UNIVERSITÉ DU QUÉBEC À TROIS-RIVIÈRES

DÉVELOPPEMENT DE MATÉRIAUX ABSORBANTS UTILISANT LE CHITOSANE ET LA CELLULOSE PHOSPHORYLÉE POUR L'ÉLIMINATION DES CONTAMINANTS TOXIQUES DES EAUX USÉES

DEVELOPMENT OF SORBENT MATERIALS USING CHITOSAN AND PHOSPHORYLATED CELLULOSE FOR THE REMOVAL OF TOXIC CONTAMINANTS FROM WASTEWATER

THÈSE PRÉSENTÉE COMME EXIGENCE PARTIELLE DU

DOCTORAT EN SCIENCES ET GÉNIE DES MATÉRIAUX LIGNOCELLULOSIQUES

PAR
RICARDO BRANDES

OCTOBRE 2020

UNIVERSITÉ DU QUÉBEC À TROIS-RIVIÈRES

DOCTORAT EN SCIENCES ET GÉNIE DES MATÉRIAUX
LIGNOCELLULOSIQUES (PhD)

Direction de recherche :

Bruno Chabot, Ph. D., Ing.
Prénom et nom — directeur de recherche

François Brouillette, Ph. D.
Prénom et nom — codirecteur de recherche

Jury d'évaluation

Bruno Chabot, Ph. D., Ing.
Prénom et nom — directeur de recherche

François Brouillette, Ph. D.
Prénom et nom — codirecteur de recherche

Jonathan Gagnon, Ph. D.
Prénom et nom — évaluateur externe

André Lajeunesse, Ph. D.,
Prénom et nom — évaluateur interne

Simon Barnabé, Ph. D.,
Prénom et nom — président de jury

Thèse soutenue le 06 10 2020

"Learning is the one thing that the mind never tires of,
is never afraid of and never regrets."

Leonardo Da Vinci

Foreword

Fresh and potable water is a limited resource, so governments and industries are setting targets to reduce unmitigated use of fresh water. Many efforts have been made in recent years, however, insufficient to avoid an environmental impact and a possible lack of drinking water in the future. Technologies capable of treating effluents in order to reuse contaminated water is in great demand today.

Heavy metals, pesticides, pharmaceuticals are among others examples of contaminants that seriously affect the production equipment and the final quality of products once the water is contaminated and recirculated in the industry. In addition, the direct disposal of these contaminants into the environment can have a severe impact on the health of living beings. Therefore, the technologies developed for the treatment and recovery of water must be simple, effective and low-cost in order to be easy to apply industrially.

The development of adsorbent media based on renewable, degradable and low-cost biopolymers seems a promising solution to meet the environmental, industrial and economic expectations mentioned above.

Acknowledgments

First of all, I would like to thank Professors Bruno Chabot and François Brouillette for accepting me in their research laboratories and to have enabled me to deepen and apply the knowledge acquired during my studies in a very promising subject.

I would also like to thank the Innovations Institute in Ecomaterials, Ecoproducts, and Ecoenergies Biomass Based (I^2E^3) and the University of Quebec at Trois-Rivières for allowing me to carry out my PhD.

I would like to thank Dr. Dan Belosinschi from Innofibre (CÉGEP de Trois-Rivières) for helping me with phosphorylated cellulose production.

I would also like to thank my colleagues from the laboratory for their support and availability, as well as all those I might have forgotten. I would also like to thank Dr. Agnès Lejeune, Isabelle Boulan and Celine Leduc for helping me with material analysis.

I thank the Natural Sciences and Engineering Research Council of Canada (NSERC) for scholarship funding.

Finally, I would like to thank all my family, my girlfriend and my friends for the support and affection.

October 2020

Résumé

La contamination de l'eau est une préoccupation mondiale croissante en raison de son importance. La croissance rapide de la population humaine et l'industrialisation mondiale ont conduit à la production de plus grandes quantités d'eaux usées contenant divers polluants, y compris des métaux lourds toxiques. Les contaminants toxiques peuvent causer de graves problèmes pour l'environnement et l'homme. Les métaux lourds sont des contaminants toxiques et dangereux. Les humains sont exposés aux métaux lourds par la consommation d'eau contaminée, ce qui entraîne toute une série d'effets néfastes importants tels que le cancer, les lésions organiques, les dommages au système nerveux et, dans les cas extrêmes, la mort. Pour prévenir les problèmes environnementaux et humains, il est nécessaire d'éliminer les métaux lourds des eaux usées. Les technologies de traitement tertiaire des eaux usées pour l'élimination des métaux lourds ont été développées et étudiées pendant plusieurs années. L'adsorption est une technologie de traitement tertiaire présentant une excellente efficacité, une hydrodynamique favorable, un débit élevé, un faible coût, une cinétique rapide et une réutilisabilité. Parmi les matériaux utilisés pour l'adsorption, le charbon actif (AC) est le plus utilisé. Sa capacité d'adsorption est efficace, mais son application est limitée par son coût élevé. Les matériaux les plus viables sont les adsorbants à faible coût. Le chitosane (CS), les fibres de cellulose phosphorylées (PCF) et les dérivés de cellulose phosphorylées sont des matériaux adsorbants peu coûteux, connus pour leur grande capacité à adsorber les contaminants et constitueraient d'excellentes alternatives pour le traitement de l'eau. Les matériaux adsorbants fonctionnent sur la base d'une surface de contact et la technique d'électrofilage est considérée comme un excellent choix pour la production de matériaux adsorbants car il s'agit d'un procédé capable de produire des nanofibres avec une surface spécifique élevée. Ainsi, ces travaux visent à mieux protéger l'environnement et à produire des bioadsorbants plus efficaces pour le traitement effluents contenant des contaminants. Pour atteindre l'objectif, des matériaux structurés à faible coût basés sur des mélanges PCF/CS avec une capacité d'adsorption améliorée des contaminants ioniques ont été développés. Ces matériaux à base de nanofibres PCF/CS ont été produits par coulée ou par électrofilage. Leurs propriétés thermiques, chimiques, électriques, mécaniques et morphologiques ont été évaluées. Des tests d'adsorption par lots ont été effectués en

utilisant des contaminants ioniques métalliques. Des modèles cinétiques et isothermes ont été utilisés pour analyser les résultats expérimentaux et les propriétés thermodynamiques ont été calculées. La réutilisabilité des adsorbants a été déterminée après les cycles d'adsorption-désorption. La capacité d'adsorption a augmenté avec la température et la concentration des ions Cd^{2+} atteignant 547 mg/g à 25°C pour les milieux adsorbants PCF/CS. Le matériau bicouche à base de PCF et de CS a permis de capturer les contaminants anioniques et cationiques, notamment le cuivre (II), le nickel (II), le cadmium (II) et le chrome hexavalent (VI). Ces résultats confirment que les supports adsorbants PCF/CS sont efficaces et relativement faciles à produire. Ils sont également respectueux de l'environnement. Ces bioadsorbants peu coûteux peuvent contribuer à la durabilité de l'eau en tant qu'excellente alternative aux technologies existantes.

Octobre 2020

Mots-clés

Durabilité de l'eau, Contaminants cationiques et anioniques, Métaux lourds, Adsorption, Chitosane, Cellulose phosphorylée, Nanofibres

Abstract

Water contamination is a growing global concern because of its importance. Rapid human population growth and global industrialization have led to the production of greater quantities of wastewater containing various pollutants, including toxic heavy metals. Toxic contaminants can cause serious problems for the environment and humans. Heavy metals are toxic and dangerous contaminants. Humans are exposed to heavy metals through the consumption of contaminated water, resulting in a range of significant adverse effects such as cancer, organ damage, damage to the nervous system and, in extreme cases, death. To prevent environmental and human problems, it is necessary to remove heavy metals from wastewater. Tertiary wastewater treatment technologies for the removal of heavy metals have been developed and studied for several years. Adsorption is a tertiary treatment technology with excellent efficiency, favorable hydrodynamics, high flow, low cost, fast kinetics and reusability. Among the materials used for adsorption, activated carbon (AC) is the most widely used. Its adsorption capacity is efficient, but its application is limited by its high cost. The most viable materials are low-cost adsorbents. Chitosan (CS), Phosphorus Cellulose Fibers (PCF) and Phosphorus Cellulose Derivatives (PCD) are low-cost adsorbent materials known for their high capacity to adsorb contaminants and would be excellent alternatives for water treatment. Adsorbent materials operate on a contact surface basis and the electrospinning technique is considered an excellent choice for the production of adsorbent materials as it is a process capable of producing nanofibers with a high specific surface area. Thus, this work aims to better protect the environment and to produce more efficient bioadsorbents for the treatment of contaminants by adsorption. To achieve the objective, low-cost structured materials based on PCF/CS mixtures with improved adsorption capacity for ionic contaminants have been developed. These materials based on PCF/CS nanofibers were produced by casting or electrospinning. Their thermal, chemical, electrical, mechanical and morphological properties were evaluated. Batch adsorption tests were performed using metallic ionic contaminants. Kinetic and isothermal models were used to analyze the experimental results and thermodynamic properties were calculated. The reusability of the adsorbents was determined after the adsorption-desorption cycles. The adsorption capacity increased with temperature and Cd^{2+} ion concentration reaching 547 mg/g at 25°C for PCF/CS adsorbent

media. The PCF/CS bilayer material allowed the capture of anionic and cationic contaminants including copper (II), nickel (II), cadmium (II) and hexavalent chromium (VI). These results confirm that PCF/CS adsorbent carriers are efficient end relatively easy to produce. They are also environmentally friendly. These low-cost bioadsorbents can contribute to the sustainability of water as an excellent alternative to existing technologies.

October 2020

Keywords

Water sustainability, Cationic and anionic contaminants, Heavy metals, Adsorption, Chitosan, Phosphorylated Cellulose, Nanofibers

Table of Contents

List of Figures

List of Tables

List of Equations

List of Abbreviations

AC	Activated carbon
MP-AES	Microwave-induced plasma interfaced to an atomic emission spectrophotometer
AFM	Atomic Force Microscopy
CS	Chitosan
DSC	Differential Scanning Calorimetry
EDTA	Ethylenediaminetetraacetic acid
EDX	Energy Dispersive X-ray Spectrometry
FTIR	Fourier Transform Infrared Spectroscopy
KF	Kraft fibers
MP-AES	Microwave Plasma-Atomic Emission Spectrometry
OM	Optical microscope
PCF	Phosphorylated cellulose fibers
PEO	Poly(ethylene oxide)
PMC	Phosphorylated microcellulose
PNC	Phosphorylated Nanocellulose
PVA	Polyvinyl alcohol
PVSK	Poly(vinyl sulfate) potassium salt
RH	Relative humidity

SEM	Scanning electron microscopy
XRD	X-ray diffraction

Chapitre 1 - Introduction

Water is an important natural resource for life on earth and an essential component for humans. The amount of fresh water in the world is 2.5% and of this volume only 10% is accessible for use, with much of it trapped in glaciers and snowfields. Some of the most populous countries with the largest economies in the world use the largest amounts of fresh water due to municipal, commercial, industrial and agricultural needs. The consumption of fresh water has increased in recent decades, due to the increase in the global population, climate change, land use change, energy choices, and global poverty, which are causing changes in the quality, availability, and quantity of fresh water [1]. It is estimated that demand for the resource will increase by 64 billion cubic meters annually. Table 1.1 shows the world's largest consumers of fresh water.

Table 1.1 World's largest users of fresh water.

Country	**Annual use of fresh water (1.0×10^9 m^3)**
India	761
China	554
USA	478
Indonesia	113
Japan	82
Mexico	81

Those countries have a high rate of water consumption. Environmentalists are increasingly concerned because the use of fresh water has been made at a higher rate each year, which raises concerns about exhaustion [2]. Fresh water is a finite resource that must be used in a sustainable way to avoid its depletion, however the contamination of rivers, lakes, oceans and groundwater have interfered with the integrity of natural resources affecting the environment and humans [3]. Industries and cities are using fresh water and generating an enormous amount of wastewater containing numerous contaminants, including agricultural chemicals, detergents, pharmaceutical derivatives and heavy metals. Sato et

al. [4] analyzed the annual volume of contaminated water and the quantity treated by some countries, as can be seen in the Table 1.2.

Table 1.2 Largest wastewater generators and volume treated in each country.

Country	Wastewater generated (Km^3/year)	Wastewater treated (%)
Canada	5	83
USA	80	71
Mexico	13	23
Brazil	2	35
Germany	6	85
France	8	84
China	59	30
India	14	31
Thailand	5	1

In many parts of the world, the wastewaters are not treated or are poorly treated, as for example in less developed and poorer countries. Even in the most developed and rich countries, with high quantities of treated wastewaters, these volumes do not reach 100%, i.e. the amount of fresh water used is still far from being fully recovered. The lack of fresh water due to contamination generates a supply water problem, affecting a significant portion of the world's population. Scarcity of fresh water affects poor people more significantly, so it is very important to implement measures that can ensure the sustainability of this important natural resource essential for life. Due to the drastic effects that a total shortage of water could cause, governments and companies have emphasized the urgency of solutions that can counter this problem [5].

From the standpoint of contaminants and their effects, contamination by heavy metals is one of the major environmental problems due to the fact that they are not biodegradable, tend to accumulate in living organisms and are known as toxic or carcinogenic [6]. The release of untreated metal contaminated effluent directly into water systems, and especially groundwater aquifers can have a large environmental, public health, and economic impact. Consumption of water contaminated with heavy metals at high

concentrations can result in serious health problems, such as cancer, lower energy levels, damage to the blood composition, organ damage (lungs, kidneys, liver and other vital organs), nervous system damage, and in extreme cases, death [7]. Common heavy metal pollutants are arsenic, cadmium, chromium, copper, nickel, lead, mercury, chrome, etc. Cadmium, a heavy metal that was most widely studied in this thesis, is mainly produced during zinc refining as a by-product of processing and refining zinc from sulfide ore concentrates.

Cadmium can cause extensive environmental contamination and health problems. It bioaccumulates in plants, invertebrates, and vertebrates. Humans may get exposed to cadmium primarily by inhalation and ingestion and can suffer from acute and chronic intoxications. A maximum acceptable concentration of 0.005 mg/L in drinking water has been established on the basis of health considerations. Also, a FAO/WHO expert committee has estimated a provisional tolerable weekly intake of cadmium for an adult to be from 0.4 to 0.5 mg [8]. Workers within the electroplating, battery production, and pigment industries are at the highest risk for exposure to cadmium. It is typically used in rechargeable batteries and special alloys and can also be found in tobacco smoke. About three-fourths of cadmium is used in alkaline batteries as an electrode component, the remaining part is used in coatings, pigments, plating and as a plastic stabilizer. However, Cd emissions decreased approximately by 35% from 1990 to 2017. This is largely due to improvements in emission reduction technologies for wastewater treatment and incinerators, and in metal refining and melting plants. Directives and regulations requiring reductions and limits on heavy metal emissions and associated permit conditions have also contributed to the reduction of Cd emissions. Emissions will continue to decrease with technological advances and the most severe regulations.

Due to the serious environmental, economic and health problems that wastewaters can cause, measures to improve the levels of treated water are being adopted. For example since 1983, Canadian municipalities have continued to upgrade their level of wastewater treatment. The percentage of Canadians on municipal sewers with secondary treatment or better has improved from 40% in 1983 to 69% in 2009, leaving approximately 18% with primary treatment or less and another 13% of Canadians using household septic systems

to treat their sewage [9]. The wastewater treatment is composed of a primary treatment which removes all materials that can easily be collected from the water before they damage or clog the primary treatment sedimentation tanks and lines. Then, a secondary treatment is applied to degrade the organic content that is derived from human waste, food waste, soaps and detergents through aerobic biological processes. Finally, a tertiary treatment is sometimes used to further improve the quality of the effluent before it is discharged into the receiving environment (sea, river, lake, wetlands, soil, etc.). Tertiary wastewater treatment technologies for contaminants removal have been extensively studied and developed. Operations including ion exchange, coagulation and flocculation, flotation, electrochemical treatment, chemical precipitation, membrane filtration, and adsorption have been used for the elimination of contaminants from aqueous environments [10].

Among these treatment technologies, adsorption is known as an economic and effective method for the removal of heavy metals, widely used due to the availability of adsorbent materials, reversibility and flexibility in design and operation [6]. Adsorption is a process that can collect ions or molecules (adsorbate) in solution to a solid surface (adsorbent). This process creates an adsorbate film onto the surface of the adsorbent. Thus, adsorption is a surface phenomenon. Materials and their characteristics are important, so they must have high abrasion resistance, high thermal stability and small pore diameters, which results in a larger exposed surface and therefore a higher adsorption capacity. Adsorbents can be used in the form of powders, spherical pellets, sticks, monoliths, membranes, etc. Most adsorbents are oxygen-containing compounds, which are hydrophilic and polar (silica gel and zeolites), carbon-based compounds which are hydrophobic and non-polar (activated carbon and graphite) and polymer-based compounds which are polar or non-polar depending on the functional groups attached to the polymer matrix. Activated carbon (AC) is the most widely used material in the production of adsorbent materials. AC is an effective adsorbent for water treatment method due to its multi-functional nature which processed to have small, low-volume pores and high degree of micro porosity that increase the surface area. However, its activation process already has a high cost and the rapid reduction of world reserves of coal-based AC sources has led to a rise in the price of this material [11].

Natural materials have been applied as low cost and high efficiency adsorbent for the removal of contaminants, therefore a promising alternative to replace traditional adsorbents. Polysaccharides, such as chitosan and cellulose have attracted attention due to their high availability and low cost. Chitosan is a material well known for its ability to remove heavy metals by the fact that it has a strong chelation potential due to its free functional groups (amine and hydroxyl) [12]. Cellulose is not an excellent adsorbent, however, chemical reaction for surface modification can significantly increase the kinetic and adsorption capacity [13]. Among them, we can mention oxidation (introduce carboxylic acid or aldehyde functionalities), esterification (sulfation and phosphorylation reactions), amidation (TEMPO oxidized cellulose), carbamation (the use of tolylene-2,4-diisocyanate (TDI) to attach functional polymers or other molecules, and the use of non-polar isocyanates) and etherification (glycidyl-trimethylammonium chloride (GTMAC) or derivatives to cationize the surface). Phosphorylation can be highlighted, which adds highly reactive phosphate groups to the cellulose surface. Among the available manufacturing technologies for the production of adsorbent materials, electrospinning is a modern process capable of producing nonwoven mats composed by nanometric fibers with large surface area and high adsorption capacity [14]. As the adsorption of contaminants is dependent on the surface area, electrospinning is a very interesting technology for the production of adsorbent media. This is a versatile process, since it allows the utilization of a wide range of materials, as well as a good control of the physical properties of the mats. Evaporation casting or dry-casting is another technology used for the production of sorbent media. It is based on the deposition of a polymer solution on a substrate, followed by the formation of a film after evaporation of the solvent. This is a practical and easy method but it does not produce materials with such high surface areas as in the electrospinning process.

Due to the importance of this issue, our research group is trying to develop sustainable and efficient solutions for wastewater treatment, which has been developing adsorbent media for the capture of heavy metals for several years. Previous works have shown that the production of chitosan nonwoven mats produced by electrospinning and evaporation casting are excellent solutions for this issue [6, 11, 12]. However, they are not competitive with conventional adsorption materials used in the market, yet. The literature review

shows that phosphorylated cellulose and its derivatives are sustainable and abundant materials with good characteristics for the adsorption of heavy metals. In addition, it was found that there are no published articles on the production of chitosan and phosphorylated cellulose composite materials using electrospinning or evaporation casting for the removal of heavy metals from aqueous solutions. In this way, the proposal of this work was to develop various types of structured sorbent media composed of chitosan and phosphorylated cellulose using electrospinning and evaporation casting processes for the removal of heavy metals from aqueous solutions. For a better understanding of these materials, the prepared solutions were evaluated in relation to their rheology, surface tension, electric conductivity and charge demand and all designed sorbent media were characterized in relation to their morphology, chemical and thermal properties. Batch adsorption experiments were carried out under controlled conditions to investigate the effects of contact time, temperature and initial metal ion concentrations on adsorption capacity. Pseudo-first order, pseudo-second order and intraparticle diffusion kinetic models were used to fit kinetic adsorption data. Langmuir, Freundlich, Temkin, Dubinin-Radushkevich isotherm models were applied to describe the adsorption equilibrium data of metal ions. The thermodynamic parameters were used to establish if the adsorption process is feasible, spontaneous and endothermic. Five adsorption/desorption cycles were evaluated for the sorbent materials in order to evaluate their reusability. The development of these new low-cost bio-adsorbents may contribute to increase the adsorption capacity and contribute to the water sustainability as an excellent alternative to existing technologies. This technology will benefit thousands of people who already suffer from lack of potable water and consequently will help prevent diseases caused by the excessive consumption of heavy metals.

1.1 Objective

The main objective of the project was to develop biosorbent composite media based on chitosan and phosphorylated cellulose and their derivatives, using electrospinning and evaporation casting processes, which is intended to be used as a tertiary treatment for the removal of heavy metals from wastewaters.

1.2 Specific Objectives

1) Develop homogeneous biopolymer solutions based on chitosan and phosphorylated cellulose and derivatives;
2) Provide accurate characterization of biopolymer's solutions based physical, chemical, optical and electrical characteristics;
3) Produce various types of sorbent media using chitosan and phosphorylated cellulose by electrospinning and evaporation casting processes;
4) Provide accurate characterization of sorbent media based on physical, chemical, thermal and electrical characteristics;
5) Perform batch adsorption experiments under controlled conditions for single-heavy metal content solution (cadmium) to investigate the effects of contact time, initial metal ion concentrations and temperature on adsorption capacity;
6) Evaluate the experimental adsorption data using the adsorption models, such as kinetic models, isotherm models and thermodynamic behavior;
7) Perform batch adsorption experiments under controlled conditions for multi-heavy metal content solution (copper, nickel, cadmium and hexavalent chromium) to investigate the effects of contact time, initial concentrations of metallic ions and temperature on adsorption capacity;
8) Study the reusability potential of the media and its degradation by performing five adsorption and desorption cycles using cadmium ion solutions.

1.3 The PhD research plan

The PhD research plan is summarized in Table 1.3:

Table 1.3 Outline of the PhD thesis

Production of electrospun chitosan/polyethylene oxide composite membranes	Production of electrospun chitosan/polyethylene oxide/nanocellulose phosphorylated composite membranes	Production of electrospun chitosan/polyethylene oxide/microcellulose phosphorylate composite membranes	Production of membranes via casting of phosphorylated cellulose fibers covered with electrospun nanofibers of chitosan/polyethylene oxide
Step 1 →	**Step 2** →	**Step 3** →	**Step 4**
✓ Solutions preparation ✓ Nanofibers production ✓ Nanofibers Neutralization ✓ Morphological evaluation	✓ Solutions preparation ✓ PNC dispersion ✓ Nanofibers production ✓ Nanofibers neutralization ✓ Morphological evaluation ✓ Chemical characterization ✓ Electrical characterization ✓ Cd^{2+} adsorption Study ✓ Kinetic models, isothermal and thermodynamic models of adsorption	✓ Solutions preparation ✓ PMC dispersion ✓ Nanofibers production ✓ Nanofibers neutralization ✓ Morphological evaluation ✓ Chemical characterization ✓ Thermal characterization ✓ Cd^{2+} adsorption Study ✓ Kinetic models, isothermal and thermodynamic models of adsorption ✓ Adsorption and desorption study	✓ Production of PCF by casting ✓ Assessment of CS/PEO nanofiber membrane coating ✓ Assessment of water permeability of membranes ✓ Heat neutralization ✓ Morphological evaluation ✓ Chemical characterization ✓ Thermal characterization ✓ Cd^{2+} adsorption Study ✓ Kinetic models, isothermal and thermodynamic models of adsorption ✓ Adsorption and desorption study ✓ Study of adsorption in a multibath with Cd (II), Cu (II), Pb (II) and Cr (VI)

Chapitre 2 - Literature Review

2.1 Water contamination

Water is the most essential natural resource for all life on earth and a precious substance for human civilization. Of the total amount of water in the world, only 2.5% exists as freshwater, while 97.5% is seawater. Considering this small proportion of freshwater, about 90% is inaccessible for our use. In many countries and regions of the world, approximately 70% of fresh water is used for agriculture. It is estimated that by 2050, in order to feed all the people on the planet, a 50% increase in agricultural production and a 15% increase in fresh water withdrawal will be necessary. Freshwater is a natural resource that needs to be very well managed, since its misuse could lead to a permanent lack of fresh water. The population growth, climate change, land use change, energy choices, and global poverty have caused precipitous changes in freshwater quantity, availability, and quality [15]. Water contamination can be defined as any matter that, when introduced into it, becomes harmful to human health and nature, creating adverse conditions for social and economic activities, affecting the sanitary conditions of the environment [16]. Water contamination is the pollution of freshwater such as lakes, rivers, oceans, and groundwater by human activities (Figure 2.1). Contamination interferes with the integrity of natural resources that preserve life in the biosphere, significantly affecting the environment [2]. The largest amount of accessible freshwater in the world is used by industries and cities, generating an enormous amount of wastewater containing numerous contaminants. The main water contaminants are suspended solids, chemical biodegradable organics, nutrients, hazardous, heavy metals, inorganic solids and biological pathogens. In many parts of the world, these contaminants are not treated or are only subjected to a treatment that does not effectively remove most of the pollutants. Human health suffers serious impacts due to the lack of drinking water, which currently affects many people in the world. Due to contamination of fresh water, the current water supply faces a major problem, where a significant proportion of people around the world still do not have access to adequate drinking water sources. This water scarcity afflicts poor people most seriously, so, it is urgent to implement basic water treatment in the affected areas mainly where water

and wastewater infrastructure are often non-existent [1]. Water scarcity places great pressure on society over its use and management.

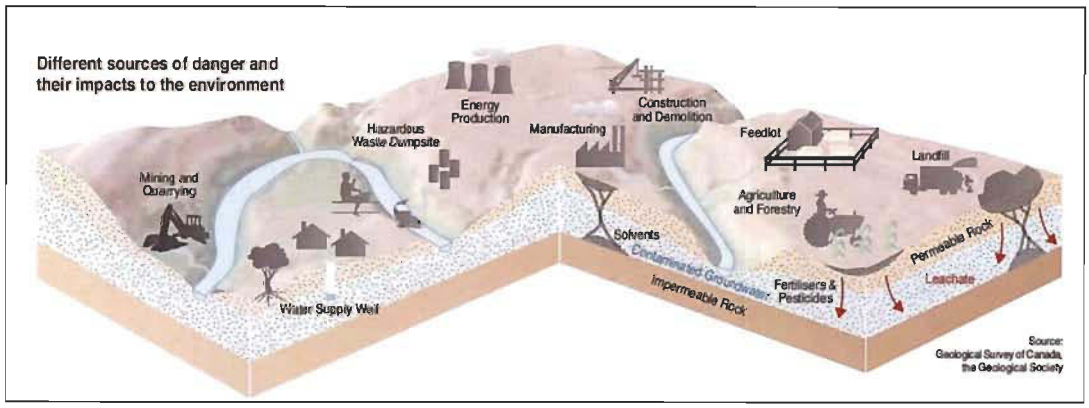

Figure 2.1 Sources of agricultural and industrial pollution and their impacts on the environment [17]

2.2 Heavy metal contamination

Industries such as metal plating, mining, fertilizers, tanneries, batteries, pulp and paper and pesticides directly or indirectly discharge their wastewater containing heavy metals into the environment [6]. Contamination with heavy metals is of particular concern because of the difficulty of treatment and its persistence in the environment. Heavy metal is the term applied to atoms that have density more than 6 g/cm^3 and occupy the central columns of the periodic table. The term heavy metal refers to a metallic chemical element that has a relatively high density and is toxic or poisonous at low concentrations. They cannot be degraded or destroyed. The toxicity of any compound, including metals, is directly related to the dose, the exposure time, the physical and chemical form of the elements, route of administration and absorption. At higher concentrations they can lead to poisoning [5]. It is believed that older people and children are more susceptible to toxic substances. Figure 2.2 shows a lake contaminated by industrial activities in China with heavy metals containing moderate to high contamination by Pb and Cr. Pollution levels were determined by checking the fish and crustaceans living in the region.

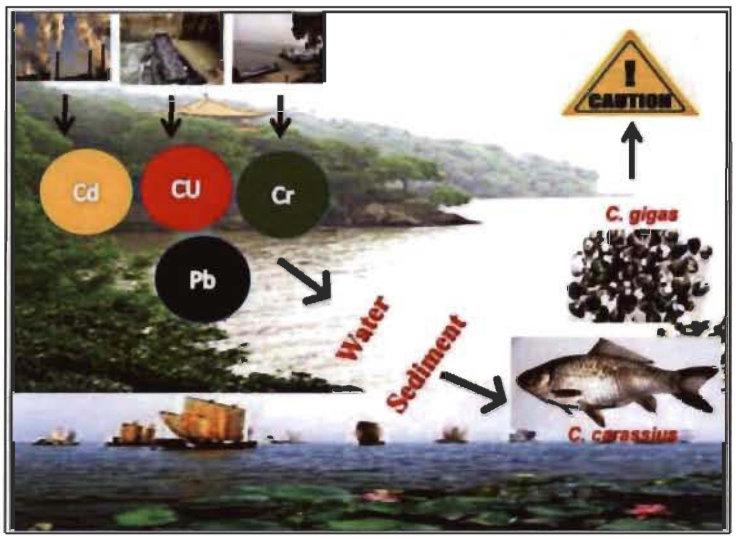

Figure 2.2 Industrial activities contaminating the lake with heavy metals in high concentrations [18].

Heavy metals in water which are most threatening due to their toxicity are arsenic, cadmium, chromium, lead, and mercury, ranking among the priority metals that are of public health significance. Other examples of toxic heavy metals are manganese, chromium, cobalt, nickel, copper, zinc, selenium, silver, antimony and thallium [3]. Economic and technical issues allied with concern about a possible shortage of fresh water lead to the seek of a cheap and efficient technique for the removal of heavy metals from wastewaters [19]. Remediation approaches, such as water reuse and recycling have been adopted in industries. However, they are not widely used due to technical and economic limitations. Therefore, the removal of heavy metals from water has become a high priority within water treatment technologies.

Heavy metals cannot be degraded or destroyed. Cadmium is one of the most polluting heavy metals which derives its toxicological properties from its chemical similarity to zinc, which is also very polluting. Cadmium is bio persistent and, once absorbed by an organism, remains resident for many years. The average daily intake for humans is estimated at 0.001 mg of water, being 1500-8900 mg considered toxic doses for humans [9]. Chromium is used in metal alloys and pigments for paints, cement, paper, rubber and other materials. Low-level exposure may irritate the skin and cause ulceration. Long-term exposure can cause damage to kidneys and liver, and circulatory and nerve tissue damage.

Chromium accumulates frequently in aquatic life, increasing the danger of eating fish that may have been exposed to high levels of chromium. Copper in high doses can cause anemia, liver and kidney damage, and stomach and intestinal irritation. Copper normally occurs in drinking water from copper pipes as well as from additives designed to control the growth of algae. High levels of exposure can result in toxic biochemical effects in humans, which in turn cause problems in haemoglobin synthesis, effects on the kidneys, the gastrointestinal tract, joints and the reproductive system, and acute or chronic damage to the nervous system. Nickel in excessive amounts, can become mildly toxic. Long-term exposure can cause decreased body weight, heart and liver damage, and skin irritation. Nickel can accumulate in aquatic life, but its presence is not magnified along food chains [1]. Chrome compounds in water-solution in the +6-oxidation state are anionic contaminants extremely toxic for humans and animals being actively transported into the cells of the body. Once Cr (VI) is inside the cells, it is converted to unstable reactive intermediates which are bonded to cells being a strong mediator of Cr (VI) toxicity and carcinogenicity [5]. The carcinogenic effects of hexavalent chromium are more evident in the respiratory tract, but more recent evidence indicates that it can lead to other cancers. Workers are exposed to Cr (VI) through inhalation which leads to lung cancer. The most contaminating and polluting industries are chrome plating, leather tanning, stainless steel production and chrome pigment manufacturing [6]. Other studies show that ingestion or skin contact with Cr (VI) can lead to its reduction to Cr (III) which connects to DNA-modifying proteins and can lead to cancer in all human organs [7].

2.3 Wastewater treatments

Wastewater treatment is a process used to remove contaminants from wastewater or sewage and convert them into an effluent that can be returned to the water cycle with acceptable impact on the environment, or reused for various purposes (called water recovery). Water recycling is a means of saving water in industries, where wastewater that would be discharged, can be used in a lower quality application. Water recovery refers to the reuse of wastewater produced elsewhere such as in industrial cooling, power generation and boiler feed. However, wastewater sometimes needs to undergo a tertiary treatment before effluents are reused or recycled, directly or indirectly in the industry [1].

Wastewater treatment usually involves four stages, called pre-treatment, primary, secondary and tertiary treatments. The pre-treatment removes all materials that can easily be collected before they damage or clog primary treatment pumps and clarifier lines. Objects normally removed during pre-treatment include garbage, tree limbs, leaves, branches and other large objects. The primary treatment consists of temporarily holding the waste in a basin where heavy solids can settle to the bottom while oil, grease and lighter solids float to the surface. The settled and floating materials are removed and the remaining liquid can be discharged or subjected to secondary treatment. Sedimentation is the most used process at this stage. The secondary treatment removes dissolved and colloidal substances remaining in water after the primary treatment. The secondary treatment involves microorganisms to digest organic contaminants. Oxygen and agitation are also supplied to water in order to keep microorganism alive. Rotating Biological Contactors (RBCs), Trickling Filters, Activated Sludge and oxidation ditches are secondary treatments. Tertiary treatment is the step of polishing the effluent to eliminate specific contaminants not removed in the primary and secondary treatment steps. Various tertiary wastewater treatment technologies for heavy metal removal have been extensively studied and developed. Operations including ion exchange, photocatalysis and adsorption have been used for the elimination of metals from aqueous environments [10]. Most of these processes are not appropriate alternatives for the elimination of trace amounts of metal ions because of driving force, inadequate reactivity and large amounts of required materials, energy consumption and high cost [6]. Among these technologies and considering the cost-benefit, adsorption can be featured as an economic and effective method for the removal of heavy metals widely used and recognized due to the availability of adsorbent materials, reversibility and flexibility in design and operation [6]. Adsorption is considered a tertiary treatment technology. Activated carbon (AC) is the most widely used adsorbent for the removal of heavy metals from wastewaters. However, the sources of commercial coal-based AC are almost depleted, resulting in the increase of price, in other words, AC is relatively expensive. So, the search for an abundant and cheap alternative to activated carbon has become a main research focus [5]. Low-cost adsorbents are recognized as effective and economic methods for low concentration heavy metal wastewater treatment. Biosorbents are low-cost and high effectiveness adsorbents

materials that has been confirmed like very promising for the removal of heavy metals from wastewaters. These biosorbents can be provided from sources such as non-living biomass, algal biomass and microbial biomass [20].

2.4 Adsorption process

Adsorption is a mass transfer operation, which studies the ability of certain solids to concentrate on its surface some substances existing in liquid or gaseous fluids, allowing the separation of the components of these fluids. Since the adsorbed components concentrate on the outer surface, the larger will be this outer surface per unit of solid mass, the more favorable will be the adsorption [17]. The component that accumulates on the interface of the material is usually referred as adsorbate, and the solid surface on which adsorbate accumulates is the adsorbent. The adsorption separation processes are based on three distinct mechanisms: the steric mechanism, the equilibrium mechanism and the kinetic mechanism. For the steric mechanism, the pores of the adsorbent material have characteristic dimensions, which allow certain molecules to enter, excluding the others. For the equilibrium mechanism, solids materials are available to accommodate different adsorbate species, which are preferentially adsorbed to other compounds. The kinetic mechanism is based on the different diffusivities of the various species in the adsorbent pores [18]. Depending on the nature of the forces involved, the adsorption can be classified according to the intensity in two types: physical adsorption (physisorption) and chemical adsorption (chemisorption). In the physical adsorption, adsorbate binding to the surface of the adsorbent involves a relatively weak interaction which can be attributed to van der Waals forces, which are similar to molecular cohesion forces. The chemisorption, involves the exchange or sharing of electrons between the molecules of the adsorbate and the surface of the adsorbent, resulting in a chemical reaction, creating strong chemical bonds [7]. Chemical adsorption is highly specific and not all solid surfaces have active sites capable of chemically adsorbing the adsorbate. It should be noted that not all molecules present in the fluid can be adsorbed chemically, only those capable of binding to the active site. Physical adsorption, unlike chemical adsorption, is non-specific. The physical adsorption occurs over the entire adsorbent surface, so it is said to be non-localized, and the chemical adsorption can only occur at the active sites, so it is said localized [7].

Adsorption phenomena are the result of a combination of the types of forces involved in physical and chemical adsorption. Thus, many factors influence the adsorption process, such as surface area, adsorbent and adsorbate properties, system temperature, solvent nature, and pH of the medium. The characteristics of the adsorbent include the surface area, pore size, density, functional groups present on the surface, and hydrophobicity of the material. The nature of the adsorbate depends on the polarity, the size of the molecule, the solubility, and the acidity or basicity. The operating conditions include, principally, temperature, pH and the nature of the solvent [7]. Figure 2.3 shows a schematic example of the adsorption of contaminants on a graphene membrane. It is possible to observe adsorption of different contaminants, which interacted with the membrane through different kinds of connections.

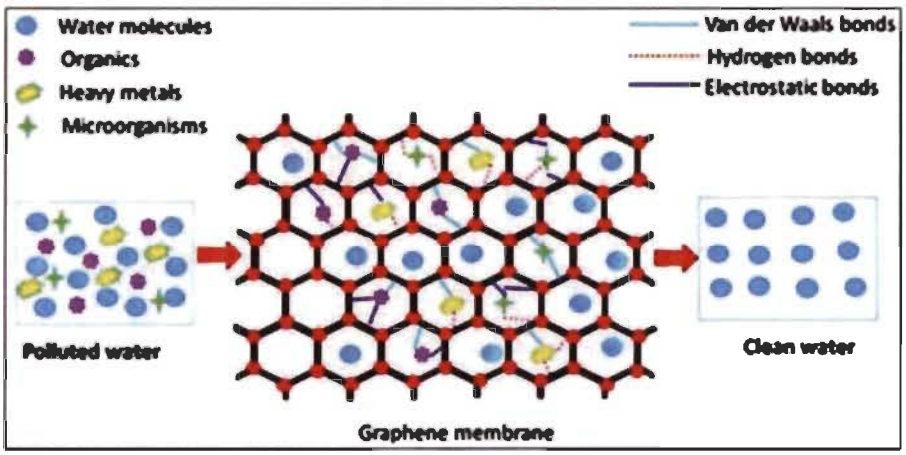

Figure 2.3 Electrospun graphene membrane eliminating by adsorption contaminants from the wastewater [12].

2.4.1 Adsorption equilibrium

When a certain amount of an adsorbent comes in contact with a given volume of a liquid containing an adsorbate, the adsorption occurs until equilibrium is reached. In the contact between the adsorbent and the adsorbate, the molecules or ions tend to flow from the aqueous medium to the surface of the adsorbent until the solute concentration in the liquid phase (C_e) remains constant. At this stage, the system is said to have reached the equilibrium state and the adsorption capacity of the adsorbent (q_e) can be determined. Weak molecular forces, such as van der Waals forces, provide the driving force for physical adsorption, while a chemical reaction forms a chemical bond between the

adsorbate and the surface of the solid provides the driving force in chemical adsorption. Obtaining an adsorption isotherm is a process where a mass of adsorbent is added in a given volume (V) of a quantity of solutions with different and known initial concentrations (C_o). When the adsorption equilibrium is reached, it is possible to evaluate the final solute concentration in the solution in equilibrium (C_e, in mg/L) and the adsorption capacity of the adsorbent (q, adsorbate mass per unit of adsorbent mass, mg/g). This information makes it possible to plot a graph of q versus C_e. To obtain the C_e values, analytical techniques can be used, such as gas or liquid chromatography, ultraviolet or visible spectroscopy, absorption or emission spectroscopy, titration or other suitable means [18]. To obtain values of q, the amount of adsorbate in the adsorbent should be equal to the amount of adsorbate removed from the solution, according to Equation 2.1.

$$q = \frac{(C_o - C_e)V}{m} \qquad \text{Eq. 2.1}$$

Where,

q = Adsorption capacity (mg/g);

C_o = Initial concentration of adsorbate (mg/L);

C_e = Concentration of adsorbate at equilibrium (mg/L);

V = Volume of the solution (L);

m = Adsorbent mass (g).

After the determinations of q and C_e, a plot of q versus C_e can be drawn. Analyzing the various forms of isotherms, provides relevant information about the process of adsorption. Many isothermal equations were proposed with two or more parameters to adjust the experimental data on the values of q versus C_e. Among these, the Langmuir, Freundlich, and Dubinin-Radushkevich models are the most applied [17].

2.4.2 Langmuir isotherm

For the Langmuir model, the following hypotheses are considered:

- The surface is assumed to be homogeneous, that is, composed of only one type of adsorption site;

- The adsorbed metal species interact with only one type of site active so that each site can accommodate only one molecule and that there is formation of a monolayer;
- Adsorption is limited to monolayer;
- It is assumed that there is no competition from species to be, so that only one can be adsorbed;
- The adsorption energy is identical in all the active sites and independent of the presence of adsorbed species at neighboring sites;
- The charged solution of metal species is diluted and the adsorption process occurs reversibly [7].

The representative mathematical expression of the Langmuir isotherm is given by Equation 2.2.

$$\frac{C_{eq}}{q_{eq}} = \left(\frac{1}{K_L q_{\max}} + \frac{C_{eq}}{q_{\max}} \right) \qquad \text{Eq. 2.2}$$

Where,

q_{eq} = amount of solute adsorbed per unit mass (mg/g);

q_{max} = maximum adsorbent capacity (mg/g);

C_{eq} = solute concentration in the liquid phase in equilibrium with solid phase (mg/L);

K_L = Langmuir constant (L/mg).

2.4.3 Freundlich isotherm

The first empirical model was developed by Freundlich and it is based on the adsorption of a multilayer type on the heterogeneous surface [17]. The heat of adsorption on the adsorbent surface is not uniform and the model is given by Equation 2.3.

$$q_{eq} = K_f C_{eq}^{1/n} \qquad \text{Eq. 2.3}$$

Where,

q_{eq} = amount of solute adsorbed per unit mass (mg/g);

C_{eq} = solute concentration in the equilibrium liquid phase with the solid phase (mg/L);

K_f = Freundlich constant (mg/g);

n = constant of the Freundlich equation related to the degree of system heterogeneity.

This expression can be linearized in the form of Equation 2.4.

$$\ln q_{eq} = \ln K_f + \left(\frac{1}{n}\right) \ln C_{eq} \qquad \text{Eq. 2.4}$$

2.4.4 Dubinin-Radushkevich isotherm

Dubinin-Radushkevich adsorption isotherm is more general than the Langmuir model, because its derivation is not based on ideal assumptions such as equipotent of adsorption sites, absence of stoic obstacle between adsorbed and incoming particles and surface homogeneity on microscopic level. It is applied to estimate the nature of adsorption process, where the mean energy free informs if it is chemical or physical. The general equation form is given by Equation 2.5.

$$q_{eq} = q_{DR} \exp\left(-\beta_{DR} \varepsilon^2\right) \qquad \text{Eq. 2.5}$$

Where,

ε = Polanyi potential;

q_{eq} = adsorption capacity at equilibrium (mmol/g);

q_{DR} = maximum theoretical adsorption capacity for formation of monolayer (mmol/g);

β = activity coefficient related to adsorption free energy (mol^2J^{-2});

Polanyi's theory considers a fixed volume of sorption space near to the sorbent surface and the existence of a sorption potential on these spaces. The potential ε is represented by Equation 2.6:

$$\varepsilon = RTln\left(1 + \frac{1}{C_e}\right) \qquad \text{Eq. 2.6}$$

Where,

R = constant of the ideal gases (8.314 J mol^{-1});

T = temperature in the thermodynamic scale (K);

C_e = concentration of the chemical species (mol/L).

The mean free energy of adsorption (E, J mol^{-1}) can be calculated by Equation 2.7.

$$E = \frac{1}{\sqrt{2\beta}} \qquad \text{Eq. 2.7}$$

This means that the adsorption free energy provides information about the adsorption mechanism. If the results found are between 8 and 16 kJ mol^{-1}, the adsorption process occurs chemically and, if the values found are less than 8 kJ mol^{-1}, the adsorption process occurs physically.

2.4.5 Thermodynamic parameters

The thermodynamic parameters are important in the adsorption process since they determine the degree of spontaneity and feasibility of the process when calculating the variation of the Gibbs free energy values and the entropy change. The variation of the Gibbs free energy change of adsorption can be calculated by following equations:

$$\Delta G^{\circ} = -RT \ln K_c \qquad \text{Eq. 2.8}$$

$$K_C = \lim_{C_{el} \to 0} \frac{C_{es}}{C_{el}} \qquad \text{Eq. 2.9}$$

R is the gas constant; T is an absolute temperature (K) and K_C is the adsorption equilibrium constant. C_{es} and C_{el} are the solid and liquid phase concentration in equilibrium (mg/L), respectively. Equilibrium constant (K_C) and temperature can be related by the Van't Hoff equation (Equation 2.10).

$$\ln K_C = \frac{\Delta S^{\circ}}{R} - \frac{\Delta H^{\circ}}{RT} \qquad \text{Eq. 2.10}$$

The entropy change of adsorption (ΔS°) and the enthalpy change of adsorption (ΔH°) can be obtained from the slope and intercept of a Van't Hoff plot of ln K_C versus $1/T$.

2.4.6 Kinetics of adsorption

The adsorption kinetics describes the rate of solute removal, being dependent on the physical and chemical characteristics of the adsorbate, adsorbent and experimental

system. The knowledge of the kinetics of adsorption serves to examine the mechanism which controls the adsorption process, such as mass transfer between phases and chemical reaction, and several kinetic models can be tested to interpret the experimental data, especially the first-order and pseudo-second order models. A good correlation of the kinetic data reveals the adsorption mechanism [17]. The pseudo-first order model assumes a physical adsorption as the dominant mechanism and it can be represented by the following equations:

$$dq/dt = K_1\left(q_{eq} - q_t\right) \qquad \text{Eq. 2.11}$$

$$\log(q_{eq} - q_t) = \log(q_{eq}) - (\frac{K_1}{2.303})t \qquad \text{Eq. 2.12}$$

Where,

q_{eq} = amount of the adsorbed metal at equilibrium (mg/g) in the first order model;

K_1 = first-order equilibrium constant (L/min);

q_t = quantity of metal adsorbed as a function of time (mg/g);

t = reaction time (min).

The pseudo-second order model assumes that chemical adsorption is the dominant mechanism [18]. The model equation can be represented by the following equations:

$$dq/dt = K_2\left(q_{eq} - q_t\right)^2 \qquad \text{Eq. 2.13}$$

$$t/q_t = \frac{1}{K_2 q_{eq}^{\ 2}} + \frac{t}{q_{eq}} \qquad \text{Eq. 2.14}$$

Where,

q_{eq} = amount of metal adsorbed at equilibrium (mg/g);

K_2 = second-order equilibrium constant (L/min);

q_t = amount of metal adsorbed as a function of time (mg/g);

t = reaction time (min).

According to the Weber and Morris model, if intraparticle diffusion is the determinant factor of the velocity, the removal of adsorbate varies with the square root of time [7]. Thus, the intraparticle diffusion coefficient (K_d) can be defined by Equation 2.15.

$$q_t = K_d t^{1/2} \qquad \text{Eq. 2.15}$$

Where, q_t is the amount of adsorbate adsorbed on the solid phase (mg/g) at time t (min) and K_d is the intraparticle diffusion coefficient (mg/g $min^{1/2}$).

2.5 Adsorbent Materials

2.5.1 Traditional adsorbents

Some of the more traditional types of adsorbents in use are: activated alumina, silica gel, activated carbon, molecular sieve coal, molecular sieve zeolites and polymeric adsorbents. Most adsorbents are manufactured; however, some occur naturally, e.g. activated carbons and some zeolites respectively. Each adsorbent material has its own characteristics, such as porosity, pore structure and nature of its surfaces. Adsorbent pore sizes can be distributed over the entire volume of the material. Pore sizes are generally classified into macropores (diameters above 50 nm), mesopores (diameters from 2 to 50 nm) and micropores (diameters below 2 nm). These traditional adsorbents can be used in differentiated applications, such as, drying of gases, refrigerants, organic solvents, transformer oils, removal of HCl from hydrogen, purification of helium, water purification, separation of olefins and aromatics from paraffins, removal of acetylene, propane and butane from air, refining of mineral oils, clean-up of nuclear off-gases, and so on. There are several studies using traditional adsorbents for the removal of heavy metals. For example, Kołodyńska *et al.* [21] made a comparison between the use of biochar and activated carbon for the removal of heavy metals. Another example is the use of Amphiphilic PMMA/PEI core-shell nanoparticles as adsorbent for the removal of heavy metals [22]. Also, Gholami and Padervant [23], used magnetic core-zeolitic shell composites functioned as adsorbents for the removal of cationic heavy metals.

2.5.2 Chitosan

Chitin is the second most abundant natural polysaccharide in the world and it is composed of (1-4)-linked 2-acetamido-2-deoxy-b-D-glucopyranose units [24]. Chitosan is an amino polysaccharide, derived from the deacetylation process of chitin, which constitutes the largest fraction of the exoskeletons of insects and crustaceans [25]. To obtain chitosan it is necessary to partially deacetylate the chitin, which is found and extracted mainly from the carapace of crustaceans, lobsters, prawns and crabs. With deacetylation, the acetamido groups (-$NHCOCH_3$) of chitin are transformed into amino groups (-NH_2), in varying degrees, forming the chitosan. The chitosan name is generally assigned to the polymer whose number of monomer units containing the NH_2 group is sufficient to render the polymer soluble in weak acids. Chitosan is reactive and can be characterized as a cationic polyelectrolyte, generally being purified in the neutral form [24]. Chitosan is a biopolymer that has a molecular structure chemically similar to cellulose, differing only in functional groups. Hydroxyl groups (OH) are arranged in the general structure of the biopolymers, but the major difference between them is the presence of amino (NH_2) groups in the chitosan. It is soluble in diluted acid medium, forming a cationic polymer, with the protonation of the amino group (NH_3^+), which confers special properties differentiated in relation to the vegetal fibers [26]. Figure 2.4 shows the chemical structure of completely acetylated chitin and completely deacetylated chitosan.

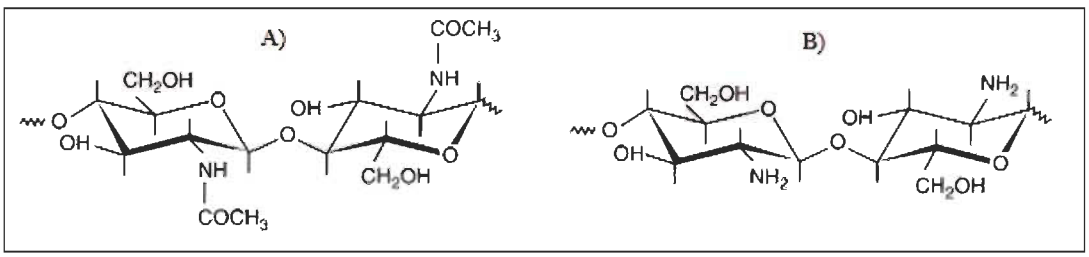

Figure 2.4 Chemical structures of (a) completely acetylated chitin and (b) completely deacetylated chitosan [27].

In the solid state, chitosan is a semi crystalline polymer. Its morphology has been studied, with mention in the literature of many polymorphisms [25]. Chitosan crystals are obtained by complete deacetylation of the low molecular weight chitin. In diluted weak acid solutions, chitosan is readily dissolved due to the protonation of the amino groups. In

neutral medium, chitosan has limitations to solubilize in water. To increase the solubility in water, it is better to use low molecular weight chitosan, which will increase the homogeneity and will decrease the viscosity of the system. It has also been used the combination of chitosan with other polymers and inorganic materials for the production of composite materials such as the polyvinyl alcohol (PVA) and the poly (ethylene oxide) (PEO) [28]. Chitosan is a biopolymer widely used and it presents potential applications in water purification, food processing and chelation of metallic ions, encapsulation of fragrances, ion exchange, protective lotions and creams, skin regeneration, bone structure regenerator, bactericidal and antiviral activities, artificial membranes, absorbent in the removal of heavy metals and support of immobilization of enzymes and microbial cells [29-31]. Chitosan nanofibers present potential applications in wastewater treatment, where the removal of heavy metal ions by chitosan through chelation has received much attention [32-34]. Chitosan is a low-cost absorbent with high removal capacities for industrial waste due to the interaction of its free amine groups with metal ions in heavy metal pollution control. The application of chitosan as an adsorbent material makes it possible to capture toxic metal ions such as Hg^{2+}, Cu^{2+}, Ni^{2+}, Zn^{2+}, Pb^{2+} and Cd^{2+} from polluted drinking water and aqueous solutions. The amine groups on the chitosan structure insert additional adsorption sites for metal chelation by coordination bond which can be formed by functional groups of chitosan and metallic ions [35].

2.5.3 Cellulose

Cellulose is the most abundant polysaccharide, cheap and easily available on earth, and can be traditionally extracted from plants or synthesized by various microorganisms such as fungi, algae and bacteria [36]. The cellulose content in the cotton fiber is 90%, in the wood is 40-50%, and in the dried hemp is 57%, approximately. Cellulose is insoluble in water and an important structural component of the primary cell wall of green plants and some types of algae. Cellulose is an organic compound with formula $(C_6H_{10}O_5)_n$ consisting of a linear chain of β (1→4) linked D-glucose units with a structural unit of repetition appointed cellobiose, formed by the union of two molecules of glucose [37]. Each glucose molecule is rotated approximately 180° relative to the neighboring molecule. The cellulose biopolymer can be very long reaching a number of glucose units

with glycan chain coming from 2000 to more than 25000 glycoside molecules [38]. Figure 2.5 shows the structure of the β (1→4) glycan chain, cellulose. Total hydrolysis of cellulose produces glucose molecules, while partial hydrolysis produces cellobiose molecules.

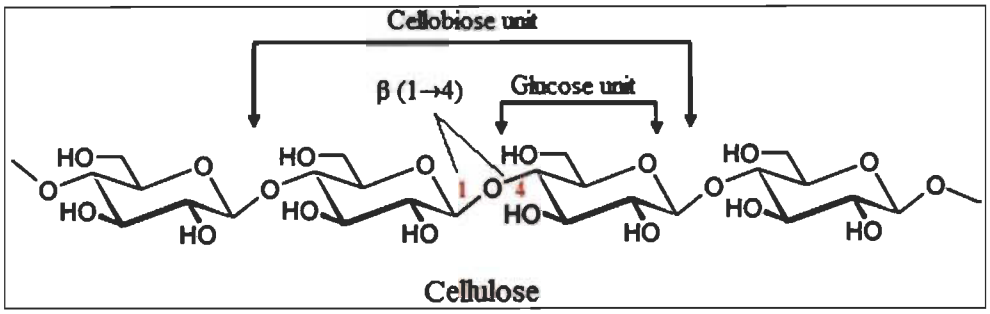

Figure 2.5 Structure of the glycan chain β (1→4) (cellulose). The cellobiose and glucose-repeating units are indicated in brackets.

A cellulose molecule can have areas with an orderly, rigid and inflexible configuration in its structure (crystalline cellulose) and other areas of flexible structures (amorphous cellulose). These differences are responsible for some variations in physical behavior, which can be observed in a cellulose molecule. For example, water absorption and swelling of a cellulose molecule is limited to the amorphous regions of the molecule [37]. The strong hydrogen bonding network of the crystalline regions prevents the occurrence of the swelling process in these areas. There are four different known forms of crystalline cellulose structures (I, II, III and IV) and only two of them are the most industrially used, numbers I and II. Type I cellulose can be synthesized by plants where their parallel chains of cellulose are arranged uniaxially, however, in type II cellulose, their chains are arranged randomly. Type I cellulose can have two formats, type Iα and Iβ where their structures are triclinic and monoclinic, respectively [39]. In nature cellulose does not exist as a single chain. The long and rigid molecules of cellulose combine to form the microfibrils, each consisting of several cellulose chains. The cellulose chains that constitute the microfibril are oriented parallel, forming intramolecular hydrogen bonds [37]. The microfibril can have approximately 36 cellulose chains, and the cellulose produced by algae can form microfibrils with more than 1200 glycan chain β (1→4) [40].

2.5.4 Phosphorylated Cellulose

Cellulose has a chemical structure that allows chemical modifications, such as phosphorylation. Phosphorylation is a esterification reaction which adds phosphate groups (PO_4) on another molecule [41]. Due to the high reactivity of the phosphate groups, polymers can be graphitized (process in which monomers are covalently bonded and polymerized as side chains onto the main polymer chain) to obtain copolymers which bring new physical and chemical properties through phosphorylation reactions [42]. The grafting reaction of phosphorus containing groups to cellulose can performed with pentavalent (V) or trivalent (III) phosphorus reagents, by direct or indirect bonding of phosphorus functions, using cellulose as substrates, in heterogeneous or homogeneous reactions [43]. The reaction of cellulose substrate with phosphoric acid in aqueous solutions is called heterogeneous and the reaction with phosphoric acid in molten urea is then called homogeneous [44], the reaction schemes can be seen in Figure 2.6.

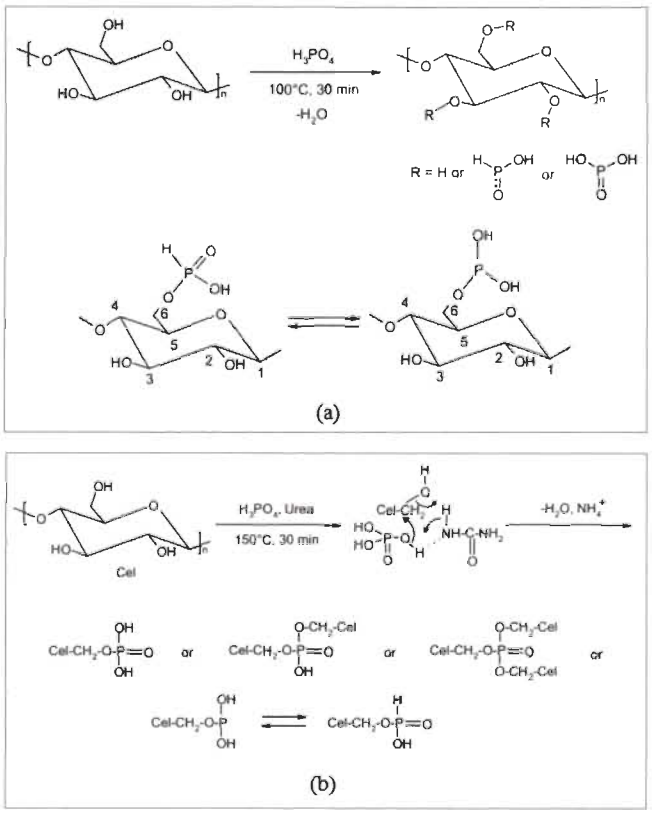

Figure 2.6 Cellulose phosphorylation with phosphoric acid in aqueous solution (a) and in molten urea (b). Formation of tautomeric phosphorylated cellulose structures [44].

The phosphoric acid is attached to the cellulose chain in the form of a phosphate acid group by one ester bond via the reactions of the cellulose hydroxyl groups, however, derivatives containing mobile hydrogen directly attached to phosphorus are in tautomeric equilibrium. The tautomeric structures with different dissociation behaviour can form a phosphide that should behave as a monobasic acid or can form two acid groups (Figure 2.6 a) [44]. In relation to the phosphorylation in molten urea, the phosphoric acid can also form structures crosslinked di-substituted and tri-substituted esters with cellulose (Figure 2.6 b) [44]. The chemical treatment applied on the cellulose substrate during the phosphorylation transform the material in nanocellulose. Phosphorus derivatives such as H_3PO_4, P_2O_5, and $POCl_3$ are the most used phosphorylating agents for pentavalent phosphorus. However, these types of reagents, usually form anionic cellulose phosphates with lower esterification reactivity than derivatives of trivalent phosphorous that cause high degradation of the cellulose [43]. Aggressive acidic environments, high temperatures and long reaction times lead inevitably to the deterioration of the fiber structure. This problem can be partially overcome if urea is introduced in the phosphorylation system as a catalyst [45]. The reaction between cellulose and phosphoric acid result in surface phosphate groups occurred predominantly at C3 and C6 positioned hydroxyl groups of cellulose monomer rings without any changing of crystalline structure. After the phosphorylation, the cellulose keeps its cellulose (I) crystal structure and crystallinity indices [46].

Phosphorylation can be provided as a mean to enhance the adsorption capacity of the cellulose [47]. Cellulose phosphates have been used for several years because of its high ability to bind calcium ions [48]. Peng *et al.* [13] used cellulose nanocrystals, phosphorylated cellulose nanocrystals and phosphorylated cellulose fibers for selective adsorption of Ag^{+}, Cu^{2+} and Fe^{2+} from industrial effluents. They observed that the introduction of phosphate groups onto cellulose surface significantly improve the metal sorption velocity and sorption capacity with immobilization nearly 100% of the metals in the aqueous solutions. Oshima *et al.* [49] used phosphorylated bacterial cellulose and plant cellulose with phosphoric acid in molten urea and observed that the degree of phosphorylation of bacterial cellulose is higher than that of plant cellulose under the same conditions.

2.6 Electrospinning process

2.6.1 Basic principle

Electrospinning is a technique that uses electrostatic forces to produce fine fibers from polymer solutions. This process is capable of producing nonwoven mats composed by nanometric fibers with large surface area and high adsorption capacity [14]. The basic process setup consists of a high voltage power supply, a syringe pump/spinneret and a collector, wherein this system is connected and grounded, according to Figure 2.7. The power source provides a direct current and a needle and syringe assembly is used as a spinneret driven by a pump with a polymeric solution stored inside the syringe. An electric field is formed when a high voltage is provided and the solution surface at the tip of the needle is charged. When the voltage increases an electrostatic repulsion is generated between the polymer chains creating forces offsetting the surface tension, which the solution will be distorted to create a conical shape (Taylor cone) [14].

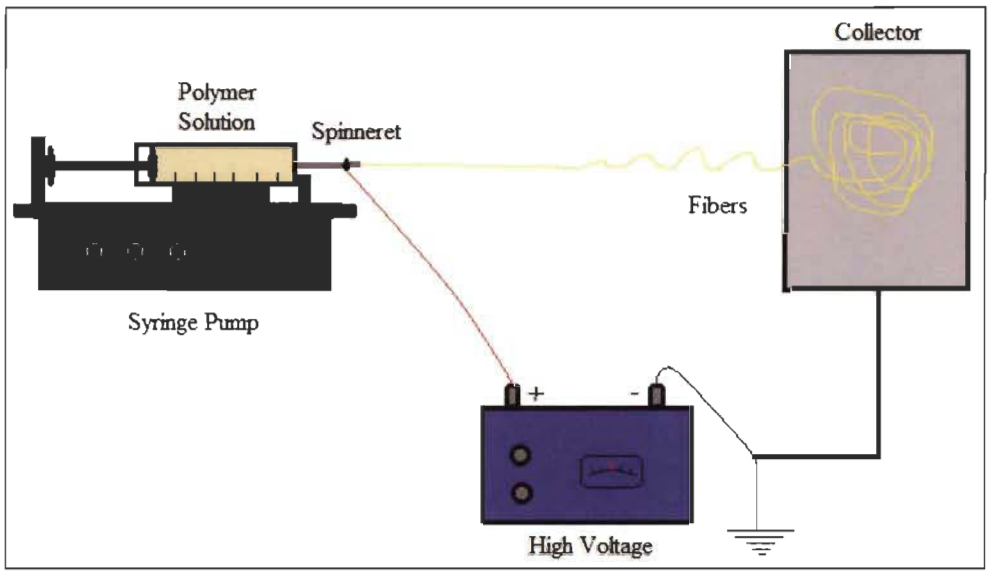

Figure 2.7 Schematic illustration of the electrospinning setup.

At this moment, a jet flow is formed and ejected from of the Taylor cone suffering stretching and elongation, then the solvent will evaporate and the jet diameter can reach nanometers. Attracted by the negatively charged collector, the nanofibers will eventually deposit on the collector's surface in a random manner, generating a nonwoven nanofiber mat [50].

2.6.2 Effect of electrospinning parameters

Electrospinning is a complex process with many parameters that drive the formation of nanofibers and consequently mats properties, among them, there are solutions, process and environmental parameters. The solutions variables are concentration, molecular weight, viscosity, surface tension and conductivity [50]. Applied voltage, flow rate, collector type and tip to collector distance are the process parameters. The environmental parameters are the temperature and the humidity. The set of parameters dictates the quality of the mats formed and that a poor choice of values parameters could generate defects on the nanofibers, such as bridging, beads, droplets, pores, heterogeneous nanofiber diameters [14].

Regarding the solution parameters, low polymer solution concentrations tend to form beads on the nanofibers and the increase generates uniform nanofibers with increased diameters. High molecular weight polymer provides a desired viscosity for the nanofiber generation, however, generating nanofibers with larger average diameters. Low viscosities tend to produce non continuous nanofibers and in high viscosities there is a difficulty in the jet formation. Viscosity, polymer concentration and molecular weight are correlated to each other. The solution's viscosity is determining the range of solutions concentrations that can produce continuous nanofibers. The high surface tension of the solutions causes instability in the jets generating sprayed droplets. Lower surface tension helps to produce mats in a lower electric field and the reduction of the solution surface tension tend to produce nanofibers without beads. The conductivity is related to the polymer type and solvent used. The increase in electrical conductivity generates lower nanofibers diameters whereas at low conductivity, insufficient elongation of the jet, produces beads and non-uniform nanofibers [51]. Regarding the process parameters, a higher voltage generates stretching of the solution due to the coulombic forces in the jet and a stronger electric field. These effects lead to lower nanofiber diameter and produce rapid evaporation of the solvent. However, a high voltage increases the chances to produce beads on the nanofibers. The flow rate influences the jet velocity and the material transfer rate, where a low rate gives enough time for the solvent to evaporate and higher rates tend to produce beads. Flat collectors have the disadvantage of difficult nanofiber mat removal

compared to rotational collectors. Rotating collectors can also be used to make mats with aligned nanofibers. Aligned nanofibers can be produced by magnetic electrospinning (MES). Aligned nanofibers can improve mechanical properties in the machine direction (MD), can be easily removed from the collector and can be efficient for tissue engineering, where acted as a guide for neural cells and were able to achieve a higher cell proliferation and migration. The distance between the syringe tip and the collector can help to control the nanofibers diameter and morphology. It is necessary to keep enough distance for the nanofibers to dry in order to avoid bridging and accumulations [52]. The temperature, an environmental parameter, can be adjusted to control nanofiber diameters. When the humidity is increased, there is a tendency to form pores on the nanofiber surface. Also, our lab experience has shown a great interference of the humidity on the nanofibers generation, where, in high humidity the surface tension of the polymer solution is drastically altered resulting in appearance of beads or non-formation of nanofibers [14].

2.6.3 CS/PEO Electrospinning

The electrospinability of chitosan is limited mainly due to its polycationic nature in solution, rigid chemical structure and specific inter and intra-molecular interactions [53]. The formation of strong hydrogen bonds avoids the free movement of chitosan chain segments exposed to the electrical field, leading to jet breakage during the process. Furthermore, the repulsive forces between the cationic groups on the chitosan can hinder the formation of sufficient chain entanglements which results in beads instead of nanofibers [54]. The method more widely applied and successful for improving the electrospinability of chitosan is mixing it with another natural or synthetic polymer which are biocompatible and biodegradable and do not restrict the final applications of chitosan nanofibers [55]. The coaxial electrospinning of chitosan with PEO is an alternative approach to overcome this problem [28]. The coaxial electrospinning is a modification of the conventional process which can electrolyte two or more polymer solutions simultaneously from coaxial capillaries. The spinnerets used share an axis, allowing one solution to be injected into the other at the tip of the needle with the core fluid to be sucked in from the outside to produce continuous or hollow coated nanofibers. The addition of PEO as a second polymer phase changes the physical and mechanical properties of

chitosan composite nanofibers. The integrity and stability of the nanofibers under different working conditions is a concern that should be taken into account for the final applications of chitosan and PEO nanofibers. Due to the excellent PEO electrospinability, a higher content of PEO will lead to an improvement in the chitosan electrospinability [55]. The literature has shown that researchers have prepared electrospinning solutions with concentrations of chitosan/PEO and acetic acid ranging from 2 to 6 wt% and 3 to 90 wt%, respectively; and the mixing ratios between chitosan and PEO range from 90/10 to 50/50 [19, 56]. The solutions can be prepared separately or not, and the mixing times usually range from 18 to 24 h. Moreover, polymer solution aging is a well-known phenomenon and chitosan/PEO solutions should be immediately electrospun after preparation. Pakravan *et al.* [55] have proved that highly concentrated acetic acid can help increase the electrospinability of chitosan by decreasing the solution surface tension, so, the surface tension decreases increasing the acetic acid concentration. Also, the increased acid concentration results in an increase in the electrical conductivity of the solution. Rosic *et al.* [57] have evaluated the properties of chitosan/PEO solutions mixed at different ratios (see Table 2.1). Results show that the increase of chitosan content leads to an increase in viscosity and conductivity, where the surface tension is not significantly affected [57].

Table 2.1 Solutions properties of chitosan/PEO (3 wt%) in different mixing ratios[57].

Chitosan/PEO ratio	Viscosity (mPas)	Surface tension (mN/m)	Conductivity (mS/cm)
100/0	725.7 ± 3.1	65.0 ± 1.2	5.1 ± 0.1
90/10	680.0 ± 12.8	61.3 ± 0.5	4.1 ± 0.1
80/20	622.7 ± 9.1	64.6 ± 0.5	3.7 ± 0.1
70/30	580.7 ± 9.0	63.4 ± 0.4	3.3 ± 0.1
60/40	544.7 ± 10.6	62.8 ± 0.9	3.0 ± 0.1
50/50	494.0 ± 10.6	63.0 ± 0.5	2.4 ± 0.1
40/60	435.3 ± 3.1	62.3 ± 0.6	2.0 ± 0.1
30/70	326.0 ± 6.6	61.4 ± 0.6	1.8 ± 0.1
20/80	295.0 ± 10.4	60.8 ± 0.8	1.6 ± 0.1
10/90	261.0 ± 7.0	61.4 ± 0.8	1.2 ± 0.1
0/100	155.7 ± 7.2	64.2 ± 0.6	0.1 ± 0.0

The viscosity of these materials shows a strong positive deviation from the additivity rule, which indicates strong interactions between PEO and chitosan chains with strong

hydrogen bonds between hydroxyl and amino groups on chitosan molecules and ether groups on PEO, according to Figure 2.8.

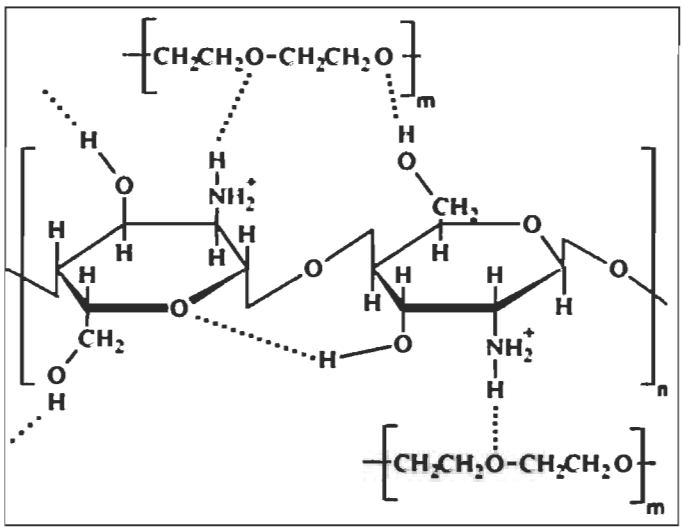

Figure 2.8 Proposed hydrogen bonding interactions between chitosan/PEO molecules [58].

The mixture between chitosan and PEO can produce nanofibers free of defects and with stable jet. According to Pakravan *et al.* [55], a higher volume of chitosan in the mixture will lead to the production of nanofibers with smaller diameters, however, it will also increase the chances of the formation of defects, such as beads. The temperature and humidity are also affecting the quality of the nanofibers produced. Higher temperatures and lower humidity tend to favor the formation of defect-free nanofibers [55]. Granja *et al.* [57] have demonstrated that parameters such as the distance between the collector and the tip of the syringe, flow rate and applied voltage generate differences in the final results of the chitosan/PEO nanofibers. Among these parameters, the applied voltages from 10 to 30 kV causes a greater impact, being that, higher voltages can reduce the diameter of the nanofibers. However, they can also increase the number of beads. Greater distances (10 – 30 cm) and lower flow rates (0.3-10 mL/h) tend to favor the evaporation of the solvent and the formation of nanofibers with smaller diameters [57].

2.6.4 Evaporation casting technology

Evaporation casting is based on the evaporation of a solvent from an initial solution and the subsequent formation of a polymeric film by precipitation. In this process, a polymer

is dissolved in a solvent and the resulting solution is poured into a previously selected cavity. The solvent then evaporates over a period of time in an inert or controlled atmosphere, inducing the polymer's precipitation and generating a film usually with a dense structure. In evaporation casting the films produced have an isotropic and less porous structure compared to dip casting, due to slower evaporation of the solvent. Many factors determine the porosity and pore size of cast films formed. If the evaporation step is prolonged, the average pore size will be larger. In general, by increasing the solvent content of the casting solution or decreasing the polymer concentration, the porosity will increase. Figure 2.9 clearly illustrates the formation of a film by deposition of a polymer solution on a support with subsequent evaporation of the solvent. This is a widespread and commonly used method. Lee *et al.* [60] developed a new model for the evaporation casting process for polymeric membrane formation that incorporates convective transport owing to density changes. Bucher *et al.* [61] showed a method to produce flat sheet membranes with thin isoporous block copolymer by profile roller coating on top a porous support membrane.

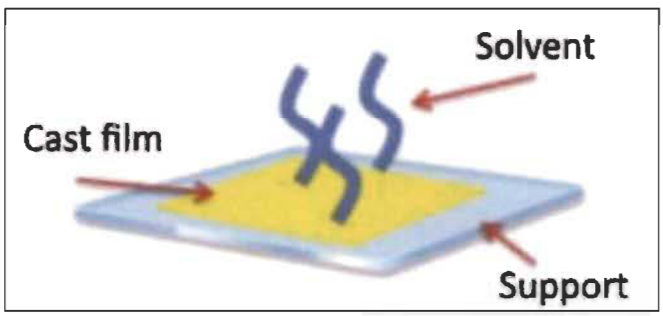

Figure 2.9 Illustration of a film formation by the evaporation casting process [59].

2.6.5 Conclusion

The literature review showed that the environmental pollution is increasing at a high rate and water pollution is a major concern. A total shortage of water could be a total disaster for humanity. Heavy metals dumped into these waters are toxic and harmful to human health and can cause serious illness when ingested. The current techniques for the removal of this type of contaminants are insufficient to remedy the problem. Thus, the development of techniques and materials that can help overcome this problem are essential and urgent. The use of biopolymer materials for the production of sorbent materials based on

electrospun nanofibers for the removal of heavy metals from aqueous solutions by the adsorption process is promising and relevant. The overall objective of the work, the materials and methods that will be employed bring a perspective of achieving excellent results. The insertion of phosphorylated nanocellulose in a chitosan matrix may increase the adsorption capacity of the current chitosan nonwoven mats produced by electrospinning technology. The characterizations that will be employed and the adsorption tests will indicate the potential of these new materials. As results, these low-cost materials will help to treat wastewater with high quality. The efficient removal of toxic heavy metals can prevent many diseases and reduce withdrawals of fresh water from natural reserves.

Chapitre 3 - Materials and Methods

3.1 Materials used for the production of sorbent media

Chitosan powder with 75-85% deacetylation (Sigma-Aldrich) with an average molecular weight of 50 000-190 000 Da was the adsorbent material used as the matrix of composites media. Acetic acid at 99.7% (Fischer Brand) was the solvent used to dissolve the chitosan.

Poly(ethylene oxide) powder (Sigma-Aldrich) with an average molecular weight of 900 000 Da was used as a polymer co-agent in order to decrease chitosan viscosity and increase the electrospinning ability to the nanofiber's generation. Distilled water was the solvent used to dissolve the Poly(ethylene oxide).

Sodium carbonate anhydrous (99% A.C.S, Fisher Chemical) Na_2CO_3 was used for the neutralization of nanofibers to improve their stability in aqueous media.

Cellulose Kraft fibers received a surface chemical treatment called esterification, which employs phosphate esters and urea. This treatment aimed at the insertion of the functional groups of phosphate on the cellulose surface. Then, phosphorylated nanocellulose and phosphorylated microcellulose were produced from phosphorylated CKF in our laboratory. All celluloses and derivatives were used as supplied.

3.2 Materials used for the adsorption

Cadmium (II) sulfate hydrate (A.C.S $\geq$ 98%, Sigma-Aldrich) is a chemical (metal ion) in crystalline form. Its chemical formula is $3CdSO_4.8H_2O$ and its molecular weight is 226.49 g/mol. This material was the basic cationic contaminant used in all stages of this work aiming to evaluate the adsorption of the produced membranes.

Copper (II) sulfate pentahydrate (A.C.S $\geq$ 99%, Sigma-Aldrich) is the pentahydrate of copper (+2) sulfate and a chemical (metal ion) bright blue solid in crystalline form. Its chemical formula is $CuSO_4.5H_2O$ and its molecular weight is 249.69 g/mol. This material was one of the cationic contaminants used in the last stage of this work in order to evaluate the adsorption in a multi-contaminant solution.

Lead (II) nitrate (A.C.S ≥ 99%, Sigma-Aldrich) is a white solid, which appears white in microcrystalline form. Its chemical formula is Pb $(NO_3)_2$ and its molecular weight is 303.26 g/mol. This material was one of the cationic contaminants used in the last stage of this work in order to evaluate the adsorption in a multi-contaminant solution.

Ammonium dichromate (A.C.S ≥ 98%, Sigma-Aldrich) is an inorganic compound with the formula $(NH_4)_2Cr_2O_7$ and molecular weight is 256.06 g/mol. In this compound, as in all chromates and dichromate, chromium is in a +6 oxidation state, commonly known as hexavalent chromium. It is a salt consisting of ammonium ions and dichromate ions. Hexavalent chromium Cr (VI) is the chromium in any chemical compound that contains the element in the +6 oxidation state. This material was the anionic contaminant used in the last phase of this work to evaluate the adsorption in a multi-contaminant solution.

3.3 Determination of heavy metal concentrations

In all cadmium ion analyses, the complexation titration method was used. Disodium ethylenediaminetetraacetic (EDTA) (A.C.S ≥ 98%, OMEGA Chemical Company) with chemical formula of $Na_2C_{10}H14N_2O_8.2H_2O$ and molecular weight of 372.24 g/mol was the compound used to determine residual cadmium ions concentration. Eriochrome Black was used as indicator for cadmium ion concentrations determination by complexometric titration procedure. A 1 mL micropipette was used to dose the solutions to be titrated. 5 mL of cadmium ion solutions were added to a 25 mL beaker. 1 mL of ammonia was added to facilitate the visualization of the titration end point. 0.01 g of Eriochrome Black T was added to the beaker as well. The titration was carried out with a 50 mL volumetric burette filled with a 0.001 M EDTA solution until the end point was achieved (change from light blue to strong blue). The volume of EDTA used was recorded and used in the calculation of the cadmium ion solution concentration.

Microwave Plasma-Atomic Emission Spectrometry (MP-AES) is a microwave-induced plasma interfaced to an atomic emission spectrophotometer (AES). It is used for the simultaneous determination of larger and smaller elements in multi-analysis and an Agilent 4210 MP-AES was the equipment employed to verify the traces of heavy metals ions concentrates in the multi-contaminant solutions.

3.4 Materials and methods

The methodology adopted as well as the material used for each stage of this project will be presented in detail in the scientific articles included in chapters 4 to 6.

Chapitre 4 - Article 1

4.1 A new electrospun chitosan/phosphorylated nanocellulose bio-sorbent for the removal of cadmium ions from aqueous solutions

4.2 Foreword

This first article is entitled "A new electrospun chitosan/phosphorylated nanocellulose bio-sorbent for the removal of cadmium ions from aqueous solutions". It has been published in Journal of Environmental Chemical Engineering, Vol. 7 (6), December 2019, 103477

Authors and their corresponding addresses are in the following order:

Ricardo Brandes, PhD student in Science and Engineering of Lignocellulosic Materials PhD program

Innovation Institute on Ecomaterials, Ecoproducts and Ecoenergies based on Biomass (I^2E^3), Université du Québec à Trois-Rivières, 3351 boulevard des Forges, Trois-Rivières, Quebec, G9A 5H7, Canada

Dan Belosinschi, PhD.

Researcher

Innofibre, Cégep de Trois-Rivières, 3351 boulevard des Forges, Trois-Rivières, Quebec, G9A 5H7, Canada

François Brouillette, PhD.

Thesis co-supervisor

Innovation Institute on Ecomaterials, Ecoproducts and Ecoenergies based on Biomass (I^2E^3), Université du Québec à Trois-Rivières, 3351 boulevard des Forges, Trois-Rivières, Quebec, G9A 5H7, Canada

Bruno Chabot, PhD.

Thesis supervisor

Innovation Institute on Ecomaterials, Ecoproducts and Ecoenergies based on Biomass (I^2E^3), Université du Québec à Trois-Rivières, 3351 boulevard des Forges, Trois-Rivières, Quebec, G9A 5H7, Canada

Authors contributions: Ricardo Brands is the main author of the article. He did all the experimental work, laboratory setup developments and wrote the manuscript. Dr. Dan Belosinschi provided the phosphorylated nanocellulose. Dr. Brouillette is the thesis co-supervisor and provided materials and laboratory facilities and he helped with manuscript corrections. Dr. Chabot is the thesis supervisor and provided materials and laboratory facilities. He provided guidance and helped in the preparation and correction of the manuscript.

4.3 Résumé

L'élimination des ions Cd (II) de la solution aqueuse a été réalisée à l'aide d'un nouveau sorbant nanofibreux, fabriqué à partir de chitosane (CS) et de nanocellulose phosphorylée (PNC). Le matériau sorbant a été caractérisé à l'aide de MEB, EDX, AFM et FTIR. La capacité de sorption a atteint 62,3 mg/g à un pH de 5,5 et à 25°C. L'adsorption du Cd (II) s'est produite rapidement et a atteint l'équilibre en 120 minutes. Le modèle cinétique d'ordre pseudo-seconde a le mieux adapté les données expérimentales. L'isotherme de sorption a également été le mieux décrit par le modèle de Langmuir. La capacité d'adsorption maximale de Langmuir était de 232,55 mg/g à 25°C, et augmentait avec la température, ce qui peut s'expliquer par la forte affinité des groupes amine et phosphate avec le cadmium à la surface des mats nanofibreux. L'étude thermodynamique a montré que l'adsorption est une réaction endothermique spontanée. Ces travaux ont confirmé qu'un tapis nanofibreux électrofilé à base de CS et de PNC peut être utilisé comme matériel de remplacement pour l'élimination des ions de cadmium, contribuant ainsi à la durabilité de l'approvisionnement en eau potable.

Mots-clés: L'eau potable, Métaux lourds, Adsorption, Chitosane, Nanocellulose phosphorylée, Nanofibres électrofilées.

4.4 Abstract

The removal of Cd (II) ions from aqueous solution was carried out using a new nanofibrous electrospun nonwoven sorbent made from Chitosan (CS) and Phosphorylated Nanocellulose (PNC). The sorbent material was characterized using SEM, EDX, AFM and FTIR. The sorption capacity reached 62.3 mg/g at pH 5.5 and 25°C. The Cd (II) adsorption occurred rapidly and achieved equilibrium within 120 minutes. The pseudo-second order kinetic model best fitted experimental data. The sorption isotherm was also best described by the Langmuir model. The maximum adsorption capacity of Langmuir was 232.55 mg/g at 25°C, and increased with temperature, which can be explained by the high affinity of amine and phosphate groups with cadmium on the surface of the nanofibrous mats. The thermodynamic study showed that the adsorption is a spontaneous endothermic reaction. This work confirmed that an electrospun nanofibrous mats based on CS and PNC can be used as an alternative material for the removal of cadmium ions, contributing to water sustainability.

Keywords: Water sustainability, Heavy metals, Adsorption, Chitosan, Phosphorylated Nanocellulose, Electrospun nanofibers.

4.5 Introduction

Water is an essential natural resource for life on earth. Fresh water accounts for less than 2.5% of the total amount of water available. Moreover, only 10% of the total fresh water is readily accessible. It is thus a finite resource that must be used in a sustainable way to avoid its exhaustion [62, 63]. However, the ever-growing demand of water in agricultural, industrial and domestic sectors lead to generation of large volume of wastewaters containing various contaminants among which agricultural chemicals, detergents, pharmaceuticals derivatives, and heavy metals. Heavy metals contamination of aquatic freshwater ecosystems is of particular concerns. They are introduced into freshwater systems as a result of the weathering of soils and rocks, from volcanic eruptions, and from

human industrial activities such as mining, metal plating, pharmaceutical, leather, paint, automobiles, chemical, cosmetic, printing, paper, polymer, etc. The most common heavy metal pollutants are arsenic, cadmium, chromium, copper, nickel, lead and mercury. The release of untreated metal contaminated effluent directly into water systems, and especially groundwater aquifers can have a large environmental, public health, and economic impact. Heavy metals are not biodegradable and tend to accumulate in living organisms [3, 5]. At high concentrations, they can lead to poisoning [6]. Consumption of water contaminated with those metals can result to serious health problems, such as cancer, lower energy levels, damage to blood composition, organ damage (lungs, kidneys, liver and others organs), nervous system damage, and in extreme cases, death [64, 65]. Cadmium is mainly produced during zinc refining as a by-product since those metals occur naturally within the raw ore mineral. Cadmium can cause extensive environmental contamination and health problems. It has a long half-life and bio accumulates in plants, invertebrates, and vertebrates. Humans may get exposed to cadmium primarily by inhalation and ingestion and can suffer from acute and chronic intoxications. A maximum acceptable concentration of 0.005 mg/L cadmium in drinking water has been established on the basis of health considerations. Also, FAO/WHO expert committee has estimated a provisional tolerable weekly intake of cadmium for an adult to be from 0.4 to 0.5 mg. Workers within the electroplating, battery production, and pigment industries are at the highest risk for exposure to cadmium. It is typically used in rechargeable batteries and special alloys and can also be found in tobacco smoke. About three-fourths of cadmium is used in alkaline batteries as an electrode component, the remaining part is used in coatings, pigments, plating and as a plastic stabilizer [66, 67].

To meet water sustainability standards, industries have the opportunity to implement or increase water recycling on site. This approach is one of the primary means of saving fresh water. However, as the recycle ratio is increased, the quality of recycled water is reduced with potentially detrimental effects on process operations as well as on product quality. Therefore, recycled water must be properly treated prior to recirculation within the process. Remediation approaches such as chemical precipitation, electrodialysis, membrane separation processes and solvent extraction are available but they present economic and technical limitations. They are also expensive and energy intensive.

Therefore, there is a demand for cheaper and more efficient techniques for the removal of heavy metals from wastewaters [12]. Tertiary wastewater treatment technologies including advanced oxidation processes, membrane filtration, and adsorption have been extensively studied [10]. Among them, adsorption is known as an economic and effective method for removal of metals. It has many interesting features such as the availability of adsorbent materials and the reversibility and flexibility in design and operation [6]. Since adsorption is a surface process, sorbent materials need high surface area and large amounts of active reaction sites that are able to interact with solutes in the adjacent aqueous phase. The chemical nature and polarity of the surface can affect the attractive forces between the adsorbent and adsorbate. A huge number of commercial adsorbents are available on the market. They can be found under various forms including powders, granules, molecular sieves, and polymeric beads. Activated carbon (AC) is the most widely used adsorbent materials. However, the rapid reduction of world reserves of coal-based AC has led to a rise in the price of this material [68]. AC can be obtained from other technologies among which biomass pyrolysis, but technical issues still need to be resolved [69]. Most of these commercial sorbents are used in fixed-bed absorbers. This system configuration is efficient, but may develop large pressure drops through the packed bed depending on adsorbent's particle size used, the smaller particles, and the higher pressure drop. Mass transfer or diffusion of contaminants into the porous bed structures is also an issue which is affecting adsorption. Electrospun nanofibrous nonwoven mat is an alternative for packed bed applications due to their high porosities and interconnected pore structures which provide a higher permeability to water and lower pressure drops. Nanofibers have high specific surface area due to their small diameters. They can also be tailor-made to adsorb specific contaminants by selecting suitable polymers or adjusting polymers ratio prior to electrospinning [70].

The search for a low-cost and abundant alternative to AC has become a research topic of growing interest [5]. Biomass-based materials are a promising replacement for AC. Polysaccharides, such as CS and cellulose, have attracted attention due to their high availability and low cost. CS is well known for its ability to remove heavy metals. It has a strong chelation potential due to the presence of free functional groups (amine and hydroxyl) on its surface [12, 71, 72]. Cellulose is not a high-performance material for the

adsorption of metals, but it can be chemically modified to increase its rate and capacity of adsorption. Phosphorylation, which adds phosphate groups to cellulose, is one of the most interesting surface modification reactions that can be used for this application. In recent works, phosphorylated cellulose and derivatives have been evaluated regarding heavy metals adsorption and the results proved the high adsorption capacity these materials [13, 43, 45, 73]. CS and PNC need to be combined into a suitable material that can be easily handled.

In this work, electrospinning was used to produce membranes composed of nanofibers with large surface area and high adsorption capacity [14]. Electrospinning is a modern and versatile process that allows the utilization of a wide range of starting materials, as well as a good control of the physical properties of the membranes. At the present time, there are no published works related to the production of electrospun nanocomposite membranes based on a CS matrix and PNC for the removal of heavy metals by adsorption. In consequence, the objective of this work is to introduce PNC in a CS matrix in order to increase the metal ion adsorption capacity of CS through the production of nanocomposite membranes by electrospinning. The combination of simple manufacturing technologies with the use of the two most abundant biopolymers on the planet would lead to a highly sustainable wastewater treatment process.

4.6 Materials and Methods

4.6.1 Materials

Chitosan of low molecular weight (75-85% deacetylated, 50 000-190 000 Da, Sigma-Aldrich) and glacial acetic acid (99.7%, Fisher Scientific) were used to prepare chitosan solutions. Poly (ethylene oxide) (PEO) (average molecular weight ~900 000 Da, Sigma-Aldrich) was used as a polymer co-agent to decrease chitosan viscosity and increase its electrospinning ability. PEO solutions were prepared with distilled water. Sodium carbonate (Na_2CO_3, A.C.S, Fisher Scientific) was used for the mat neutralization treatment. Phosphorylated nanocellulose (PNC, 2 wt%) was produced from a bleached softwood Kraft fibers (KF) provided by a local paper mill (Trois-Rivières, Canada),

according to the procedure described by Noguchi *et al.* [46]. Cadmium sulfate ($CdSO_4$, Fisher Scientific) was used as the model contaminant for adsorption studies.

4.6.2 CS/PEO solution preparation

CS (3 wt%) was prepared with 90% acetic acid/10% distilled water (v/v). PEO solution (3 wt%) was prepared with distilled water. Both solutions were prepared at room temperature and properly mixed using a magnetic stirrer for 24h until complete dissolution. Then, CS and PEO solutions were mixed at a 60/40 mass ratio with a magnetic stirred at room temperature for 24h, until homogeneous solutions were obtained. The final solution was sonicated in a Branson 2800 ultrasonic bath for 15 min and left to rest for 3h before electrospinning. An overview of the preparation procedure for the CS/PEO solutions is shown in Figure 4.1.

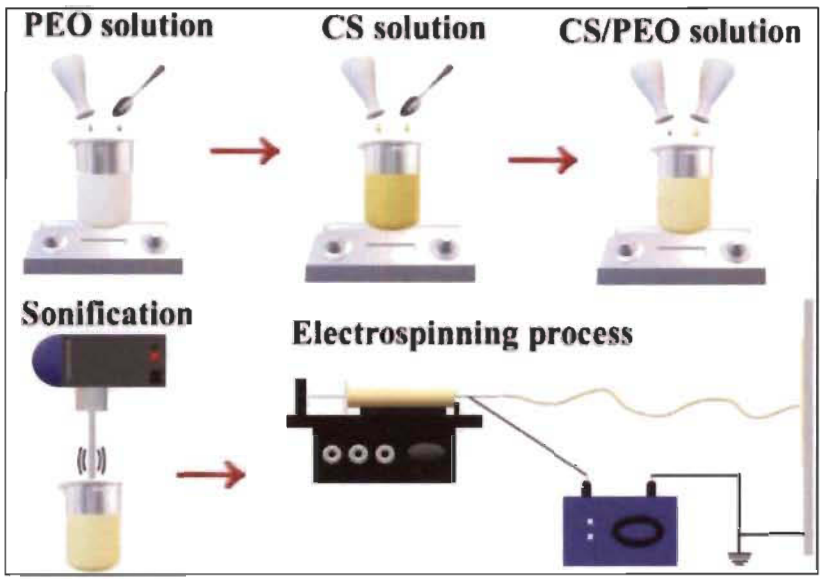

Figure 4.1 Procedure for the preparation of CS/PEO electrospinning solution.

4.6.3 CS/PEO/PNC dispersion preparation

The PNC dispersion and 90% acetic acid/10% distilled water (v/v) were dispersed in a beaker using a Silverson L4RT-A laboratory high shear mixer at 7000 rpm during 10 min. CS powder was added to the previously prepared PNC/acetic acid dispersion and kept under mixing with a magnetic stirrer for 24h to complete dissolution. At the same time, PEO powder and distilled water were combined in a beaker and mixed with a magnetic

stirrer for 24h to prepare a PEO solution. Finally, the CS/PEO/PNC dispersion solution was blended with a magnetic stirrer at a 54/36/10 mass ratio for a total weight of 30 g and stirred at room temperature for 24h, until homogeneous dispersion. The final dispersion was sonicated in the Branson 2800 ultrasonic bath for 15 min and rested for 3h before electrospinning. An overview of the preparation procedure for the CS/PEO/PNC dispersion is shown in Figure 4.2.

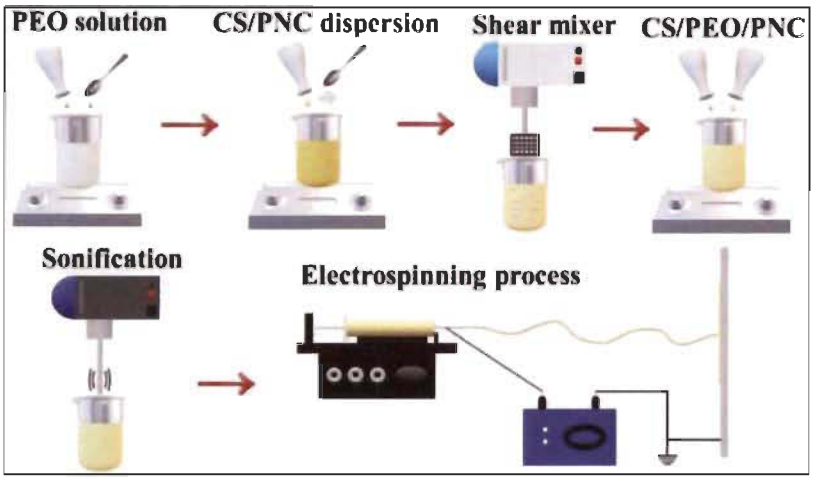

Figure 4.2 Procedure for the preparation of CS/PEO/PNC electrospinning solution.

4.6.4 Characterization of the electrospinning dispersions

The dispersion of PNC particles in the electrospinning polymer solution was determined by flow birefringence. The experimental setup for this test consists in a light source, a magnetic stirrer, and two cross-polarized filters. The solutions were positioned between the two filters under stirring and the flow birefringence was captured using a digital camera. The flow birefringence of the PNC particles (0.1 wt%) dispersed in distilled water was used for the comparison of the dispersions according to Naseri *et al.* [31].

The electrical conductivity of the dispersions was measured using a Mettler-Toledo Seven Multi Dual pH/conductivity meter with an InLab 731conductivity probe. All samples were measured three times at room temperature and average values were reported.

A particle charge analyzer was used to determine the surface charges of dispersions. Poly (vinyl sulfate) potassium salt (PVSK, negatively charged, 0.1000N, Mütek) was the

polyelectrolyte used for the titrations. An amount of 0.15 g of each sample was mixed with 100 mL of distilled water and dissolved for 30 min with a magnetic stirrer. A volume of 10 mL of each previously prepared solution was titrated with the negatively charged polyelectrolyte to neutralize the cationic charge. This titration was performed on a Mütek PCD 03 particle charge detector combined with a PCD T3 automatic titrator that uses the streaming potential technique to detect the titration end-point. The surface charge density was calculated according to the amount of PVSK adsorbed to the weight of the sample [70].

The viscosity of electrospinning polymer solution was measured using a Brookfield Synchro-Lectric Viscometer model LVT (D.W. Brookfield Ltd.) at a rotation frequency of 60 rpm, needle #4 and a factor of 100. The measurements were made at a depth of 7 cm in a 250 mL glass beaker. The viscosity values were reported as the average of five measurements.

4.6.5 Preparation of nonwoven nanofibrous mats

Nanofibrous mats were produced by electrospinning. For that, a 5-mL plastic syringe equipped with a 20-gauge stainless steel needle (Kimble Chase) was filled with CS/PEO or CS/PEO/PNC solutions. The polymer solutions were fed by a programmable micro-syringe pump (KD Scientific, model 100). The flow rate, the applied voltage and the tip to collector distance were adjusted to obtain defect free nanofibers nonwoven mats. A high voltage DC generator (Gamma High Voltage Research, USA) was used to provide a high voltage between the tip of the needle and the collector. An aluminum foil was used to collect electrospun nanofibers. These parameters were selected based on a literature review and preliminary tests. All tests were performed at room temperature. The solution's parameters, as well as the optimized processing parameters, are summarized in Table 4.1.

Table 4.1 Electrospinning and solution's parameters.

Sample	CS/PEO (wt%)	PNC (wt%)	Acetic acid (%)	Final conc. (wt%)	Applied voltage (kV)	Distance (mm)	Flow rate (mL/h)
CS/PEO	60/40	0	90	3.00	21	240	0.6
CS/PEO/PNC	54/36	10	90	2.85	19	220	0.5

The electrospun nanofibrous mats were detached from the aluminum foil at the end of the electrospinning process. They were dried in a vacuum oven at 70°C overnight. Then, they were immersed in a sodium carbonate solution (0.1 M) for 1h and washed with distilled water until a neutral pH was obtained. Finally, they were kept at room temperature during 24h.

4.6.6 Nanofibrous mats characterization

A Zeiss Axio Scope A1 FL-LED equipped with an AxioCam ERC 5 optical microscope (OM) was used to visualize electrospun mats and solutions surfaces. Each sample was analyzed at five different locations.

Scanning electron microscopy (SEM) and Energy Dispersive X-ray Spectroscopy (EDX) were used to investigate the surface morphology and chemical composition of the mats. The samples were inserted in an aluminum stub and fixed on a carbon double-sided tape. Samples were covered with a 30 nm gold layer. SEM/EDX analyzes were performed with a HITACHI SU 1510 microscope at 15 kV giving a magnification up to 15 000x and an Aztec X-MAX 20 EDX microanalysis system (Oxford Instruments). The mean diameter of the nanofibers was determined from approximately 100 measurements using the Image-J software (National Institutes of Health).

Atomic Force Microscopy (AFM) (Asylum Research 3D Stand Alone) equipped with a silicon AFM probe (Tap 300 Al-G), resonant frequency of 300 kHz and force constant of 40N/m was used in tapping modes in order to analyze the morphology of nanofibers. For AFM analysis, 2g of electrospun nanofibrous mats for each sample were dried under vacuum at ambient temperature on a glass slide.

The presence of typical functional groups on the nanofibrous materials was determined by Fourier Transform Infrared Spectroscopy (FTIR) analyzes. A Spectrum ATR-FTIR 2000 Spectrometer (PerkinElmer) was used to acquire spectra in the 400-4000 cm^{-1} range at a resolution of 4 cm^{-1} and averaged over 30 scans.

4.6.7 Adsorption tests

Batch adsorption tests were carried out to investigate the adsorption of cadmium ions by nanofibrous mats. For kinetic experiments, a 30 mg mass (m) of materials and a 60 mL volume (V) of a 100 ppm Cd^{2+} (C_0) solution were added in a 250 mL Erlenmeyer flask. The flasks were agitated using an orbital shaker (Lab-line Instrument) at room temperature, pH 5.5, and 200 rpm. Agitation was provided until the equilibrium concentration (C_e) was reached. The amount of adsorbed metal ions, q (mg/g), was calculated using Equation 4.1 at various contact times (10-300 min.). The residual cadmium concentrations were determined by EDTA titration according to the procedures described by Prasad and Raheem [74].

$$q = \frac{(C_0 - C_e)V}{m} \qquad \text{Eq. 4.1}$$

Kinetic models were used to determine the dominant mechanism involved in the adsorption process of cadmium ions on electrospun mats: physical adsorption (pseudo-first order model, non-linear form, Equation 4.2 or chemical adsorption (pseudo-second-order model, non-linear form, Equation 4.3.

$$q_t = q_e(1 - \exp^{(-k_1 t)}) \qquad \text{Eq. 4.2}$$

$$q_t = \frac{(k_2 q_e^2 t)}{(1 + (k_2 q_e t))} \qquad \text{Eq. 4.3}$$

Where:

q_e = Amount of adsorbed metal ions at equilibrium (mg/g);

q_1 = Amount of metal adsorbed at time t (mg/g);

t = Reaction time (min);

k_1 = First-order equilibrium constant (min^{-1});

k_2 = Second-order equilibrium constant (g $(mgmin)^{-1}$).

The initial adsorption rate h (mg ($gmin^{-1}$)) can be determined with k_2 and q_e values of the pseudo-second order model, Equation 4.4:

$$h = k_2 q_e^2 \qquad \text{Eq. 4.4}$$

The Weber and Morris model was also used to evaluate the influence of intra-particle diffusion on the adsorption of cadmium ions. The removal of adsorbate varies with the square root of time when intra-particle diffusion is the velocity determinant. The intra-particle diffusion coefficient (K_d) can be obtained from Equation 4.5:

$$q_t = K_d t^{1/2} + C \qquad \text{Eq. 4.5}$$

Where:

C = Constant related to diffusion resistance (mg/g);

K_d = Intra-particle diffusion coefficient ($mgg^{-1}min^{-1/2}$).

The constant C gives an idea of the thickness of the boundary layer: the larger the value of C, the greater the effect of the boundary layer.

For equilibrium experiments, the same procedure as kinetics tests was performed, but using varying Cd^{2+} concentrations C_0 (50-300 ppm) at 25°C. The contact time used in the isotherms was 4 h. The linearized Langmuir (Equation 4.6) and Freundlich (Equation 4.7) isotherm models were applied to the results.

$$\frac{C_e}{q_e} = \left(\frac{1}{K_L q_m} + \frac{C_e}{q_m} \right) \qquad \text{Eq. 4.6}$$

$$\ln q_e = \ln K_f + \left(\frac{1}{n} \right) \ln C_e \qquad \text{Eq. 4.7}$$

Where:

q_m = Maximum adsorbent capacity (mg/g);

K_L = Effective dissociation constant (L/mg).

K_f = Freundlich constant [(mg/g) (mg/L)$^{1/n}$];

n = Constant related to system heterogeneity.

The Dubinin-Radushkevich (D-R) model was also applied to the adsorption data. It was originally developed for adsorption processes based on pore filling. The average adsorption energy value (E) of the D-R model provides valuable information on the nature of the adsorption and is used to differentiate the adsorption of metals as physical or chemical. The linearized form of the D-R model is given by Equation 4.8:

$$\ln q_e = \ln q_m - \beta\varepsilon^2 \qquad \text{Eq. 4.8}$$

Where ε is the Polanyi potential (Equation 4.9) and β is the activity coefficient (a constant) associated to the adsorption energy E (kJ/mol) through Equation (4.10):

$$\varepsilon = RTln(1+\frac{1}{C_e}) \qquad \text{Eq. 4.9}$$

$$E = \frac{1}{\sqrt{2\beta}} \qquad \text{Eq. 4.10}$$

Thermodynamic parameters can be found through the application of Equations (4.11) and (4.12). Enthalpy change (ΔH^0), and entropy change (ΔS^0) were obtained respectively, from the slope and the intercept of van't Hoff plot according to Equation 4.11. R is the universal gas constant (8.314 J/mol K^{-1}) and T is the absolute temperature (K). Gibbs free energies (ΔG^0) were determined by Equation 4.12.

$$ln[q_{eq} / C_{eq}] = \frac{\Delta S^0}{R} - \frac{\Delta H^0}{RT} \qquad \text{Eq. 4.11}$$

$$\Delta G^0 = \Delta H^0 - T\Delta S^0 \qquad \text{Eq. 4.12}$$

4.7 Results and discussion

4.7.1 Characterization of the electrospinning dispersions

Figure 4.3 shows the flow birefringence and optical microscopy images for the PNC dispersion, CS/PEO and CS/PEO/PNC electrospinning solutions. Figure 4.3 a shows a strong birefringence pattern for the PNC dispersion due to the presence of highly negatively charged phosphate groups, which can form liquid crystalline phases and stable colloidal system [31, 75-77]. The birefringence pattern for CS/PEO (Figure 4.3 (b) and CS/PEO/PNC (Figure 4.3 (c)) solutions are similar to the PNC dispersion, demonstrating the non-aggregation and well-dispersed state of these electrospinning solutions. The background optical microscope images in Figure 4.3 show, for each sample, no significant particle agglomeration. Figure 4.3 (a) shows no visible agglomeration, confirming a successful dispersion. Figure 4.3 (b) shows good dispersion and chemical compatibility between CS and PEO. Figure 4.3 (c) exhibits aggregates attributed to the interaction between the functional groups present in CS and PNC. Electrospinning solutions with PNC weight concentration higher than 10% present a very high level of coagulation and agglomeration.

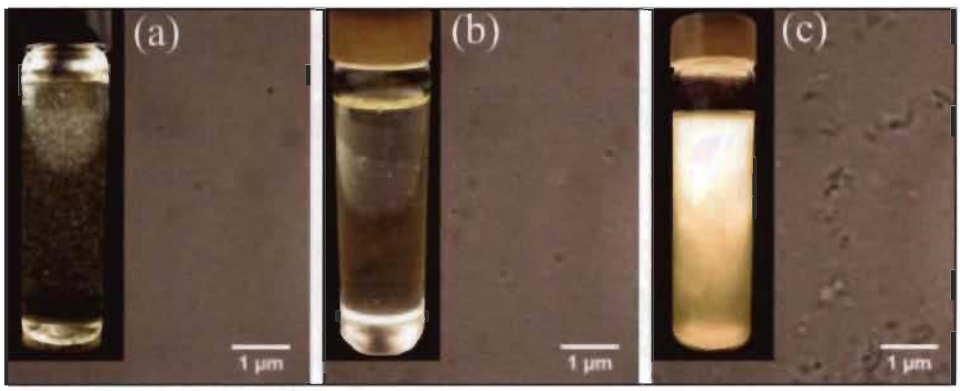

Figure 4.3 Flow birefringence and optical microscopy images (background) of PNC dispersion (a), CS/PEO electrospinning solution (b) and CS/PEO/PNC electrospinning solution (c).

Table 4.2 shows the electrical conductivity of the electrospinning solutions. Greater conductivities facilitate the formation of nanofibers and decrease the nanofiber diameter [50, 78]. The conductivity increased because PNC is based on a phosphorus salt. In water dispersions, PNC is negatively charged while CS is positively charged. Negatively

charged polyelectrolytes such as PVSK interact with positive charges and can be used for quantitative analyzes. Table 4.2 shows the total charge density for CS/PEO and CS/PEO/PNC electrospinning solutions. The anionic charge demand gives an indication of the effect of the addition of PNC to CS/PEO solutions. The total charge for the CS/PEO solution is higher than CS/PEO/PNC solution due to the presence of negative charges provided by phosphate groups present in PNC structure.

According to the viscosity data (Table 4.2), the CS/PEO solution showed the highest viscosity and the addition of 10 wt% of PNC significantly decreased the viscosity. The reduction in weight of highly viscous chitosan in the solution and the addition of the low viscosity PNC suspension to the electrospinning solution can be the cause of the viscosity reduction, being in agreement with Naseri *et al.* [79]. These results show the effect of PNC addition on the CS/PEO matrix.

Table 4.2 Electrical conductivity and particle charge demand for electrospinning solutions.

Sample	Electrical conductivity (mS/cm)	Total charge (meq/g)	Viscosity (mPas)
CS/PEO	2.30 ±0.02	- 4.33 ±0.05	3600
CS/PEO/PNC	2.74 ±0.04	- 3.22 ±0.04	2300

4.7.2 Electrospun nanofibrous mats production and characterization

The electrospinning process parameters (solution concentration, voltage, relative humidity, distance, flow rate) have been adjusted to obtain defect free nanofibers. Lower polymer concentrations produced nanofibers with smaller diameters, but increased the formation of defects such as beads or even prevented the generation of nanofibers. Higher polymer concentrations promoted more continuous and homogeneous defect free nanofibers. However, very high concentrations increased the mean diameter of the nanofibers and, at a certain point, prevented the formation of a jet.

The increase in voltage generated nanofibers with smaller diameters. However, high voltages can cause beads [14, 78]. Voltages lower than 15 kV did not exhibit a continuous jet formation, alternating between the formation of droplets at the tip of the needle and a continuous jet. Voltages ranging from 19 to 21 kV formed stable and continuous jets for

CS/PEO and CS/PEO/PNC solutions, respectively. Finally, at higher voltages, spreading or dividing of the jet beam occurred.

Relative humidity (RH) is a parameter that greatly influences the production of nanofibers. Electrospinning at around 20% RH gave the best results. However, electrospinning at RH higher than 50% gave erratic results with the production of a high amount of beads and reduced diameters [80, 81].

The needle tip to collector surface distance can be adjusted to control solvent evaporation. Distances of 24 and 22 cm were used for CS/PEO and CS/PEO/PNC solutions, respectively. Larger distances tend to increase solvent evaporation but an increase in voltage was required [50].

The polymer solutions flow rate influenced nanofiber diameter, porosity, and geometry. An increase in diameter and pore size of electrospun nanofibers can be associated with an increased flow rate [82]. In this case, the flow rates selected were 0.6 and 0.5 mL/h for CS/PEO and CS/PEO/PNC, respectively.

The electrospinning device produced nanofiber mats on the aluminum foil during 3h for both compositions. Figure 4.4 (a) and Figure 4.4 (b) show the optical microscope images of the nanofibers after 1 min electrospinning under the optimized processing parameters, which were presented previously in Table 4.1. Nanofibers are randomly oriented, homogeneous and continuous with no evidence of typical defects such as beads and flat fibers. Figure 4.4 (c) and Figure 4.4 (d) show electrospun mat samples after the neutralization treatment for CS/PEO and CS/PEO/PNC, respectively. Stable random mats of CS/PEO and CS/PEO/PNC were obtained after electrospinning for about 60 min. After neutralization and drying, the nanofibrous mats were weighted and the average dry mass measured was of 40±3 mg. No macroscopic defects were visible. The nanofiber deposition process on the aluminum foil was quite stable during the production of the membranes. Both samples are visually homogeneous and weight on average 50 mg after the neutralization treatment.

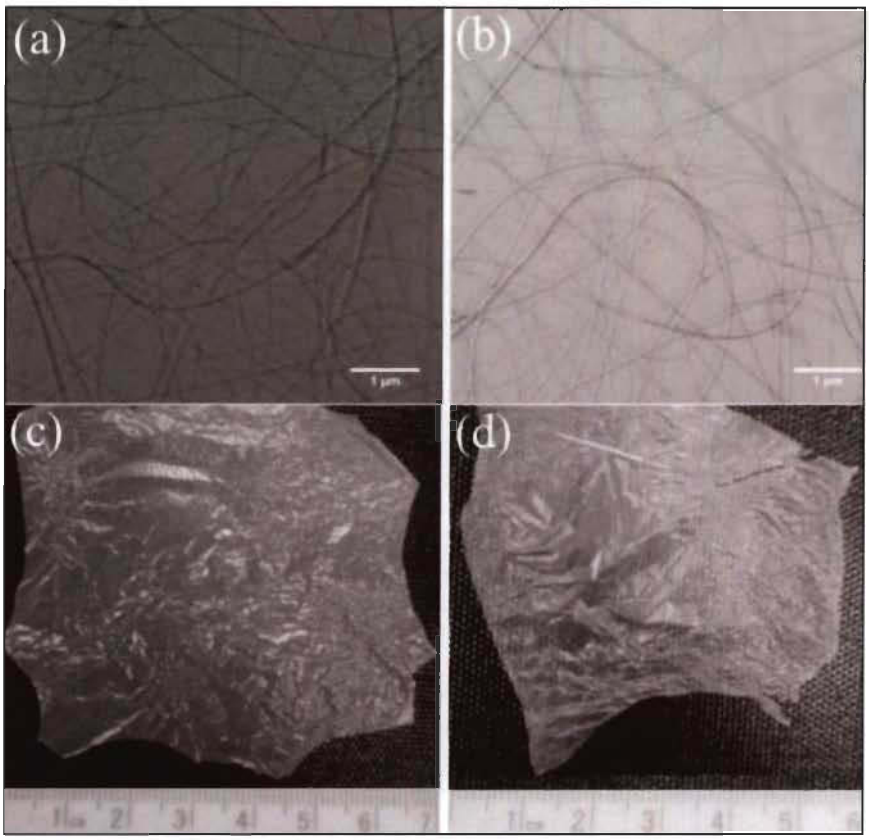

Figure 4.4 Optical microscopy images of electrospun nanofiber mats: (a) CS/PEO and (b) CS/PEO/PNC nanofibers. The visual appearance of electrospun nonwoven mats: (c) CS/PEO and (d) CS/PEO/PNC.

Figure 4.5 (a) and (b) show SEM images of CS/PEO and CS/PEO/PNC electrospun nanofibers with their respective average diameter. Figure 4.5 (c) and (d) show the AFM images of the same samples. Figure 4.5 (a) and (b) show randomly oriented nanofibers with a porous structure for both samples, which is consistent with the information obtained by optical microscopy. For CS/PEO (Figure 4.5 (a)) and CS/PEO/PNC (Figure 4.5 (b)) mats, the compatibility of the constituent materials resulted in the formation of uniform nanofibers, confirming the successful production of defect-free mats [45, 68, 79].

Nanofiber mean diameters were measured using the ImageJ software. The mean diameter was 255±6 nm for CS/PEO nanofibers and 217±5 nm for CS/PEO/PNC nanofibers. This is attributed to a decrease of the viscosity of the solutions with the incorporation of cellulose nanocrystals into the polymeric solutions prior to electrospinning. This results

in the stretching of the nanofibers and a reduction of average nanofiber diameters [31, 79]. Changes in process and solution parameters also impact the nanofiber diameter.

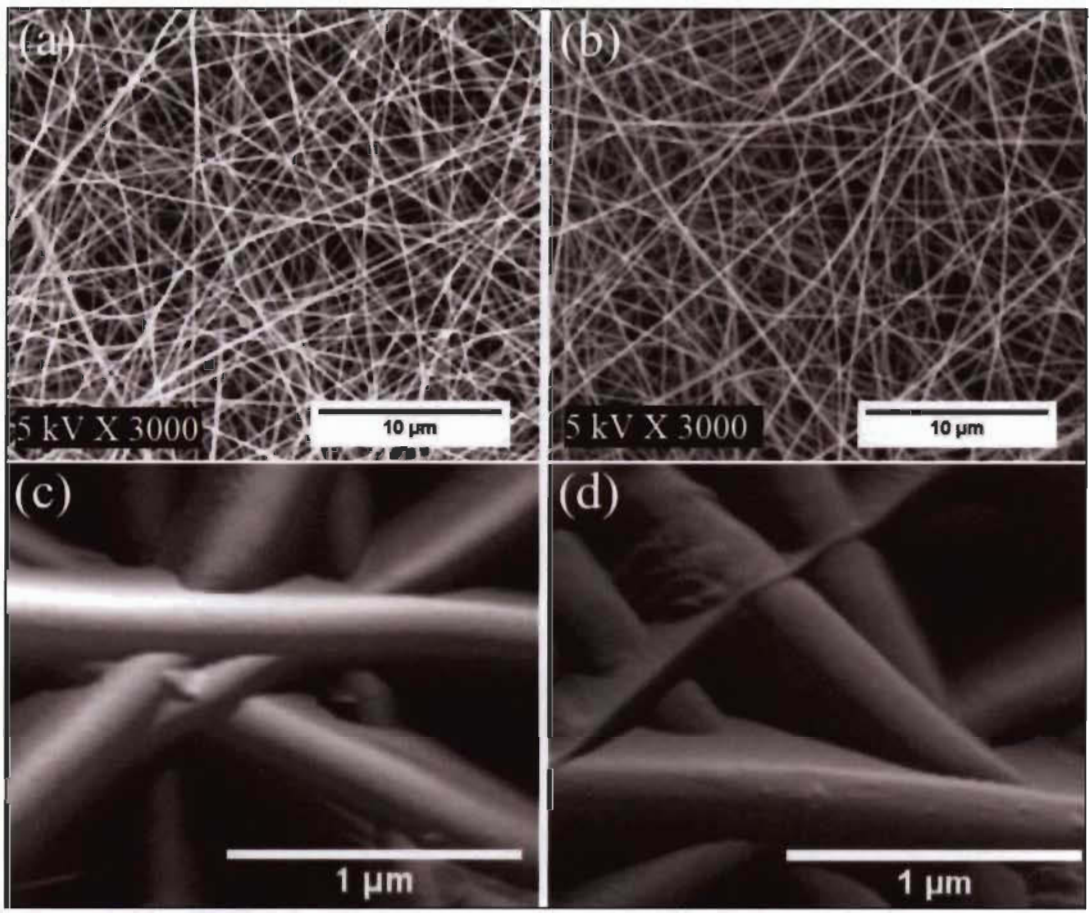

Figure 4.5 SEM images of the electrospun nanofibers (a and b) and AFM images of the surface of nanofibers (c and d).

The electrospun nanofibers were observed under AFM to evaluate the nanostructured surface morphology and the effect of PNC addition in more details. Fig. 4.5c and Figure 4.5d show single-phase structures indicating a homogeneous production of nanofibers with good dispersion of the materials [31].

The EDX analyses of the samples were also evaluated and the spectra are presented in Figure 4.6. CS/PEO nanofiber surface showed the predominance of carbon and oxygen, where an aluminum peak was present being an artefact of the aluminum foil used in the electrospinning device. The presence of PNC in the CS/PEO/PNC nanofiber mats was

confirmed by the phosphorous peaks attributed to phosphate groups. The presence of sodium peak can be attributed to the neutralization treatment with sodium carbonate.

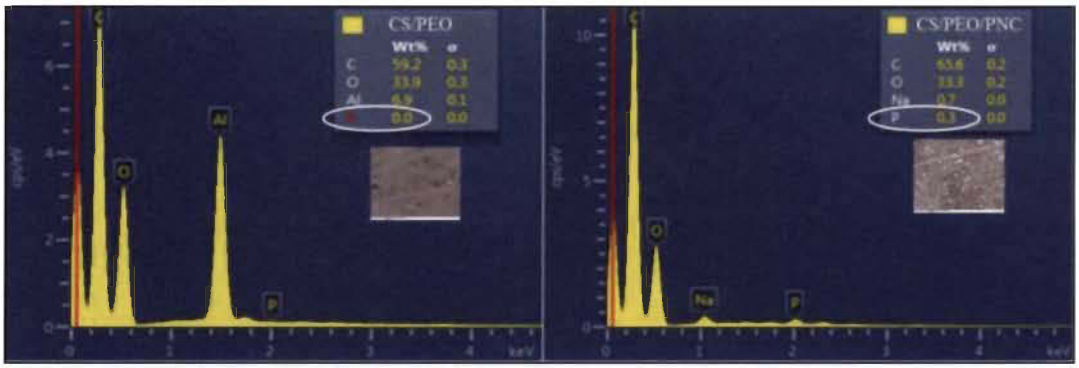

Figure 4.6 EDX spectra of CS/PEO and CS/PEO/PNC nanofiber mats.

Figure 4.7 shows FTIR spectra for CS/PEO and CS/PEO/PNC nanofibers.

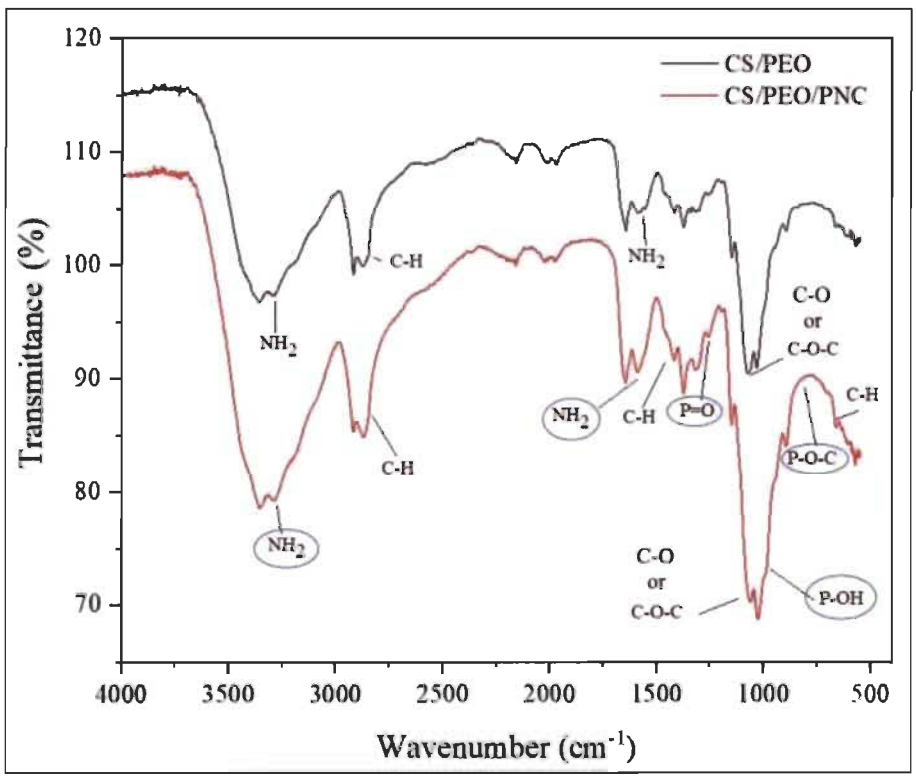

Figure 4.7 ATR-FTIR spectra of CS/PEO and CS/PEO/PNC electrospun nanofibers.

The absorption peak observed at ~1112 cm^{-1} is typical of the vibration stretching of the ether C-O-C group or assigned to C-O group in Chitosan and C-H bending in ~2781 cm^{-1} from PEO. In the amine (NH_2) stretching region, the peaks observed at ~1555 and ~3300

cm^{-1} are attributed to the amine bands and C-H vibration in ~710 cm^{-1} from CS [81, 82]. These groups are present in the CS/PEO spectrum. The presence of peaks between 920 and 1000 cm^{-1} is attributed to the P-OH stretching vibration mode of the phosphate group, a band at ~1240 cm^{-1} corresponding to the P=O stretching mode and P–O–C at 819 cm^{-1} corresponding to phosphate groups [43]. Intensities of the crystalline-sensitive peaks at 2900 cm^{-1} (C-H) and bending at 1430 cm^{-1} (CH_2) were greatly increased in the CS/PEO/PNC spectrum and are attributed to PNC [44, 55]. Differences between both spectra may be attributed to the interaction between CS/PEO and PNC which is proving the presence of PNC phosphorous groups.

4.7.3 Adsorption kinetics

Figure 4.8 shows the evolution of cadmium ions adsorption with time for CS/PEO and CS/PEO/PNC electrospun nanofibers. Electrospun nanofibers have a high adsorption potential toward cadmium ions. The removal capacity of cadmium increases gradually with time until reaching a maximum value corresponding to the equilibrium time after approximately 3h. Under experimental conditions used, adsorptions at the equilibrium time were 58.2 mg/g for the CS/PEO nanofiber mats and 62.3 mg/g for the CS/PEO/PNC mats, respectively.

The mechanism controlling the adsorption process was investigated through the application of kinetic models. These models also served as testing and validating tools for experimental data and kinetic parameters. Several kinetic models are used to determine mechanisms controlling the adsorption process: chemical reaction, diffusion control, and mass transfer. Pseudo-first order and pseudo-second order non-linear models were fitted to experimental data to evaluate the nature of cadmium ions adsorption mechanism onto nanofibers as can be seen in Figure 4.8 (a) and (b) respectively. The values of k_1, k_2, and q_e for Cd ions are listed in Table 4.3 together with the correlation coefficients (R^2). Results indicate that the pseudo-second-order kinetic model provides a better fit of the experimental data for both nanofibrous mats with R^2 values of 0.984, showing that chemical adsorption was the rate-determining step, in agreement with the results of Zhou *et al.* [83]. The pseudo-second order model provided initial adsorption rates of 9.72

mg/(g.min) for CS/PEO and 14.87 mg/(g.min) for CS/PEO/PNC. These values suggest that the presence of PNC promotes a faster initial adsorption rate. After 30 min, CS/PEO/PNC electrospun nanofibers were able to remove approximately 53 mg/g of cadmium (equivalent to 85% of the equilibrium content value). These results suggest that the reaction rate of Cd ions adsorption depends on the number of active sites and the rate limiting step must be chemical adsorption [84].

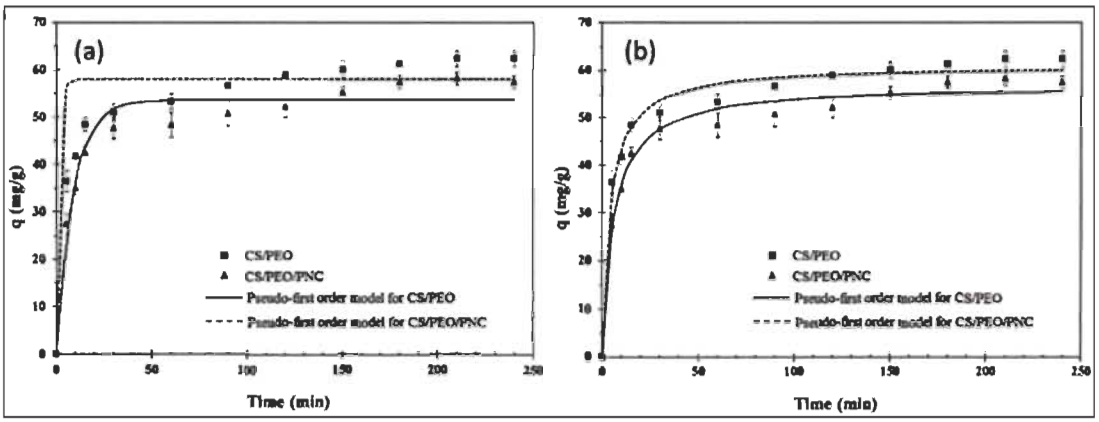

Figure 4.8 Experimental data and non-linear plot of Pseudo-first order (a) and Pseudo-second order (b) adsorption kinetic models of cadmium ions for CS/PEO and CS/PEO/PNC electrospun nanofibers.

Chitosan is known to bind metal ions through chelation by sharing amino and hydroxyl group electron pairs helping in the fixation of metal ions [19]. The presence of phosphate groups in the CS/PEO/PNC mat increases the number of adsorption sites which can lead to an even more rapid adsorption of Cd^{2+} through ion exchange [19, 69]. This is probably the main factor that can explain the higher rate and adsorption capacity of the PNC containing mats. Figure 4.9 shows a proposed scheme for the interaction between CS/PEO/PNC nanofibers and cadmium ions.

The pseudo-first and pseudo-second-order kinetic equations cannot be used to identify the diffusion mechanism. Therefore, the intra-particle diffusion model was applied. The plot of q_t versus $t^{1/2}$ did not provide a straight line. Therefore, the sorption process is not controlled by intra-particle diffusion only. A good fitting of the experimental data by the model was achieved, exhibiting two-linear plots, typical of a two steps sorption process. The straight lines are due to the difference in mass transfer rates in the initial and final adsorption zones. This indicates that diffusion within pores is not the only rate-controlled

step. Table 4.3 shows the related data in two steps equivalent to the two straight lines. The first straight portion represents the diffusion in macropores and mesopores and the second represents the diffusion in micropores.

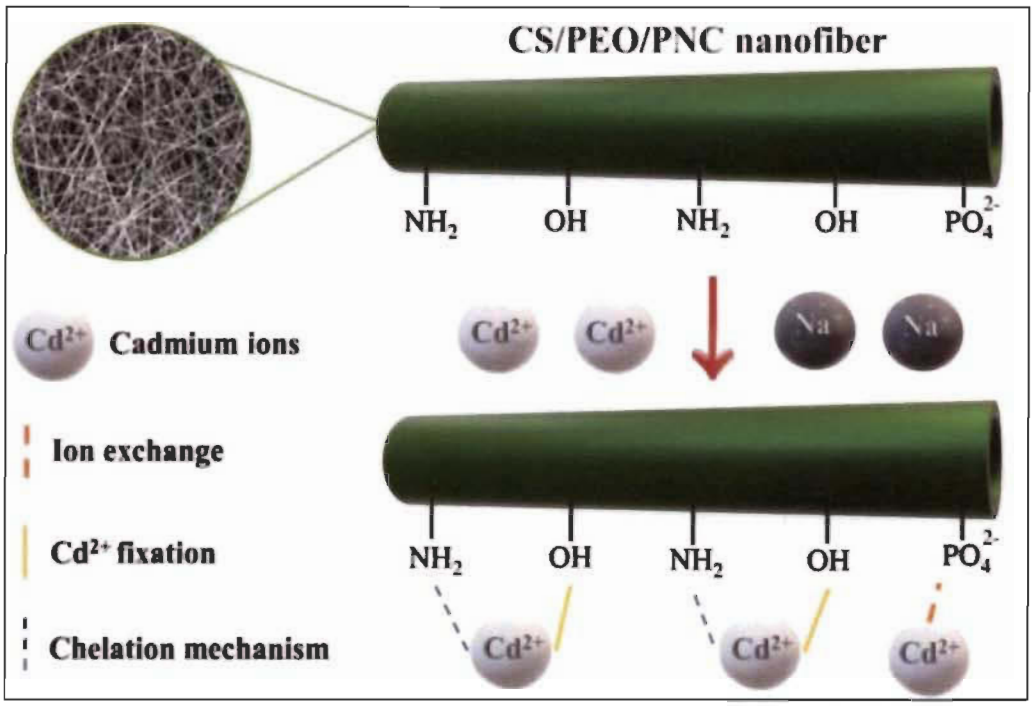

Figure 4.9 Proposed scheme for the interaction of Cd^{2+} with CS/PEO/PNC nanofibers.

Table 4.3 Kinetic parameters for cadmium ion adsorption on nanofibers.

Sample	Exp. data	Pseudo-first order model			Pseudo-second order model			
	q_e (mg/g)	k_1 (min^{-1})	q_e (mg/g)	R^2	k_2 (mg/mg.min)	q_e (mg/g)	h (mg/g.min)	R^2
CS/PEO	58.2	0.1125	53.62	0.954	0.003	56.95	9.72	0.984
CS/PEO/PNC	62.3	0.1474	58.04	0.944	0.004	60.98	14.87	0.984

Sample	Exp. data	Intra-particle diffusion model					
		Zone I			Zone II		
	q_e (mg/g)	K_d ($mg.g^{-1}min^{-1/2}$)	C (mg/g)	R^2	K_d ($mg.g^{-1}min^{-1/2}$)	C (mg/g)	R^2
CS/PEO	58.2	9.10	6.79	0.994	1.19	40.10	0.941
CS/PEO/PNC	62.3	7.24	19.79	0.978	1.20	44.76	0.972

Webber and Morris suggest that if zone I has an intra-particle diffusion coefficient equal to zero, then the intra-pore diffusion controls the adsorption process. Figure 4.10 presents

the linear regression from Eq. (5) for CS/PEO and CS/PEO/PNC. It is clearly observed that multilinear relationship is involved in both cases with two distinctive zones.

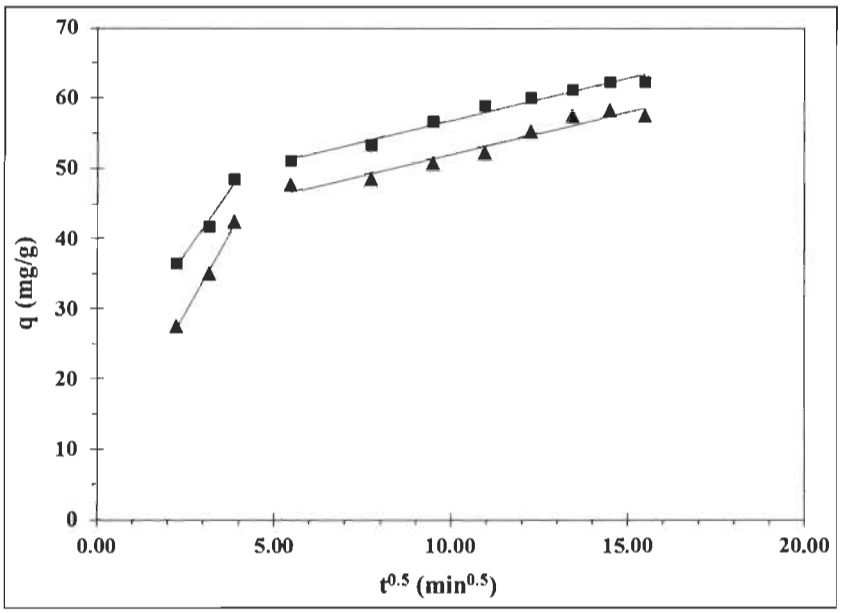

Figure 4.10 Intra-particle-diffusion plot of Cd^{2+} adsorption kinetic models for CS/PEO and CS/PEO/PNC electrospun nanofibers.

Results in Table 4.3 show that for the 5-15 minutes time interval (zone I), the intra-pore diffusion was not the predominant mechanism in the adsorption and then the process controlling the adsorption may be intra-film diffusion. If the linear coefficient is nonzero, then the process controlling the adsorption may be an intra-film diffusion whose thickness is attributed to the linear coefficient in mg/g. The CS/PEO/PNC nanofiber mats present a higher diffusion coefficient at the boundary layer. Zone II is the phase of gradual adsorption where the intra-particle diffusion is limited. The intra-particle diffusion velocity gradually decreases due to the low concentration of solute and the smaller amount of available adsorption sites. A reduction of the zone II intra-particle diffusion coefficient occurred for both materials. This effect indicates a decrease of diffusion until equilibrium is reached.

4.7.4 Adsorption isotherms

Adsorption of heavy metals is strongly dependent of the surface chemistry, adsorbent surface area and precipitation reactions. Cadmium ions adsorption capacity was

determined by plotting q_{eq} versus C_{eq} at 25, 40 and 60°C for CS/PEO/PNC electrospun nanofibers, as can be seen in Figure 4.11 (a). In order to better understand the cadmium ions adsorption isotherms, the Langmuir, Freundlich and Dubinin-Radushkevich models were used in fitting the experimental data.

The Langmuir model assumes that the adsorption occurs in a monolayer on the homogeneous surfaces with definite number of sites where these sites have equivalent energy and the adsorbed molecules do not interact with each other and each site contain only one adsorbed molecule. Therefore, based on the Langmuir linearized Eq. (6), a plot of C_e/q_e versus C_e produced a straight line with slope $1/(K_L q_m)$ and intercept $1/q_m$, as shown in Figure 4.11 (b) [68].

The Freundlich model is an empirical equation based on a multilayer adsorption appears on the heterogeneous surfaces and the adsorption amount increases infinitely with increasing concentration. The Freundlich parameters K_f and $1/n$ are related to the adsorption capacity and intensity of the sorbent, respectively. Based on the Freundlich linearized Eq. (7), a plot of $\ln q_e$ versus $\ln C_e$ curve produced a straight line with slope $\ln K_f$ and intercept $1/n$, as shown in Figure 4.11 (c) [68].

Table 4.4 shows the results for the adsorption parameters and linear regression factors for Langmuir, Freundlich, and Dubinin-Radushkevich models at different temperatures. The Langmuir model fitted very well the experimental adsorption data. The maximum adsorption capacity (q_m) of cadmium ions increased with temperature, due to the increase of energy supplied to the system which facilitates the adsorption. The CS/PEO/PNC mats exhibited a higher affinity for Cd ions, as reflected by their higher maximum adsorption capacities (q_m= 232.55, 263.15 and 270.27 mg/g). These increased sorption capacities can be explained by the high affinity of amine and phosphate groups with cadmium on the surface of the mat, bonding for electrostatic attraction and complexation due to the abundant surface functional groups ($-NH_2$, $-PO_4$), as demonstrated by Lakhdhar et al. [68] and Shi et al. [45]. The percentages of phosphate groups in the adsorbent is estimated at 0.7% and of amine groups is approximately 75%. Considering the adsorption results and the approximate amount of functional groups present on the surface of this adsorbent, results show a higher affinity of phosphate groups for cadmium ions. This can probably

be attributed to a lower energy requirement for ion exchange compared to competing groups (amine) coming from chitosan, which form a complex by chelation. A higher value of K_L indicates strong bonding of cadmium ions to nanofibers at studied temperatures. The increase in the initial concentration provides a greater flow of particle exchange with the mat providing an increase in the adsorption capacity. The favorable nature of the adsorption, an essential characteristic of the Langmuir equation, can be expressed as a dimensionless separation factor R_L, (Equation 4.13):

$$R_L = \frac{1}{1 + K_L C_0} \qquad \text{Eq. 4.13}$$

Where K_L is the Langmuir constant (L/mg) and C_0 is the initial concentration of adsorbate (mg/L). R_L values indicate the type of isotherm: irreversible (R_L=0), linear (R_L=1), favorable (0<R_L<1), or unfavorable (R_L>1) [68]. The R_L values calculated for the adsorption of cadmium ions on CS/PEO/PNC nanofibers were within a range between 0.28 and 0.76. These results suggest that the adsorbate prefers the solid to the liquid phase and the adsorption is said to be favorable.

The Freundlich model fitted the experimental adsorption data well and the high R^2 coefficients suggest that the model is suitable for describing equilibrium data of cadmium ions adsorption on CS/PEO/PNC nanofibers, too. The exponent n of Freundlich model is often used to calculate the favorability of sorption. The values calculated at all studied temperatures were between 0 and 1, which indicate that the adsorption of cadmium ions using CS/PEO/PNC nanofiber mats was favorable.

The D-R isotherm model describes in a very satisfactory way adsorption of organic compounds in gas phase on solid adsorbents. The D-R equation was originally developed for adsorption processes based on the filling of pores of non-homogeneous adsorbents by subcritical vapors and, in general, is used in the description of mechanisms of adsorption, considering Gaussian distribution of energy and heterogeneous surfaces. Based on the D-R linearized Eq. (8), the plot of Lnq_e versus ε^2 produced a straight line with slope Lnq_m and intercept K, as shown in Figure 4.11 (d) [68]. Table 4 also shows the calculated parameters for the D-R isotherm. This was the model that worst fitted the experimental

data. Since all calculated E values were smaller than 8 kJ/mol, the adsorption was considered to be physical for this model. These results are in good agreement with those from Lakhdhar *et al.* [19] and Mautner et al. [73].

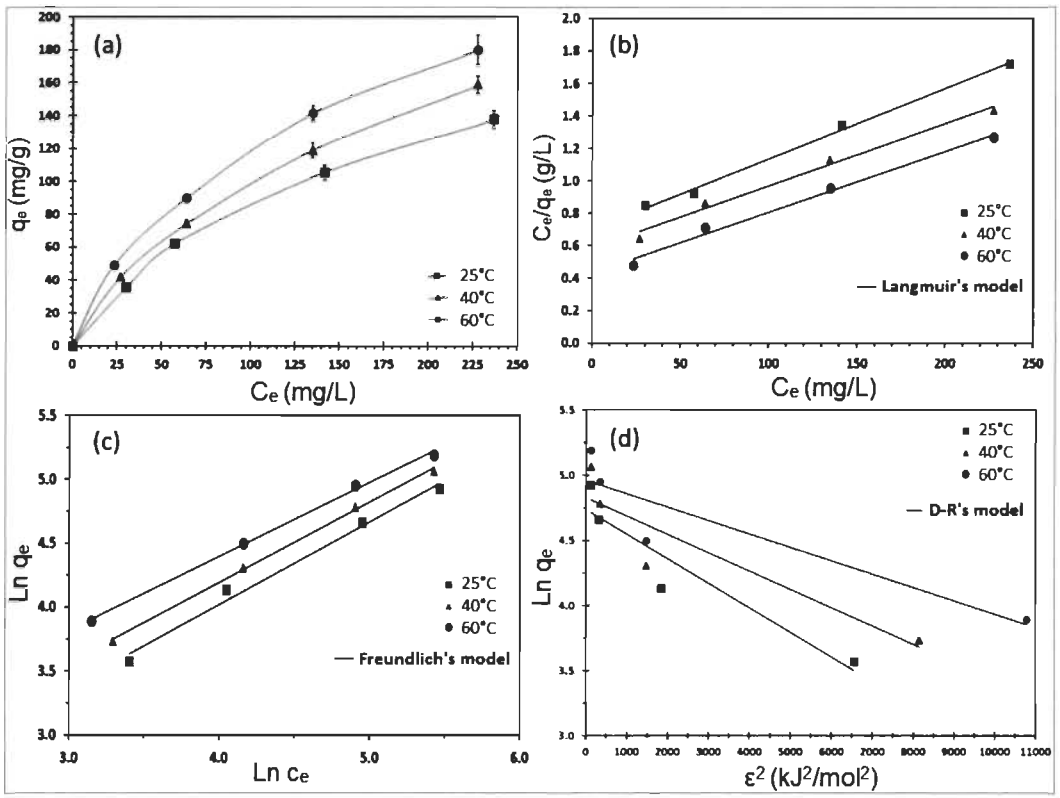

Figure 4.11 Equilibrium isotherms plot of cadmium ions (a) and linearized Langmuir (b), Freundlich (c) and D-R (d) adsorption isotherms of Cd^{2+} on CS/PEO/PNC nanofibers.

The Chi-square test was used to compare the isotherms on the same axial setting and to verify whether the experimental data was related to the theoretical data. The Chi-square (κ^2) value was defined by Equation 4.14:

$$\chi^2 = \sum \frac{(q_e - q_{e,m})^2}{(q_{e,m})} \qquad \text{Eq. 4.14}$$

Where $q_{e,m}$ is the adsorption capacity at equilibrium obtained from the isotherm model (mg/g) and q_e is the adsorption capacity at equilibrium (mg/g) from the experimental data. The Chi-square results indicated the "closeness" between the experimental data with the isotherms. When the Chi-square value approaches to 0, the experimental data is behaving

more toward the isotherm. Table 4.4 shows the relationship between the X^2 and R^2 values for each isotherm. The κ^2 values suggested that all isotherm provided a good model of the sorption system.

The Anderson-Darlin test was performed using Origin software in order to assess the normality of the data. At the 0.05 level, all the data were significantly drawn from a normally distributed population. These results confirm the validity of our results.

Table 4.4 Langmuir, Freundlich and D-R isotherm parameters and Chi-squares, κ^2 of isotherms for Cd^{2+} adsorption on CS/PEO/PNC nanofibers.

T (°C)	Langmuir				Freundlich			
	K_L (L/mg)	q_m (mg/g)	R^2	κ^2	K_f [(mg/g) (mg/L)/n]	1/n	R^2	κ^2
25	0.0061	232.55	0.995	0.134	26.50	0.6487	0.988	0.875
40	0.0065	263.15	0.987	0.436	47.21	0.6292	0.998	0.149
60	0.0085	270.27	0.988	0.788	104.08	0.5925	0.994	0.560

T (°C)		Dubinin-Radushkevich			
	$q_{D\text{-}R}$ (mol/g)	K (mol^2/J^2)	E (kJ/mol)	R^2	κ^2
25	114.19	0.00021	1.543	0.892	0.311
40	124.76	0.00017	1.715	0.836	0.004
60	142.65	0.00012	2.041	0.839	0.003

4.7.5 Effect of temperature on cadmium ions adsorption

Temperature is an important feature for adsorption. Thermodynamic parameters calculated for the adsorption of cadmium ions by CS/PEO/PNC nanofibers are reported in Table 4.5. The adsorption ability of cadmium ions was improved with increasing temperature. Results show that Gibbs free energy values (ΔG^0) started positive at 25°C and get negative at 40 and 60°C, indicating the spontaneous nature of cadmium ion adsorption on CS/PEO/PNC nanofibers. The ΔG^0 values became more negative at higher temperature, which means that the degree of spontaneity increased with temperature, which implies a larger driving force for the adsorption and is mainly due to chemisorption rather than physisorption [85]. These results are also in agreement with data from Lakhdhar *et al.* [19]. Positive enthalpy (ΔH^0) value was attributed to the endothermic nature of the adsorption process. The positive value of ΔS^0 shows an increase of the

randomness degree of the adsorbent-adsorbate system, and indicates that the interaction of functional groups with cadmium could change the structure of CS/PEO/PNC, which is in agreement with Aliabadi et al. [70], Zhou et al. [83] and Deng et al. [86].

Table 4.5 Thermodynamic parameters for Cd^{2+} adsorption on CS/PEO/PNC nanofibers.

Temperature (°C)	R^2	ΔH (kJ)	ΔS (kJ/K)	ΔG (kJ)
25	0.9997	6.967	0.0224	0.288
40				-0.047
60				-0.495

4.7.6 Comparison of cadmium adsorption with various adsorbents

The adsorption capacity of the CS/PEO/PNC mats has been compared with other adsorbents materials data reported in the literature. The q_m of Langmuir at 25°C of the present investigation was compared with reported values. Results presented in Table 4.6, revealed that the CS/PEO/PNC adsorbent have higher adsorption capacity than the other absorbents analyzed. It is important to note that the biosorbent developed in this work is based on chitosan and Phosphorylated Nanocellulose and those materials are renewable, biodegradable, cheap, and easily available.

Table 4.6 Comparison of the adsorption capacity of Cd^{2+} of different adsorbents at 25°C.

Adsorbent	q_m (mg/g)	Reference
Coffee grounds	15.65	[87]
Phosphogypsum	131.57	[88]
Orange peels	4.9	[89]
Nano-hydroxyapatite modified chitosan	123.5	[90]
Rice Husk	21.28	[91]
Cellulose nanocrystals	1.9	[92]
Sulfurized activated carbon	142.86	[93]
Activated carbon	26.36	[94]
Canna indica derived biochar	140.01	[95]
Egyptian bentonitic clay	8.2	[96]
Chitosan/rectorite nano-hybrid microspheres	16.53	[97]
Chitosan saturated montmorillonite	23.03	[98]
	60.85	[99]
CS/PEO/PNC electrospun nanofibers	232.55	Present study

4.8 Conclusions

A new electrospun Chitosan/Phosphorylated Nanocellulose biosorbent was developed for the removal of cadmium ions from aqueous solutions. Homogeneous electrospun CS/PEO and CS/PEO/PNC nanofibrous mats were produced successfully. EDX and FTIR spectra confirmed the presence of phosphate groups in electrospun CS/PEO/PNC nanofibers. The morphological analysis showed the formation of defect free random nanofibers with nanometric diameters. Batch adsorption tests showed that the equilibrium time was reached in 3h and the presence of PNC increased the rate and adsorption capacity. The pseudo-second order kinetic model best fitted experimental data and the results evidenced that the reaction rate of Cd ions adsorption was dependent on the number of active sites and the rate limiting step must be chemical adsorption with intra-film diffusion controlling the adsorption process. Equilibrium studies showed that the Langmuir isotherm model better fitted the experimental data. The maximum adsorption capacity obtained for cadmium ions adsorbed on CS/PEO/PNC nanofibers was 232.55 mg/g at 25°C, and increased with temperature. The maximum adsorption capacity achieved is higher than other reference values found in literature. Thermodynamic parameters showed that cadmium ions adsorption onto CS/PEO/PNC nanofibers is a spontaneous reaction of endothermic nature.

This work presented the synthesis of a new and original biosorbent material with promising potential for cadmium removal from aqueous solutions. However, due to chemical compatibility issues between CS and PNC, the PNC content was limited to 10 weight total percent. Further works will be required to find ways to increase PNC content into the mats and improve adsorption removal capacity.

Chapitre 5 - Article 2

5.1 Cd^{2+} removal by nonwoven Chitosan/Phosphorylated Microcellulose Nanocomposite

5.2 Foreword

This second article is entitled "Cd^{2+} removal by nonwoven Chitosan/Phosphorylated Microcellulose Nanocomposite". It has submitted to Water, Air, & Soil Pollution, March 2020.

Authors and their corresponding addresses are in the following order:

Ricardo Brandes, PhD student in Science and Engineering of Lignocellulosic Materials PhD program

Innovation Institute on Ecomaterials, Ecoproducts and Ecoenergies based on Biomass (I^2E^3), Université du Québec à Trois-Rivières, 3351 boulevard des Forges, Trois-Rivières, Quebec, G9A 5H7, Canada

François Brouillette, PhD.

Thesis co-supervisor

Innovation Institute on Ecomaterials, Ecoproducts and Ecoenergies based on Biomass (I^2E^3), Université du Québec à Trois-Rivières, 3351 boulevard des Forges, Trois-Rivières, Quebec, G9A 5H7, Canada

Bruno Chabot, PhD.

Thesis supervisor

Innovation Institute on Ecomaterials, Ecoproducts and Ecoenergies based on Biomass (I^2E^3), Université du Québec à Trois-Rivières, 3351 boulevard des Forges, Trois-Rivières, Quebec, G9A 5H7, Canada

Authors contributions: Ricardo Brands is the main author of the article. He did all the experimental work, laboratory setup developments and wrote the manuscript. Dr. Brouillette is the thesis co-supervisor and provided materials and laboratory facilities and he helped with manuscript corrections. Dr. Chabot is the thesis supervisor and provided materials and laboratory facilities. He provided guidance and helped in the preparation and correction of the manuscript.

5.3 Résumé

La croissance rapide de la population humaine et l'industrialisation mondiale ont entraîné la production de plus grandes quantités d'eaux usées contenant divers polluants comme les métaux lourds toxiques. L'adsorption est efficace à cet effet, mais son utilisation est limitée dû aux coût élevé des matériaux adsorbants. Le Chitosane et les fibres cellulosiques phosphorylées ont un potentiel élevé en tant que biopolymères adsorbants car ils sont peu coûteux et efficaces pour l'assainissement de l'eau. Des nattes de nanofibres CS/PMC non tissées ont été produites par électrofilage avec jusqu'à 50% en poids de PMC. Les propriétés thermiques, chimiques et morphologiques des membranes ont été étudiées. Des essais d'adsorption par lots ont été réalisés en utilisant des ions Cd^{2+}. Des modèles cinétiques et isothermes ont été testés par rapport aux résultats expérimentaux et les propriétés thermodynamiques ont été calculées. Les résultats ont montré que le modèle d'ordre pseudo-seconde était le mieux adapté et ont suggéré la chimisorption comme mécanisme d'élimination du Cd^{2+}. L'isotherme de Langmuir a le mieux décrit les données d'équilibre atteignant la capacité d'adsorption maximale de 283 mg/g. Cette valeur élevée a été attribuée principalement à la grande quantité de groupes phosphate, qui nécessitent moins d'énergie pour capturer les cations métalliques. L'évaluation thermodynamique a suggéré que l'adsorption est une réaction endothermique spontanée. Ces résultats confirment que les membranes CS/PMC sont faciles à produire à faible coût. Elles sont également respectueuses de l'environnement et présentent une grande efficacité d'adsorption.

Mots-clés: l'adsorption du Cd^{2+}, Chitosane, Microcellulose phosphorylée, Groupes phosphates, Nanofibres électrofilées.

5.4 Abstract

The rapid growth of human population and global industrialization has resulted in the generation of larger amounts of wastewater containing various pollutants, among which toxic heavy metals. Adsorption is efficient for this purpose, but its application is limited by the high cost of adsorbent materials. Chitosan and phosphorylated cellulosic fibers have a high potential as low-cost and effective adsorbent biopolymers for water remediation. Nonwoven chitosan/phosphorylated microcellulose nanofiber mats were produced by electrospinning with up to 50% by weight of PMC. The thermal, chemical and morphological properties of the membranes were studied. Batch adsorption trials were carried out using Cd^{2+} ions. Kinetics and isotherm models were tested against experimental results and the thermodynamic properties were calculated. The results showed that the pseudo-second order model best fitted and suggested chemisorption as the mechanism for Cd^{2+} removal. Langmuir isotherm best described equilibrium data reaching the maximum adsorption capacity of 283 mg/g. This high value was attributed mainly by the large amount of phosphate groups, which require less energy to capture the metal cations. Thermodynamic evaluation suggested that the adsorption is a spontaneous endothermic reaction. These results confirm that CS/PMC membranes are easy to produce at low cost. They are also environmentally friendly and have high adsorption efficiency.

Keywords: Cd^{2+} adsorption, Chitosan, Phosphorylated Microcellulose, Phosphate groups, Electrospun nanofibers.

5.5 Introduction

Raising awareness of the rational use of natural resources and developing technologies that minimize environmental impacts are increasingly prominent due to the great concern of the world population, governments and industries [100]. The need to preserve the environment requires increasingly efficient and feasible methods for the removal of pollutants. Among the environmental components most affected worldwide are the bodies of water. Water pollution is a serious problem in the world due to the scarcity of this natural resource, compromising the development of plant cultures and the survival of animals and humans [101]. The problem is already a reality in various parts of the world,

leading to the adoption of laws and measures to prevent waste and degradation, and to promote a more sustainable use of water reserves across the Earth. The release of effluents with contaminants such as heavy metals into fresh water bodies represents a serious environmental problem. The main sources of contamination by heavy metals in fresh waters are the electroplating, foundry, mining, pigmentation, metallurgy and paper industries [83, 102]. Therefore, the urgency for new public policies and alternative technologies for the treatment of these wastewaters is of great importance. Toxic metals such as Cd (II), have become an ecotoxicological hazard of fundamental interest and growing importance due to their tendency to accumulate in vital organs of humans and animals. Cadmium poisoning has been reported as one of the global health problems. Long-term exposure to cadmium through water leads to cancer and organ system toxicity [103, 104].

In recent decades, new methods and materials for the removal of heavy metals have been developed with an economic and environmental appeal, mainly due to increasingly strict laws. In the treatment of wastewaters, primary and secondary methods are usually used. However, these technologies are inefficient in the removal of heavy metals in low concentrations [105, 106]. An alternative is the process of removal of heavy metals by the adsorption technique, which consists of a physical-chemical process where the molecules can be attracted to the surface of the adsorbent. This technology has been used due to its simplicity, economy, efficiency in the removal, recovery and recycling of wastewater. Although the adsorption technique is simple and efficient, the high cost with adsorbent materials limits its use, mainly the activated carbon [107]. In view of this problem, researchers have been motivated to search for cheaper adsorbents that are naturally available and do not require high processing steps to increase adsorption capacity. By-products of industry, agriculture and biomass, such as biopolymers are easily available, renewable and cheap. Among those, chitin, cellulose, chitosan and starch are of particular importance due to their chemical structures, physicochemical characteristics, chemical stability, high reactivity and selectivity for metal ions [108].

Chitosan is a linear polysaccharide, obtained by deacetylation of chitin and based on D-glucosamine units. They are widely described in the literature as an effective matrix for

removal of heavy metal ions from industrial effluents, since the amine and hydroxyl groups present in their structures can act as coordination sites [109, 110]. The use of chitosan as an adsorbent for the treatment of effluents has great advantages, since it is a by-product of the fishing and crabbing industries with great volume of production [111]. Cellulose is particularly attractive since it is available at a low cost, is a renewable source, presenting excellent mechanical properties, thermal resistance and dimensional stability. In addition, the hydroxyl groups present on the cellulose can be chemically modified to provide novel properties. The surface of this material can be modified by introducing binder groups that have the ability to interact with metals by means of low-cost chemical processes to produce materials with considerable adsorption and ion exchange capacities [112-114]. Several methods, both physical and chemical, have been used to modify the natural cellulose. The phosphorylation via esterification reaction is an example of surface modification of cellulose for the introduction of phosphate groups, which can interact easily and strongly with metal cations [44, 46, 79]. Phosphorylated cellulose has shown high capacities and adsorption rates for heavy metals capture [13, 73]. Electrospinning is currently used to make nonwoven mats of fibers in the nanometer scale, thus increasing the surface area to volume ratio with the contaminants [115-117]. Researches have focused on the production of electrospun chitosan nonwoven mats and the results referring to the removal of heavy metals are good. However, there still a need to find more efficient materials to overcome the contamination problem [118, 119].

Faced with this reality, this study is aiming at the development of an electrospun nanocomposite mat based on chitosan and phosphorylated microcellulose (PMC). The idea is to produce a composite with a surface containing a larger number of phosphate groups compared to the previously produced CS/PEO/PNC adsorbent. The limit was the high surface area of the PNCs which reacted and agglomerated easily with the chitosan, limiting the addition of only 10 wt% PNC. The use of PMC with a smaller surface area and less reactant allowed the addition of a larger quantity by weight of PMC. We are also investigating their adsorption capacity for the removal of cadmium ions from aqueous solutions. To better understand the behavior of this new material, morphological and chemical analyzes were performed. Conductometric titration analysis was performed in order to evaluate the presence of acidic groups. Finally, a study of the contact time,

adsorption kinetics, adsorption isotherms, thermodynamic and sorption-desorption trials were performed in order to evaluate the effectiveness of this material.

5.6 Materials and Methods

5.6.1 Materials and chemicals

Low molecular weight Chitosan powder (MW 50 000-190 000 Da), with deacetylation degree of 75-85% (Sigma-Aldrich) and glacial acetic acid 99.7% (Fischer brand) were used to prepare chitosan solutions. Poly (ethylene oxide) (PEO) powder with average molecular weight of 900 000 Da (Sigma-Aldrich) dissolved in distilled water was used as a polymer co-agent in order to improve electrospinability. Kraft fiber (KF) samples were provided by Kruger Inc. KF were then phosphorylated using a phosphate ester having a 12 C atoms alkyl chain and urea. Sodium carbonate anhydrous (Na_2CO_3) (A.C.S, Fisher Chemical) was used for the neutralization and stabilization of mats. Cadmium sulfate anhydrous ($CdSO_4$) (Fisher Scientific Co.) was the heavy metal used for adsorption tests. Ethylenediaminetetraacetic acid (EDTA) (OMEGA Chemical) and ammonium hydroxide (Fisher Scientific Co.) were employed to determine residual ions concentration. Eriochrome Black T (Fischer Scientific Co.) was used as indicator of concentrations determination by complexometric titration.

5.6.2 Phosphate ester and phosphorylated microcellulose preparation

For the preparation of phosphate ester, 210 g of 99% decanol were added in a beaker (2000 mL) and shaken at 80°C for 30 min. Then, 60 g of poly-phosphoric acid at a concentration of 115% as phosphoric acid (APP 115) were added and mixed slowly. Finally, 60g of phosphorus pentoxide (P_2O_5) was added to the mixture and kept under stirring for 12 h[120]

For the preparation of phosphorylated microcellulose, 148 g of phosphate ester and 56 g of urea were mixed on a glass plate (150x100 mm) and heated in an oven at 150°C for 15 min. Then, 31.5g of Kraft fibers were added and kept in an oven at 145°C for 60 min. The resulting fibers were washed with distilled water and then crushed with a mechanical

mixer. The suspension was filtered and washed with denatured alcohol. Finally, the fibers were dried in a vacuum oven (Fisher Scientific, model 282A) at 105°C for 120 min and then disintegrated with a mechanical mixer for 10 min.

5.6.3 Phosphorylated microcellulose characterization

A Zeiss Axio Scope A1 FL-LED optical microscope equipped with an Axio Cam ERC 5 was used to analyze the PMC particles. 0.1 g of PMC particles were mixed with 200 mL of distilled water. The small sample of the dispersion was deposited on a microscope glass slide and dried. The images were captured at 10x magnification. The diameter of the PMC particles was determined using the L&W fiber tester Plus+ (Lorentzen & Wettre). About five thousand measurements were carried out to provide a statistically significant particle size distribution of the material.

1.2 g of PMC microparticles and 3 mL of hydrochloric acid (HCl, 36.5-38%) were added in a 300 mL beaker with 250 mL of distilled water. The mixture was then stirred for about 30 min. The PMC were filtered on the Buchner funnel with distilled water and acetone. Then, 0.6 g of PMC, 0.07 g of NaCl and 500 mL of distilled water were added in a 600 mL beaker and stirred. The total charge and acid groups were evaluated by conductometric titration using a conductometer (Thermo Orion 150) and an automated titrator (Metrohm 765 Dosimat). The prepared sample was titrated with 0.1 M NaOH.

5.6.4 CS/PEO/PMC mat preparation and electrospinning process

CS and PEO were dissolved separately in acetic acid and distilled water, respectively. 0.9 g of CS was dissolved in 29.1 g of 90% acetic acid (3 wt% CS) and 0.9 g of PEO was dissolved in 29.1 g of distilled water (3 wt% PEO). 0.9 g of PMC were dispersed in 29.1 g of distilled water (3 wt% PMC). CS and PEO solutions and PMC dispersion were mixed at a mass ratio of 40/10/50, i.e., 12 g of CS solution, 3 g of PEO solution and 15 g of PMC dispersion were mixed in a 125 mL beaker. The final constituent was 30 g. added and mixed with the PEO solution, then mixed with the CS solution. The final mixture was stirred on a magnetic stirrer for 24 h at room temperature. Then, this mixture was sonicated for 15 min and rested for 3 h before electrospinning. For electrospinning, a 60 mL plastic

syringe with a 20-gauge stainless blunt end steel needle (Kimble-Chase) was filled with 15 g of CS/PEO/PMC solution. The solution was pumped by a programmable micro-syringe pump (Harvard Apparatus 44) and kept under stirring by a magnetic stirrer positioned below the syringe. A high voltage DC power supply (Gamma High Voltage Research) was used to provide the appropriate voltage. An aluminum foil was used to collect electrospun nanofibers. The tests were performed at room temperature. The solution parameters, as well as the optimized processing parameters, are summarized in Table 5.1.

Table 5.1 Electrospinning and solution parameters

Parameter	CS/PEO mats	CS/PEO/PMC mats
CS/PEO/PMC ratio (wt%)	60/40/0	40/10/50
Acetic acid (%)	90	90
Final concentration (wt%)	3	4
Voltage (kV)	21	15
Distance (mm)	240	200
Flow rate (mL/h)	0.6	0.3

The nonwoven mats were collected from the collector, dried in a vacuum oven at 70°C overnight, neutralized and stabilized in a sodium carbonate solution (0.1 M) for 2 h. Finally, the mats were washed in distilled water until a neutral pH was reached and then kept drying at room temperature during 24 h.

5.6.5 Nanocomposite mats characterization

Scanning electron microscopy (SEM) was used to study the nanofibers mat morphology. The mat samples were inserted in an aluminum stub and fixed on a carbon double-sided tape. The nanofibers were covered with a 30 nm gold layer. SEM evaluations were performed with a Hitachi VP-SEM SU1510. The mean diameter of the nanofibers was determined using Image-J software after 300 measures per sample.

The microscope is equipped with an EDX microanalysis system from OXFORD Instruments, model Aztec x-max 20. The EDX analyzes were performed on mat samples at five different locations.

FTIR was used to determine the presence of functional groups in relation to the main bands of the infrared spectrum. A Perkin Elmer Spectrum FTIR 2000 Spectrometer equipped with a Michelson interferometer accessory from solid samples and over the range 400-4000 cm^{-1} (medium infrared region) at a resolution of 4 cm^{-1} and averaged over 30 scans were used to record the IR spectra of the samples.

Differential scanning calorimetry (DSC) were performed in a DSC 2500 modulus (TA Instruments, USA). The DSC curves were performed under dynamic nitrogen atmosphere (50 - 100 $mLmin^{-1}$) using 5 mg sample material and a heating rate of 10°C min^{-1}. Accurately weighed samples were placed into a covered aluminum sample holder with a central pin hole. The samples were heated from 25 up to 400°C.

X-ray diffraction (XRD) was carried out to study the crystallography of the mats, by means of a D8 Focus X-ray Diffractometer (Bruker, USA) using a CuKα radiation (source conditions: 40 kV and 50 mA).

5.6.6 Adsorption tests

Batch tests were performed to evaluate the adsorption of Cd^{2+} by nanocomposite mats. For kinetic experiments, a 30 mg mass (m) of adsorbent and a 60 mL volume (V) of a 100 ppm Cd^{2+} (C_0) solution were mixed in a 250 mL Erlenmeyer flask. The flasks were agitated using an orbital shaker (Lab-line Instrument) at temperature of 25°C, pH 5.5, and 200 rpm. Agitation was provided until the equilibrium concentration (C_e) was reached. The amount of adsorbed cadmium ions, q (mg/g), was calculated using Equation 5.1 at various contact times (10-300 min.).

$$q = \frac{(C_0 - C_e)V}{m} \qquad \text{Eq. 5.1}$$

Kinetic adsorption models were applied to set the mechanism involved in the adsorption process of Cd^{2+} by the adsorbent materials: pseudo-first order model according to the non-linear form (Equation 5.2), which suggests a physical adsorption and pseudo-second-order model according to the non-linear form (Equation 5.3), which suggests a chemical

adsorption. The initial adsorption rate h (mg ($gmin^{-1}$)) can be determined with the k_2 and q_e values of the pseudo-second order model (Equation 5.4).

$$q_t = q_e(1 - \exp^{(-k_1 t)}) \quad \text{Eq. 5.2}$$

$$q_t = \frac{(k_2 q_e^2 t)}{(1 + (k_2 q_e t))} \quad \text{Eq. 5.3}$$

$$h = k_2 q_e^2 \quad \text{Eq. 5.4}$$

Where,

q_e = Amount of adsorbed cadmium ions at equilibrium (mg/g);

q_t = Amount of adsorbed cadmium ions at time (mg/g);

t = Reaction time (min);

k_1 = First-order equilibrium constant (min^{-1});

k_2 = Second-order equilibrium constant ($mg/mgmin^{-1}$);

For equilibrium experiments, the same procedure as kinetics tests was performed, but at the Cd^{2+} concentrations C_0 of (50, 100, 200, and 300 mg/L) and at temperatures of 25, 40 and 60°C. The contact time used in the isotherms was 4 h. The non-linearized Langmuir, (Equation 5.5), Freundlich,(Equation 5.6), Dubinin-Radushkevich, (Equations 5.7 and 5.8) isotherm models were applied to the results.

$$q_e = \frac{q_{\max} K_L C_e}{1 + K_L C_e}; \; R_L = \frac{1}{1 + K_L C_o} \quad \text{Eq. 5.5}$$

$$q_e = K_F C^{1/n} \quad \text{Eq. 5.6}$$

$$q_e = q_{D\text{-}R} \exp^{(-K\varepsilon^2)} \quad \text{Eq. 5.7}$$

$$E = \frac{1}{\sqrt{2K}} \quad \text{Eq. 5.8}$$

Where,

q_{max} = Maximum adsorption capacity (mg/g);

K_L = Effective dissociation constant (L/mg);

R_L = Separation factor;

K_F = Freundlich constant [(mg/g) $(mg/L)^{1/n}$];

N = Constant related to system heterogeneity.;

$\mathcal{E}$ = Polianyi potential;

K = Constant associated to the adsorption energy (mol^2/J^2);

E = Adsorption energy (kJ/mol).

Thermodynamic parameters were found using Equations 5.9 and 5.10. Enthalpy change (ΔH^0), and entropy change (ΔS^0) were obtained respectively, from the slope and the intercept of van't Hoff plot according to Equation 5.10. R is the universal gas constant (8.314 J/mol K^{-1}) and T is the absolute temperature (K). The variation of the standard Gibbs free energies (ΔG^0) were determined by Equation 5.10. All equations are listed below:

$$Ln(q_e / C_e) = \frac{\Delta S^0}{R} - \frac{\Delta H^0}{RT} \qquad \text{Eq. 5.9}$$

$$\Delta G^0 = \Delta H^0 - T\Delta S^0 \qquad \text{Eq. 5.10}$$

5.6.7 Sorption-desorption study

For the adsorption cycles, 10 mg of CS/PEO/PMC mat was added in a flask with 20 mL of Cd^{2+} (100 mg/L) at 25°C, 200 rpm and a pH of 5.5. After 4h under agitation, the mat was removed and washed three times with deionized water to remove any residual Cd^{2+} on the surface. Then, the final concentration of Cd^{2+} was measured by complexometric titration and the adsorption capacity was determined according to Equation 5.1. For the regeneration and desorption evaluation, the same mat was placed in an Erlenmeyer flask containing 20 mL of HNO_3, HCl and EDTA (0.05 and 0.10 M, respectively) [121] and

HNO_3, Ca $(NO_3)^2$, EDTA (0.10 and 0.01 M, respectively) [122]. The flask was agitated with an orbital shaker for 4 h at 25°C and 200 rpm. Then, the final concentration of Cd^{2+} was measured by complexometric titration and the adsorption capacity was determined according to the Equation 5.1. After desorption and regeneration, the amount of metal ions adsorbed on the mat and the residual metal ion concentration in desorption were calculated according to Equation 5.11. The sorption/desorption experiments were performed in duplicate.

$$\text{Desorption ratio (\%)} = \frac{\text{Amount of metal ions desorbed}}{\text{Amount of metal ions adsorbed}} \times 100 \qquad \text{Eq. 5.11}$$

5.7 Results and Discussion

5.7.1 Phosphorylated microcellulose characterization

Figure 5.1 (a) shows samples of Kraft fibers, Phosphorylated Kraft fibers, Phosphorylated Microcellulose powder and Phosphorylated Microcellulose powder dispersed in water. Each sample shows the shapes of the materials until reaching the final powder and its homogeneous dispersion in water media. Optical microscope (OM) was used to get images of the phosphorylated microcellulose dispersion as an easy way to evaluate their morphology. Figure 5.1(b) is an OM image of the phosphorylated microcellulose and shows a dispersion of particles which are on the microscale. Figure 5.1(c) presents the size distribution of the Phosphorylated Microcellulose in water. The average fiber length was 193 μm (+/- 92) and the average fiber width was 32 μm (+/- 9), proving that this phosphorylated cellulose is on the microscale.

Kraft fibers and Phosphorylated Microcellulose total charges were -83±7 meq/g and -3036±160 meq/g, respectively. Those results evidence the surface modification of Kraft fibers after phosphorylation reaction, since that high value of the negative charges can be attributed to the phosphate groups added on the fiber surface.

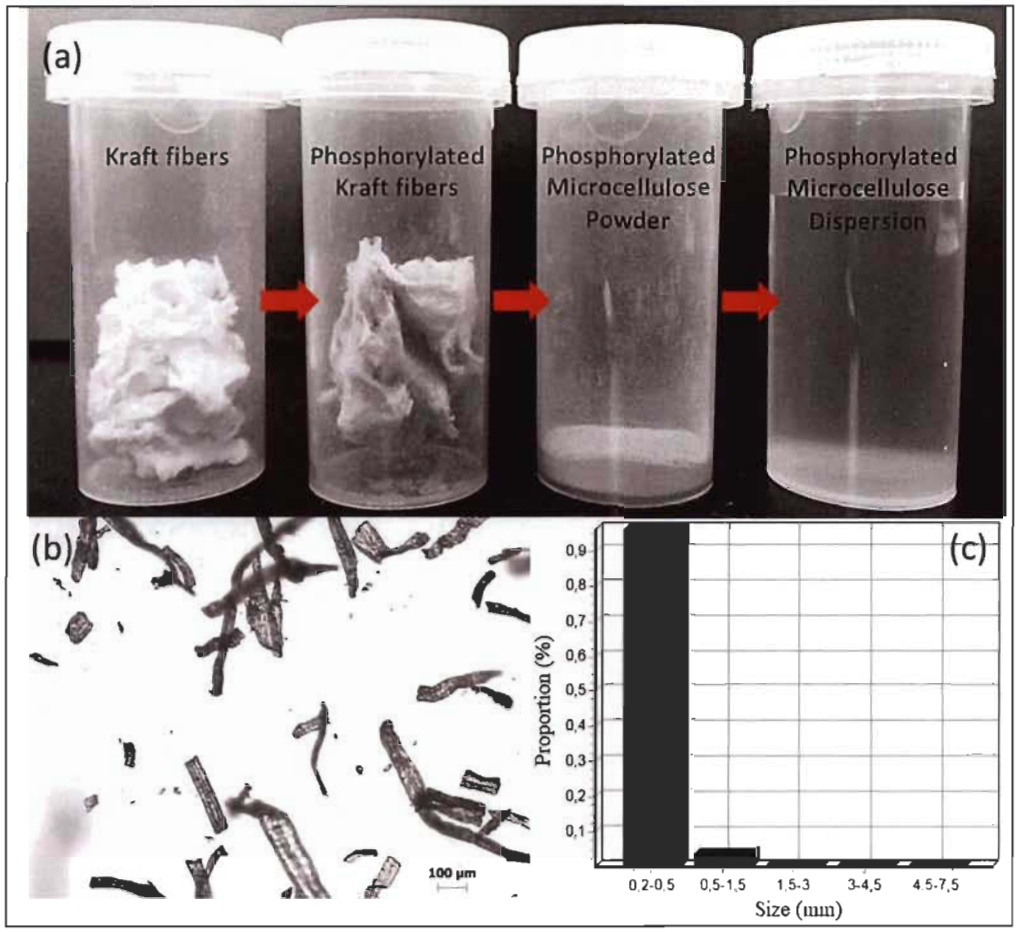

Figure 5.1 Photographs of the Kraft fibers, Phosphorylated Kraft fibers, Phosphorylated Microcellulose Powder and Phosphorylated Microcellulose Dispersion (a). Optical microscope of the Phosphorylated Microcellulose Dispersion (b), and Fibers size distribution of the PMC particles (c)

5.7.2 PMC fibers and nanofiber mat characterization

EDX analyzes for the PMC fibers and CS/PEO/PMC mat showed spectra containing peaks of carbon, nitrogen, oxygen, sodium and phosphorous, as can be seen in Figure 5.2. Carbon and oxygen came from polymer molecules and nitrogen came probably from the chitosan and PMC molecules. The presence of phosphorous peaks can be attributed to the phosphate groups from phosphorylated microcellulose and the sodium peak can be attributed to the stabilization/neutralization treatment with sodium carbonate [123]. Although EDX is not a technique with optimum quantitative accuracy, it is notable that the average phosphorous peaks for pure PMC mats were approximately 6.6 wt%, while

for CS/PEO/PMC-based mats, they were 1.7 wt%. The expected results for the composite mat were close to 3.3 wt%. The authors believe that some microparticles of PMC may have clustered inside the syringe and others could not fix and store themselves on the collector. Some microparticles may have reached the collector and fall out due to the lack of fixation. Others may have been lost on the way between the tip of the needle and the collector.

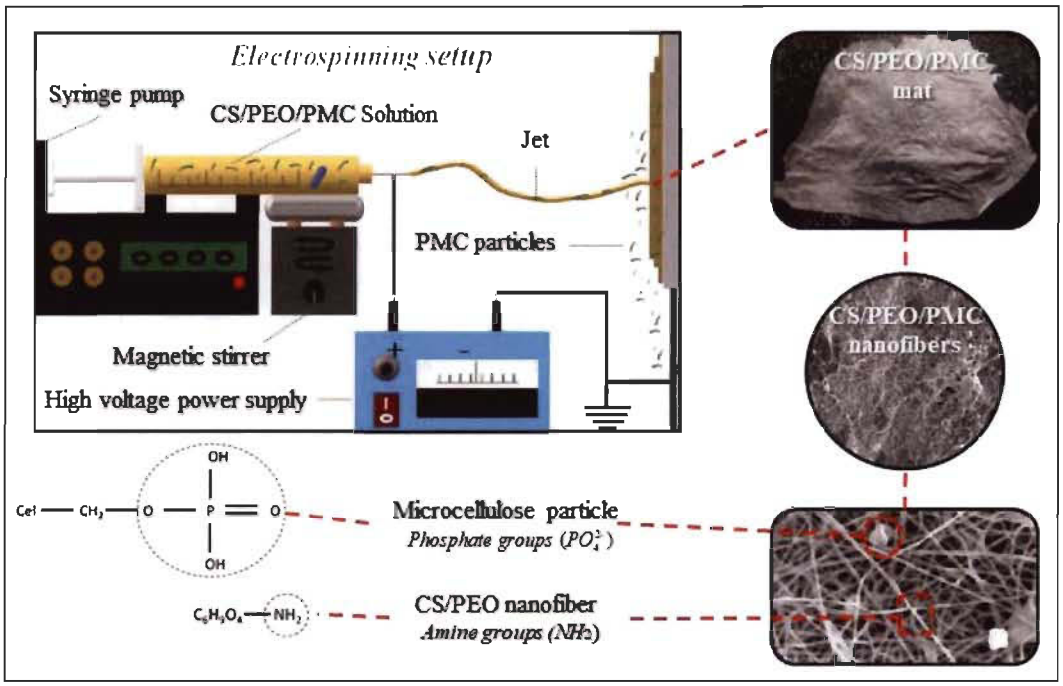

Figure 5.2 Schematic proposal for the electrospinning process of the CS/PEO/PMC mat and SEM images

5.7.3 CS/PEO/PMC nanofiber mats and electrospinning process

For the fabrication of the nanofiber mat, a CS/PEO/PMC electrospinning solution was prepared at a mixing ratio of 40/10/50 as described in Table 5.1. Therefore, 50% of PMC's were well dispersed into the CS/PEO polymer solution. To ensure that PMC are always well dispersed during the electrospinning process, a small magnetic bar was inserted into the syringe container near the exit port, and a magnetic stirrer was positioned below the syringe (see Figure 5.3). The magnetic bar was kept in rotation until the end of the electrospinning process. For the processing of the CS/PEO/PMC nonwoven mat, a voltage of 15 kV, a flow rate of 0.3 mL/h and a distance between the tip of the needle and the

aluminum foil collector of 20 cm were used. These settings provided a continuous jet formation without spreading and a stable production of the mat.

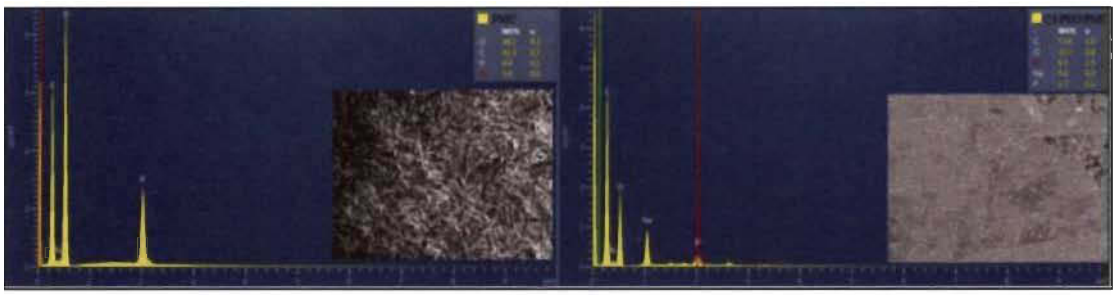

Figure 5.3 EDX spectra of PMC and CS/PEO/PMC nanofibers

Figure 5.4 shows SEM images of the CS/PEO/PMC mat where it is possible to see PMC anchored within CS nanofibers. Therefore, it is expected to find both phosphate and amine groups on the nanofiber mat surface.

Figure 5.4(a) and (b) show SEM of electrospun nanofibers before the Na_2CO_3 treatment. Figure 5.4(c) and (d) show the same samples after the Na_2CO_3 treatment. The average nanofiber diameters were 111.2 ($\pm$33.1) nm before treatment and 139.7 ($\pm$41.6) nm after sodium carbonate treatment, being in agreement with Lakhdhar *et al.* [19] and Aliabadi *et al.* [70]. The image presented in Figure 5.4(b) evidence the presence of phosphorylated microcellulose particles, which appear entangled within the nanofiber's matrix proving the theory suggested in the previous section. The neutralization treatment with sodium carbonate is used to preserve the mat's structure. Without such neutralization, it partially dissolves when immersed in water. However, this neutralization step generates a film-like structure which can be seen visually by comparing the mats presented in the Figure 5.4(b) and (d), clearly showing that the nanofibers are different [124, 125].

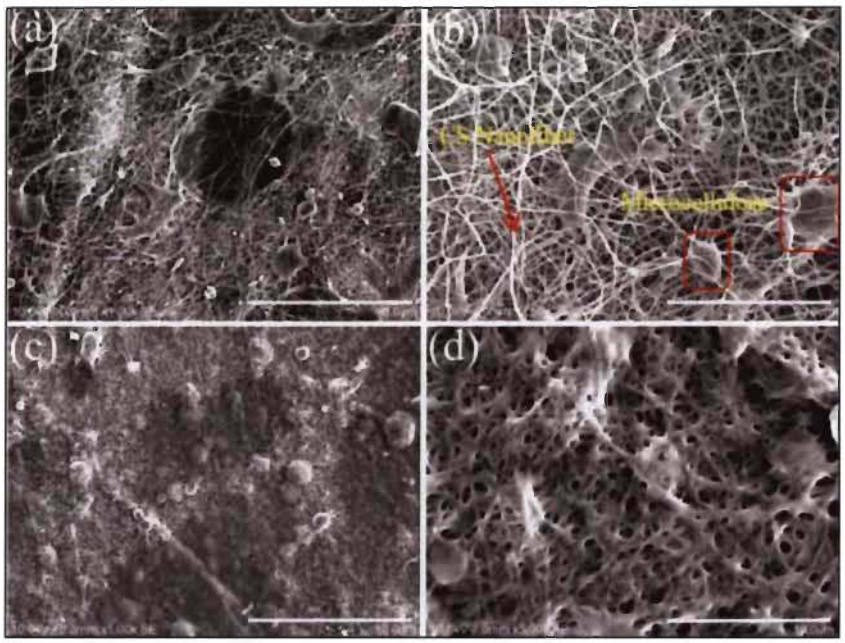

Figure 5.4 SEM images of the CS/PEO/PMC electrospun nanofibers, before (a and b) and after (c and d) sodium carbonate treatment

However, based on particle size distribution of PMC's dispersion (see Figure 5.1c) and the EDX analysis of CS/PEO/PMC mats (see Figure 5.2), it is believed that some PMC microparticles never reached the foil collector during electrospinning. According to Figure 5.4 b, very few PMC microparticles are found, at least on the surface of the mat. This may be one of the reasons to explain the low amount of phosphorous element detected by EDX analysis. It is also possible that even with the magnetic bar mixing setup used inside the syringe; there was some level of PMC aggregation and sedimentation, which limited their flow up to the collector.

Figure 5.5 presents FTIR spectra of CS/PEO and CS/PEO/PMC mats. The typical PEO absorption peaks at 1112 cm^{-1} (vibration stretching of the ether C-O-C group) and at 2781 cm^{-1} (C-H bending) were found in both spectra [126]. Chitosan typical absorption peaks were found at 3450 cm^{-1} (OH hydroxyl group), at 3360 cm^{-1} (NH group-stretching vibration), 1590 cm^{-1} (NH_2 amine group) and at 1560 cm^{-1} (NH-bending vibration in amide group) for both mats [127]. However, for the CS/PEO/PMC, new absorption peaks were found at 920 cm^{-1} (P-OH stretching vibration of the phosphoric group), at 1215 cm^{-1} (P=O stretching), at 1050 and 785 cm^{-1} (P-O-C bands) [123], both corresponding to

phosphorylated microcellulose particles, which confirm the presence of phosphorous groups.

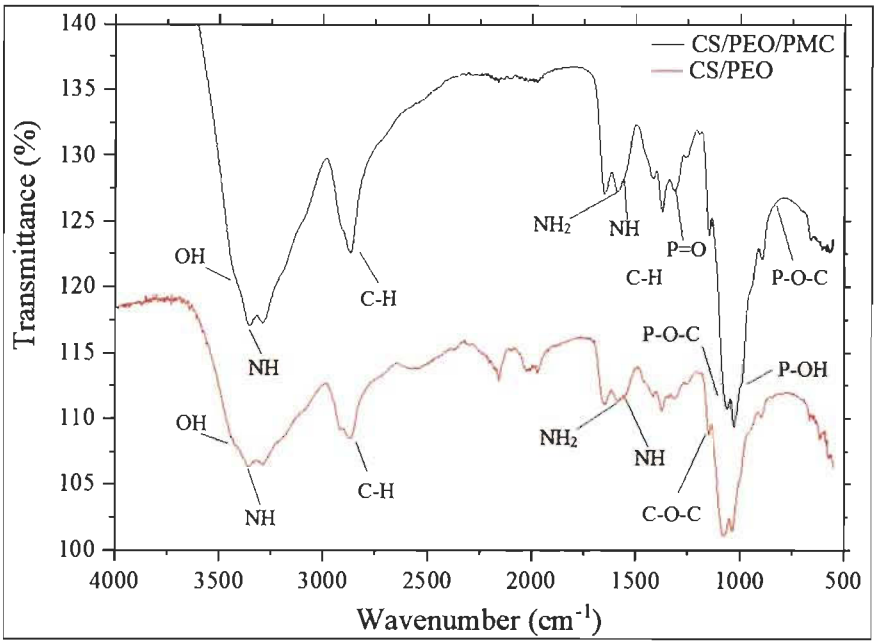

Figure 5.5 FTIR spectra of CS/PEO and CS/PEO/PMC electrospun mats

Figure 5.6 shows DSC spectra for CS/PEO and CS/PEO/PMC mats.

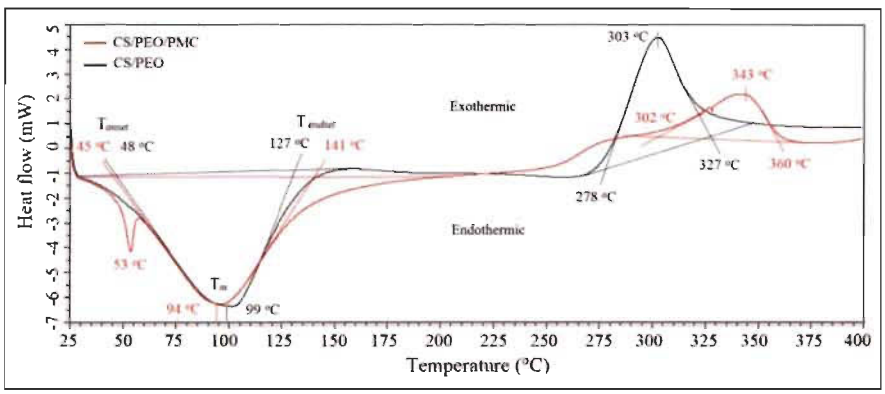

Figure 5.6 DSC spectra of CS/PEO and CS/PEO/PMC electrospun mats

The CS/PEO curve begins its thermal event at 48°C (onset temperature), with an endothermic peak or melting temperature at 99°C and an endset temperature at 127°C. By increasing the temperature, the material has an exothermic peak with an onset temperature at 278°C, a peak at 303°C and an endset temperature of 327°C. This peak can be characterized as a cross-linking event. For composite material based on CS/PEO/PMC, at

a temperature of 53°C, it is possible to see a small endothermic peak, which is typical of an impurity. For this material, the onset temperature is at 45°C, with melting temperature at 94°C and endset temperature at 141°C. The exothermic event presented onset at 302°C, peak at 343°C and endset at 360°C. The endothermic peak corresponds the fusion transition or a first order transition, due to the size distribution of crystalline regions present in macromolecules. The temperature at which crystallinity completely disappears is referred to as the fusion point of the material and corresponds approximately to the maximum melting peak in the DSC curve. These results showed that the addition of PMC increased the endothermic peak area increasing the final melting temperature of the composite material. In other words, the material requires more energy to merge completely all the crystalline domains. The crystallization process is the opposite of the fusion process, that is, it is accompanied by latent heat release, which generates a well-defined exothermic peak in the DSC curves.

The XRD spectra of CS/PEO and CS/PEO/PMC samples are shown in Figure 5.7.

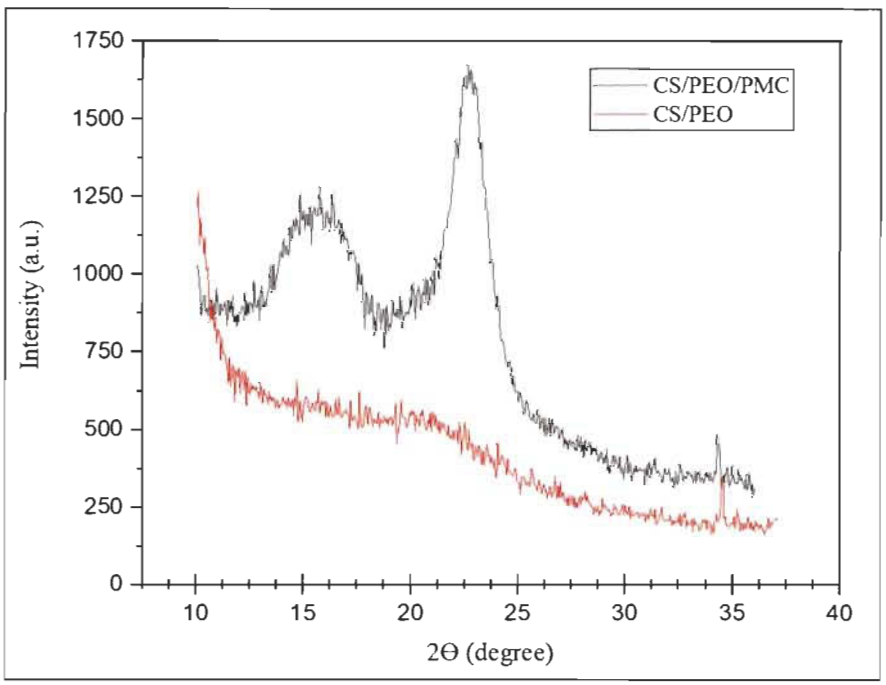

Figure 5.7 XRD spectra of CS/PEO and CS/PEO/PMC electrospun mats

CS/PEO/PMC sample presented three typical cellulose I diffraction peaks at (020) in diffractograms at 22.4°, as well as intensities of (101) and ($10\bar{1}$) lattice diffractions at 14.8°

and 16.1°, being typical diffraction patterns of cellulose I [44, 128]. In other words, PMC preserved the essential spectra features of cellulose I displayed by their native ones. These peaks confirm the presence of PMC in the CS/PEO/PMC composite material. Chitosan normally presents peaks at 10.67° (020) and 19.92°, however, they were not clear in the CS/PEO spectrum. The percentage crystallinity calculated using Seagal's equation from diffractograms was found to be around 78% and 80% for native CS/PEO and CS/PEO/PMC, respectively, being increased after PMC addition.

5.7.4 pH effect

The pH is an important variable for heavy metals adsorption. The effect of the solution pH on Cd^{2+} adsorption by CS/PEO/PMC at equilibrium was investigated for initial solution pH ranging between 3.0-8.0, at 25°C (Figure 5.8), the other adsorption parameters were kept constant.

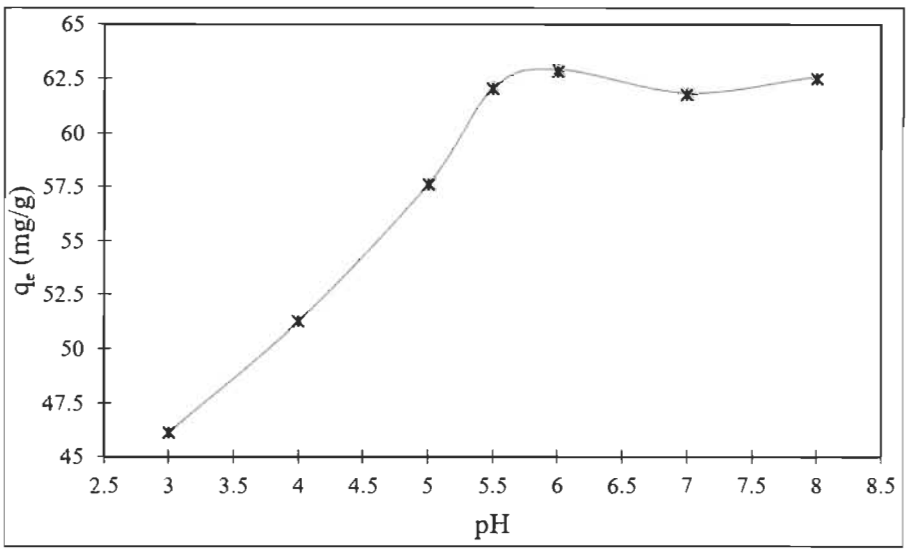

Figure 5.8 pH effect on the Cd^{2+} adsorption for a CS/PEO/PMC nanofiber mat

The desired pH's were adjusted by addition of hydrochloric acid solution or sodium hydroxide solution. The chitosan contains amine groups ($-NH_2$) and the PMC contains phosphate groups (PO_4^-) which are responsible for heavy metals adsorption. Therefore, the charge of the adsorbent surface determines the type of bond between the metal ion and the adsorbent surface. Below pH 7, the solution becomes more acidic (more H^+ ions) and above pH 7 the solution becomes more alkaline (more OH^- ions). At pH 3, the groups

from CS and PMC are in the protonated form and the adsorption of Cd^{2+} is close to zero, but with the increase of the pH, the groups start to dissociate and the Cd^{2+} adsorption increases until the pH is around 6.5 [73, 129]. Over this value, the amount of Cd^{2+} adsorption by CS/PEO/PMC is almost constant. A maximum adsorption was observed between pH 5.5 and pH 7.0, as the pH of the solution increased above 8, cadmium started to precipitate from solution, value that is according to the Cd (II) speciation table [130].

5.7.5 Effect of contact time

Figure 5.9 (a) and (b) show the effect of the contact time on Cd^{2+} removal by CS/PEO and CS/PEO/PMC electrospun nanofibers. The experimental data show a gradual increase in the adsorption capacity with time until a maximum value is achieved for both materials. This value corresponds to the equilibrium time (3h in both cases). CS/PEO/PMC and CS/PEO mats reached a maximum adsorption capacity of Cd^{2+} of 72.64 mg/g and 58.20 mg/g, respectively.

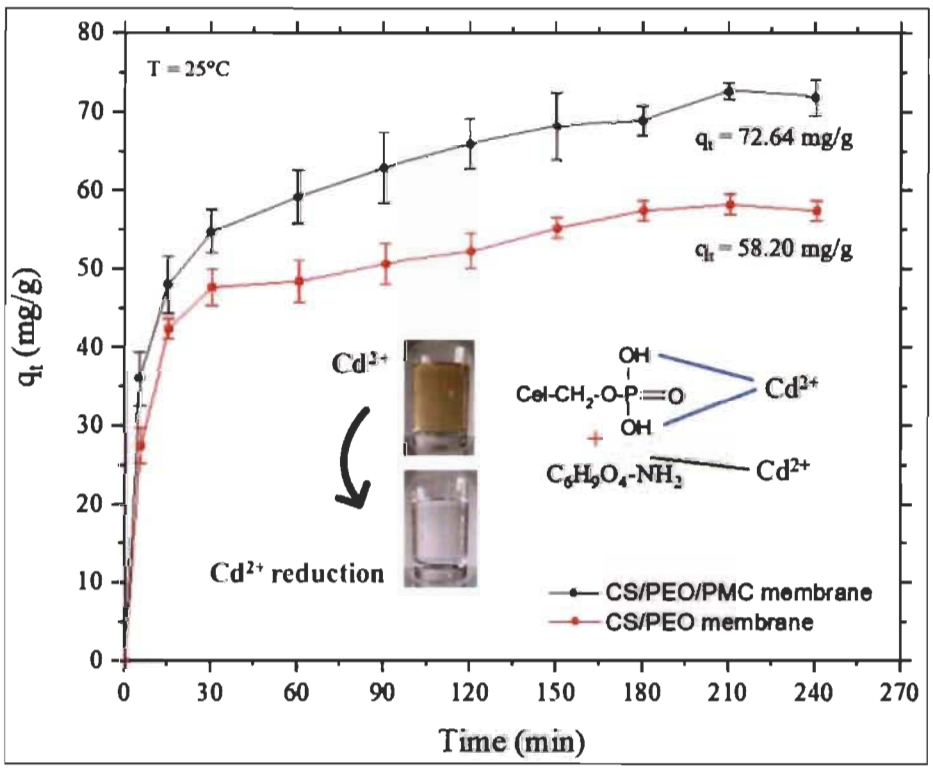

Figure 5.9 Effect of contact time on Cd^{2+} removal by CS/PEO and CS/PEO/PMC electrospun nanofibers

5.7.6 Adsorption kinetics

The non-linear pseudo-first order and pseudo-second order models were applied to the experimental data in order to investigate the mechanisms that control the adsorption process, validate the experimental data and provide the kinetic parameters. Figure 5.10 (a) shows the pseudo-first order fit plot and Figure 5.10 (b) the pseudo-second order fit plot for the CS/PEO and CS/PEO/PMC mats. It is clear that the pseudo-second order model better fit the experimental data.

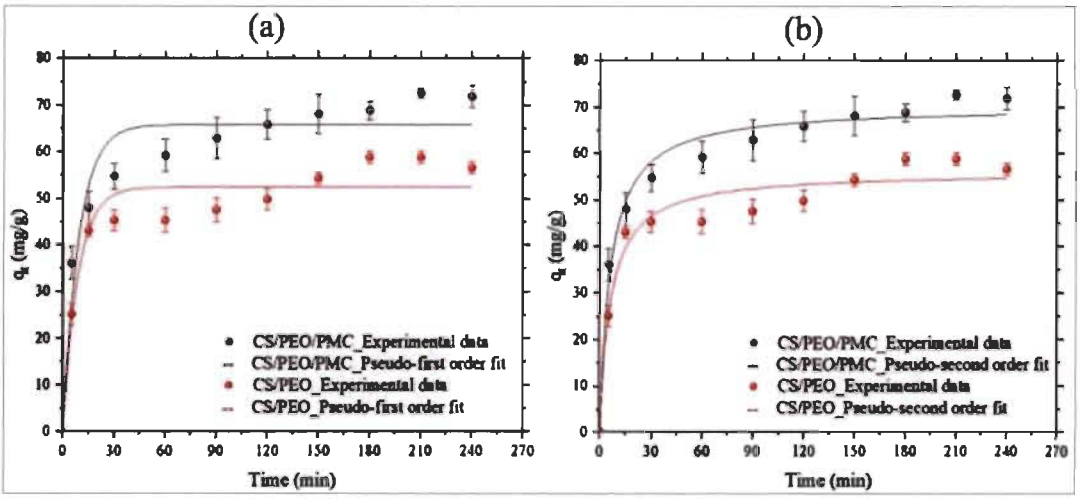

Figure 5.10 Kinetic models plot of Cd^{2+} on CS/PEO and CS/PEO/PMC electrospun nanofibers

Chitosan is a recognized metal chelating agent for removal of metallic impurities in wastewaters. It has a high chelating ability of more than 1 mmol/g for heavy metals. Kinetic parameters for both models are presented in (Table 5.2).

Table 5.2 Kinetic model parameters for Cd^{2+} adsorption on CS/PEO and CS/PEO/PMC nanofibers

Kinetic model parameter	*CS/PEO nanofibers*	*CS/PEO/PMC nanofibers*
Pseudo-first order model		
R^2	0.921	0.922
K_1 (min^{-1})	0.1162	0.1083
q_e (mg/g)	52.48	65.87
Pseudo-second order model		
R^2	0.955	0.976
K_2 (mg/mg min^{-1})	0.0028	0.0023
q_e (mg/g)	56.10	70.17
h (mg/g.min)	8.81	11.32

A higher R^2 value confirmed that the pseudo-second-order model provides a better correlation with experimental data for both materials [131]. The pseudo-second order model suggests a chemisorption mechanism, where for the CS/PEO/PMC mat, occurs an electron exchange between phosphate groups and Cd^{2+} and sharing of electrons between Cd^{2+} and amine groups in binding sites. The initial adsorption rates calculated with the pseudo-second order model were 8.81 and 11.32 mg/g.min and the equilibrium adsorption capacities were 56.10 and 70.17 mg/g for CS/PEO and CS/PEO/PMC mats, respectively. The approximate 25% increase in initial adsorption rate and adsorption capacity at equilibrium for the CS/PEO/PMC mat can be attributed to the phosphate groups that can adsorb faster and more the Cd^{2+} on the accessible sites through ion exchange.

5.7.7 Equilibrium adsorption

When the adsorbate is placed in contact with the adsorbent, the ions tend to flow from the aqueous medium to the surface of the adsorbent until the solute concentration in the liquid phase (C_{eq}) remains constant. At this stage, the system has reached the equilibrium state and the adsorption capacity of the adsorbent (q_{eq}) is determined. Figure 5.11 shows the plot of q_{eq} versus C_{eq}, for Cd^{2+} initial concentration ranging from 50 and 300 mg/L, at temperatures of 25, 40 and 60°C. Results indicate that the adsorption capacity increases with an increase in the Cd^{2+} initial concentration. When the initial concentration was 300 mg/L at 25°C, the adsorption capacity reached 152.14 mg/g, almost four times higher than the capacity when the initial concentration was 50 mg/L (38.60 mg/g). At 300 mg/L, there is a higher concentration gradient transferring more cadmium ions due to the driving force. This gives more opportunities for the ions to contact the adsorbent, bonding more ions to the active sites. Regarding the temperature, the adsorption capacity increased gradually.

5.7.8 Adsorption isotherms

For isotherm models, the relation of q_{eq} versus C_{eq} can be expressed in mathematical form, and the maximum adsorption capacity of an adsorbent can be predicted. Adsorption isotherm models were applied to experimental data in order to determine the efficiency and maximum adsorption capacity [131, 132]. Non-linear Langmuir, Freundlich and Dubinin-Radushkevich

models were used to describe the adsorption isotherms. The plot, fitting and corresponding parameters of the models are shown in Figure 5.11 and Table 5.3.

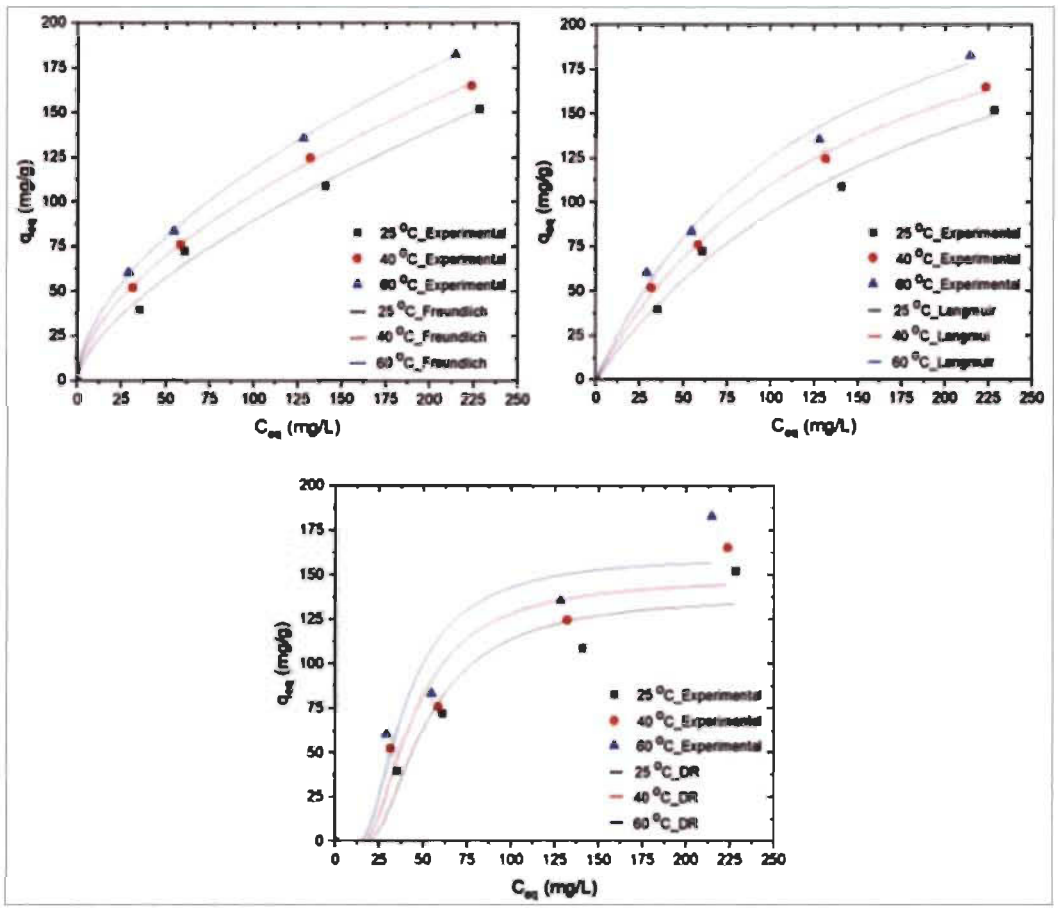

Figure 5.11 Non-linear isotherm models of Cd^{2+} adsorption on CS/PEO/PMC mats

The curves in Fig. 11 are a favorable isotherm, which informs that the mass of the adsorbate retained per unit mass of the adsorbent is high for a low equilibrium concentration of the adsorbate in the liquid phase [133]. Results indicate that the R^2 values were higher for the Langmuir model. This result evidences that Cd^{2+} adsorption occurred in an ideal monolayer on the homogeneous surface of the CS/PEO/PMC mat. The maximum adsorption capacity (q_{max}) found was 283 mg/g at 60°C. The K_L values increased with increasing temperature, confirming the endothermic nature of the adsorption. The degree of development of the adsorption process (R_L) were less than 1, then the adsorbate prefers the solid to the liquid phase and the adsorption is said to be favorable [134]. The experimental data fitted better to the model proposed by Langmuir, so we can consider: that there is a defined number of sites on the mat (which have equivalent energy), the adsorbed molecules do not

interact with each other, adsorption occurs on a monolayer and each site can contain only one adsorbed molecule.

Table 5.3 Parameters obtained from the plots of Langmuir, Freundlich, and Dubinin-Radushkevich isotherm non-linear models for Cd^{2+} adsorption on CS/PEO/PMC nanofibers

Isotherm model parameter	$T = 25$ °C	$T = 40$ °C	$T = 60$ °C
Langmuir			
R^2	0.989	0.997	0.990
K_L (L/mg)	0.0051	0.0069	0.0079
q_{max} (mg/g)	275.86	267.89	283.13
R_L	0.670	0.616	0.592
Freundlich			
R^2	0.990	0.999	0.999
K_f [(mg/g) (mg/L)$^{1/n}$]	4.73	7.25	8.97
$1/n$	0.639	0.578	0.560
Dubinin-Radushkevich			
R^2	0.921	0.893	0.872
K (mol^2/J^2)	28.77	16.18	17.32
q_{DR} (mol/g)	138.76	148.69	160.95
E (kJ/mol)	0.187	0.249	0.240

5.7.9 Adsorption mechanisms

Figure 5.12 Scheme presenting the adsorption mechanisms on CS/PEO/PMC mat presents in a simplified way the binding mechanisms that occur between cadmium ions and the CS/PEO/PMC material in aqueous solution. The solution is basically composed of Na^+, Cd^{2+} and H_2O at pH 5.5. The amino groups available on the surface of chitosan can chemically interact with Cd^{2+} through a chemical complexation process, where two electrons are shared between Cd^{2+} and the amino group. Already the phosphate groups present on the surface of phosphorylated cellulose can interact chemically with Cd^{2+} through ion-exchange, where 2 Na^+ can be replaced by Cd^{2+}.

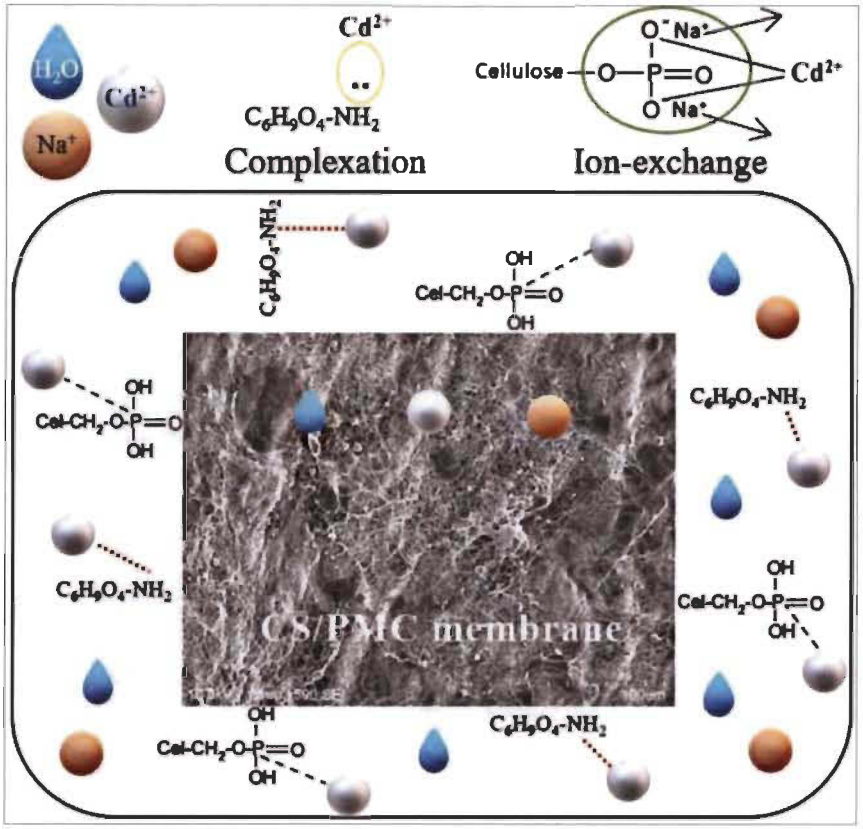

Figure 5.12 Scheme presenting the adsorption mechanisms on CS/PEO/PMC mat

5.7.10 Thermodynamic study

Thermodynamic parameters for the adsorption of Cd^{2+} by CS/PEO/PMC mats are shown in (Table 5.4).

Table 5.4 Thermodynamic parameters for Cd^{2+} adsorption on CS/PEO/PMC mats

Temperature (°C)	R^2	ΔH (kJ)	ΔS (kJ/K)	ΔG (kJ)
25	0.999	6.9689	0.0224	0.2883
40	-	-	-	-0.0477
60	-	-	-	-0.4958

The flow of energy between the system and the neighborhood can be employed with the criterion of spontaneity. Those in which energy leaves the system are termed exergonic (ΔG <0) and thus spontaneous. Conversely, when the energy brings into the system (ΔG >0), the process is said to be endergonic, and is not spontaneous. The Gibbs free energy

values (ΔG) calculated went from positive to negative, which suggests a spontaneous adsorption of Cd^{2+}. The positive values of enthalpy (ΔH) and entropy (ΔS) found are assigned to the endothermic nature of the process and show an increase of the randomness degree of the adsorbent-adsorbate system, respectively. These results agree with Lakhdhar *et al.* [19] and Aliabadi *et al.* [70].

5.7.11 Cd^{2+} sorption-desorption study

The removal rates for Cd^{2+} of regenerated CS/PEO/PMC mat and the residual weight after up to five consecutive adsorption–desorption cycles are presented in Figure 5.13 (a-b). Results show that after 5 cycles, the material loses approximately 42% of its adsorption capacity. This can be explained by the degradation of functional groups caused by the regeneration step performed with EDTA after each cycle. CS/PEO/PMC weight loss after 5 cycles was around 3.5%, which can be considered a low value.

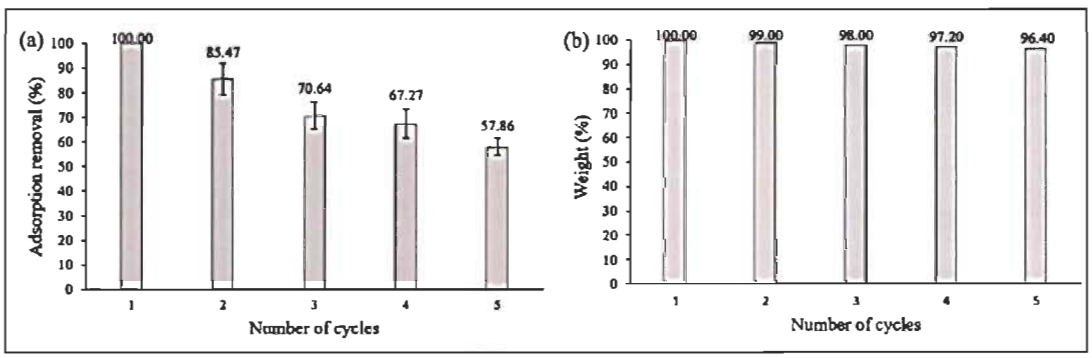

Figure 5.13 Adsorption-desorption evaluation of the CS/PEO/PMC nanofibers. Adsorption capacity (a) and residual weight (b) after 5 cycles

5.8 Conclusions

CS/PEO/PMC electrospun mat was successfully developed for Cd^{2+} removal from aqueous solutions. Morphological analysis showed a material containing phosphorylated microcellulose and CS/PEO nanofibers. The microparticles were mechanically anchored among the nanofiber matrix. EDX analysis confirmed the presence of phosphorous peaks and FTIR and XRD the presence of phosphate groups. DSC analysis showed that the melting temperature was not drastically affected by the addition of PMC. The contact time evaluation reported an equilibrium time of 3h and the application of the pseudo-second

order model best fitted with the experimental data, suggesting a chemisorption mechanism. Equilibrium analysis showed that the adsorption capacity increased at higher temperatures and initial concentrations. Among the isotherm's models tested, Langmuir best fitted experimental data. The maximum adsorption capacity for Langmuir model at 25°C was 283 mg/g. The thermodynamic study revealed an exergonic and endothermic nature of the reaction. The sorption-desorption study showed that the adsorption mat lost approximately 42% of its adsorption capacity and 3.5% of their weight after 5 recycling stages, which was considered acceptable. The development of this electrospun nanocomposite mat is very promising and appropriate since it has shown a high efficiency, in addition to having used of two renewable biopolymers, and the possibility of easy production. Certainly, this material is a strong ally in the preservation and recovery of the environment.

Chapitre 6 - Article 3

6.1 Phosphorylated cellulose/electrospun chitosan nanofibers media for removal of heavy metals from aqueous solutions

6.2 Foreword

This third article is entitled "Phosphorylated cellulose/electrospun chitosan nanofibers media for removal of heavy metals from aqueous solutions". It has submitted to Journal of Applied Polymer Science, May 2020.

Authors and their corresponding addresses are in the following order:

Ricardo Brandes, PhD student in Science and Engineering of Lignocellulosic Materials PhD program

Innovation Institute on Ecomaterials, Ecoproducts and Ecoenergies based on Biomass (I^2E^3), Université du Québec à Trois-Rivières, 3351 boulevard des Forges, Trois-Rivières, Quebec, G9A 5H7, Canada

François Brouillette, PhD.

Thesis co-supervisor

Innovation Institute on Ecomaterials, Ecoproducts and Ecoenergies based on Biomass (I^2E^3), Université du Québec à Trois-Rivières, 3351 boulevard des Forges, Trois-Rivières, Quebec, G9A 5H7, Canada

Bruno Chabot, PhD.

Thesis supervisor

Innovation Institute on Ecomaterials, Ecoproducts and Ecoenergies based on Biomass (I^2E^3), Université du Québec à Trois-Rivières, 3351 boulevard des Forges, Trois-Rivières, Quebec, G9A 5H7, Canada

Authors contributions: Ricardo Brands is the main author of the article. He did all the experimental work, laboratory setup developments and wrote the manuscript. Dr. Dan Belosinschi provided the phosphorylated nanocellulose. Dr. Brouillette is the thesis co-supervisor and provided materials and laboratory facilities and he helped with manuscript corrections. Dr. Chabot is the thesis supervisor and provided materials and laboratory facilities. He provided guidance and helped in the preparation and correction of the manuscript.

6.3 Résumé

La contamination des ressources hydriques par des métaux lourds et toxiques a des répercussions importantes sur l'environnement et la santé humaine. Leur élimination des milieux aqueux est essentielle pour assurer la durabilité de l'eau et pour fournir de l'eau douce fraiche à la population. Les tapis non tissés en chitosane électrofilé sont efficaces pour éliminer les métaux lourds des milieux aqueux. Cependant, ils souffrent d'une faible perméabilité et d'une faible résistance mécanique. Ils sont également incapables d'éliminer les contaminants de manière non sélective. Un milieu absorbant bicouche composé d'un substrat poreux de cellulose phosphorylée recouvert de nanofibres de chitosane électrofilées a été mis au point pour surmonter ces faiblesses. Le composite hydrophile présente une bonne perméabilité à l'eau et une bonne résistance mécanique avec des caractéristiques thermiques et chimiques appropriées. Les tests d'adsorption avec le Cd (II) indiquent que les modèles de pseudo-seconde ordre et de Langmuir correspondent le mieux aux données expérimentales, avec une capacité d'adsorption maximale de 591 mg/g à 25°C. L'adsorption avec des échantillons multi-éléments contenant du Cr (VI), du Cu (II), du Cd (II) et du Pb (II) révèle également leur capacité à les éliminer de manière sélective. Ce milieu adsorbant, mécaniquement résistant, hydrophile et perméable a été capable de capturer les contaminants métalliques tant cationiques qu'anioniques, montrant un énorme potentiel d'application dans les systèmes de filtration, ce qui pourrait améliorer considérablement l'efficacité de ces systèmes et contribuer également à la conservation de l'environnement.

Mots-clés: Traitement des eaux usées, Adsorption, Fibres de cellulose phosphorées, Nanofibres de chitosane, Nanocomposite biosorbant.

6.4 Abstract

Contamination of water resources by toxic heavy metals has significant impacts on environmental and human health. Their removal from aqueous media is essential to ensure water sustainability and to provide safe freshwater availability to population. Electrospun chitosan nonwoven mats are efficient at removing heavy metals from aqueous media. However, they suffer from low permeability and low mechanical strength. They are also unable to remove contaminants in a non-selective way. A bi-layer sorbent media made of a porous phosphorylated cellulose substrate covered by electrospun chitosan nanofibers was developed to overcome those weaknesses. The hydrophilic composite shows good water permeability and mechanical strength with appropriate thermal and chemical characteristics. Adsorption tests with Cd(II) indicate that pseudo-second order and Langmuir models best fitted experimental data, with a maximum adsorption capacity of 591 mg/g at 25°C. Adsorption with multi-element samples containing Cr(VI), Cu(II), Cd(II) and Pb(II) also reveal their capability to remove them in a selective way. This mechanically resistant, hydrophilic and permeable adsorbent media was able to capture both cationic and anionic metallic contaminants, showing an enormous potential for application in filtering systems, which could greatly improve the efficiency of these systems and also help in environmental conservation.

Keywords: Wastewater treatment, Adsorption, Phosphorylated cellulose fibers, Chitosan nanofibers, Biosorbent nanocomposite.

6.5 Introduction

Tertiary water treatment processes are much more efficient to remove them. Unfortunately, most of them are expensive or present operational and economic limitations, especially for developing countries. Since fresh water is a finite resource, a shortage or lack of it could have catastrophic consequences for humanity [117, 135-138].

Among those, the adsorption/filtration process is one of the most promising technology to meet those purposes [139]. The process uses materials with high specific surface area and surface functional groups to capture contaminants. Biopolymers such as phosphorylated cellulose fibers (PCF) and chitosan (CS) are attractive materials for such purposes. They contain free functional groups on their surfaces such as phosphate and amine groups, respectively to interact with ionic contaminants [140, 141]. Phosphate groups has the ability to adsorb mainly cationic contaminants such as Cu(II), Cd(II), Pb(II) while amine groups can adsorb anionic species such as Cr(VI). Most of those biopolymers come from renewable sources, such as wood, plants, crabs or shrimps. They are also biodegradable [142].

Two technologies are widely used for water treatment applications, membrane filtration and adsorption [143]. Porous membranes are manufactured via casting, lamination, extrusion, etc. They remove contaminants by a screening process. Particles larger than pore diameters are simply retained on one side of the membrane while smaller ones are allowed to permeate through the pores. Adsorption is a surface phenomenon where surface interactions are involved between contaminants and chemical groups. Porous materials are required to provide high specific surface area. The larger the available surface area, the higher the adsorption capacity. However, both technologies present inherent limitations. Membrane technologies are energy intensive since they require powerful pumps to overcome large pressure gradients, especially for those with very small pore diameters such as those used in nanofiltration and reverse osmosis. They are also prone to reversible and irreversible fouling leading to lower permeate flux with time. For adsorption, large surface area as well as surface functionality of the adsorbent have a significant effect on the process. Therefore, materials with high porosity, small particle size and contaminant-specific functional groups are required to achieve a high removal efficiency. The development of a material combining both features would thus provide a significant technological edge to the water treatment field.

Electrospun nonwoven mats are widely studied for adsorption of various contaminants in water [141, 144]. They are made of randomly laid nanofibers forming a thin porous structure. Nanofibers surface functionality is controlled by appropriate selection of

polymers or polymer's mixture prior to electrospinning. An experimental set-up consisting of a high voltage power supply, a pump/syringe system and a metal collector is used to make them [145].

Chitosan-based electrospun membranes have been widely studied as adsorbent for heavy metal uptake in aqueous solutions. They show good efficiency in single-contaminant environments. However, not many studies report using chitosan membranes for multi-heavy metal mixtures or even solutions containing both anions and cations, which may compete for active adsorption sites [146, 147]. Typical nonwoven electrospun mats present several disadvantages such as low mechanical strength and low liquid permeability. Those weaknesses are thus limiting their filtration ability in continuous adsorption configuration, which is more closely simulating industrial processes.

In this study, a two-layer adsorbent media made of a porous phosphorylated cellulose substrate coated by electrospun chitosan nanofibers was developed to overcome those weaknesses. Morphological, mechanical, thermal and chemical characterizations were performed. The adsorption capability was carried out with cadmium ions. Finally, the effect of multi-heavy metal contents was studied using a solution containing cationic ions (Cd(II), Cu(II), Pb(II)), and anionic ions (Cr(VI)) to establish their potential competing role for adsorption sites during experimentation.

Fresh water availability is important for the living beings. However, over the years this resource has been used and contaminated by human activities. Fresh water is extensively used by several industrial sectors such as mining, papermaking, tanneries, pesticides and pharmaceuticals in their production processes. It is also widely used for agriculture. Water pollution by heavy metals is one of the consequences [148-150]. Heavy metals such as cadmium, copper, lead or even hexavalent chromium are considered very toxic to living beings. Consumption of contaminated water by humans in significant doses can cause serious health problems, such as cancer. Contamination levels higher than 10 mg/L have been observed in various countries. However, it is known that levels as low as 0.5 mg/L could be at risk for humans [151, 152]. Heavy metals are difficult to remove by standard primary and secondary water treatment processes [153]. Tertiary water treatment processes are much more efficient to remove them. Unfortunately, most of them are

expensive or present operational and economic limitations, especially for developing countries. Since fresh water is a finite resource, a shortage or lack of it could have catastrophic consequences for humanity. The preliminary wastewater treatment seeks to remove grains and solids. Bar grids or mechanical screens remove paper, rags and other large solids. Sand and grit are removed by gravity, settling in a grit chamber. After the preliminary treatment, the water passes to a clarifier or decantation tank, which is called primary treatment. The sewage solids are deposited at the bottom of the tank. The solids that accumulate at the bottom of the tank are called primary sludge and are pumped from the tank for treatment elsewhere in the plant. The secondary or biological treatment is performed in a tank containing microbes called activated sludge. The microorganisms in this aeration tank use the dissolved and particulate organic matter as food, producing more microorganisms that can be collected and separated from the water in the next step. It then remains to separate the microorganisms (activated sludge) so that only clean water is left. This is done in a secondary clarifier that operates in the same way as the primary clarifier described above. The tertiary treatment, also called advanced waste treatment, provides the removal of contaminants in addition to that obtained in the primary (physical settlement) or secondary (biological) treatment. It can include additional removal of organic matter or solids, reductions in the concentration of nutrients such as nitrogen and phosphorus or treatment of toxic substances, such as heavy metals [140-143].

Research efforts are actually focusing on the development of cheaper and more efficient tertiary treatment technologies [154, 155]. Among those, the adsorption/filtration process is one of the most promising technologies to meet those purposes [146]. The process uses materials with high specific surface area and surface functional groups to capture contaminants. Biopolymers such as phosphorylated cellulose fibers (PCF) and chitosan (CS) are attractive materials for such purposes. They contain free functional groups on their surfaces such as phosphate and amine groups, respectively to interact with ionic contaminants [147, 148]. Phosphate groups has the ability to adsorb mainly cationic contaminants such as Cu (II), Cd (II), Pb (II) while amine groups can adsorb anionic species such as Cr (VI). Most of those biopolymers come from renewable sources, such as wood, plants, crabs or shrimps. They are also biodegradable [149].

Two technologies are widely used for water treatment applications, membrane filtration and adsorption [150]. Porous membranes are manufactured via casting, lamination, extrusion, etc. They remove contaminants by a screening process. Particles larger than pore diameters are simply retained on one side of the membrane while smaller ones are allowed to permeate through the pores. Adsorption is a surface phenomenon where surface interactions are involved between contaminants and chemical groups. Porous materials are required to provide high specific surface area. The larger the available surface area, the higher the adsorption capacity. However, both technologies present inherent limitations. Membrane technologies are energy intensive since they require powerful pumps to overcome large pressure gradients, especially for those with very small pore diameters such as those used in nanofiltration and reverse osmosis. They are also prone to reversible and irreversible fouling leading to lower permeate flux with time. For adsorption, large surface area as well as surface functionality of the adsorbent have a significant effect on the process. Therefore, materials with high porosity, small particle size and contaminant-specific functional groups are required to achieve high removal efficiency. The development of a material combining both features would thus provide a significant technological edge to the water treatment field. Electrospun nonwoven mats are widely studied for adsorption of various contaminants in water [144, 156]. They are made of randomly laid nanofibers forming a thin porous structure. Nanofibers surface functionality is controlled by appropriate selection of polymers or polymer's mixture prior to electrospinning. An experimental set-up consisting of a high voltage power supply, a pump/syringe system and a metal collector is used to make them [145]. Chitosan-based electrospun membranes have been widely studied as adsorbent for heavy metal uptake in aqueous solutions. They show good efficiency in single-contaminant environment. However, not many studies are reported using chitosan membranes for multi-heavy metal mixtures or even solutions containing both anions and cations, which may compete for active adsorption sites. Typical nonwoven electrospun mats present several disadvantages such as low mechanical strength and low liquid permeability. Those weaknesses are thus limiting their filtration ability in continuous adsorption set-up configuration, which is more closely simulating industrial processes. There are some studies in the literature that use materials to adsorb multi-cationic contaminants in aqueous solutions. Bouhamed *et*

al. [157] used activated carbon to adsorb Cu^{2+}, Ni^{2+} and Zn^{2+} using a real wastewater aiming at the treatment of contaminated effluents. However, Taha *et al.* [158] applied an Egyptian Na-activated bentonite adsorbent in the desalination of seawater to capture Cd (II), Pb (II) e Ni (II). Phosphorylated cellulose produced in different shapes for the adsorption of heavy metals has been confirmed as an excellent adsorbent. For example, Shahi *et al.* [159] used a phosphorylated triacetate-silica composite adsorbed Ni (II), Luo *et al.* [160] produced phosphorylated cellulose microspheres to adsorb the Pb (II) and Ojima *et al.* [161] produced a phosphorylated dry baker's yeast to adsorb a large number of metal cations, such as Cd (II), Cu (II), Pb (II), Zn (II) and even rare earth ions, including Ce (III), Dy (III), Gd (III), La (III), Nd (III), Y (III) and Yb (III). In another way, for the capture of metal anions, some authors used the chitosan successfully. For example, Sessarego *et al.* [159] used phosphonium-enhanced chitosan and Zhang *et al.* [162] used multicavity triethylenetetramine-chitosan/alginate composite beads for Cr (VI) adsorption. Although we have found in literature several works with different adsorbents for the capture of different metallic contaminants, we have not found works reported to produce a phosphorylated cellulose/chitosan based composite capable of capturing anions and metallic cations on the same material.

Thus, in this study, a bi-layer adsorbent media made of a porous phosphorylated cellulose substrate covered by electrospun chitosan nanofibers was developed to overcome those weaknesses. Morphological characterizations were performed using optical microscope (OM), scanning electron microscope (SEM), contact angle and X-ray diffraction (XRD). The mechanical properties were tested through the tensile strength test. The thermal behavior was studied using differential scanning calorimetry (DSC), and the chemical characteristics were assessed via energy-dispersive X-ray spectroscopy (EDX) and Fourier-transform infrared spectroscopy (FTIR). Adsorption study was carried out with cadmium ions. Finally, the effect of multi-heavy metal contents was studied using a solution containing cationic ions (Cd (II), Cu (II), PB (II)), and anionic ions (Cr (VI)) to establish their potential competing role for adsorption sites during experimentation.

6.6 Materials and Methods

6.6.1 Materials and chemicals

Chitosan powder, low molecular weight with deacetylation of 75-85% (Sigma-Aldrich) and glacial acetic acid 99.7% (Fischer brand) were used to prepare chitosan electrospinning solutions. Poly (ethylene oxide) (PEO) powder with average molecular weight of 900 000 (Sigma-Aldrich) dissolved in distilled water was used as a polymer co-agent in order to increase the electrospinning ability. Cellulose Kraft fibers (CKF) were supplied by a local paper mill (Trois-Rivières, Canada). Cadmium (II) sulfate anhydrous ($CdSO_4$) (Sigma-Aldrich) was used as the model contaminant for adsorption studies. Ethylenediaminetetraacetic acid (EDTA) (OMEGA Chemical) and ammonium hydroxide (Fischer brand) were employed to determine residual ions concentration. Eriochrome Black T (Fischer Scientific Co.) was used as indicator of concentrations determination by complexometric titration. Copper (II) sulfate pentahydrate ($CuSO_4.5H_2O$) (Sigma-Aldrich), lead (II) nitrate (Pb $(NO_3)_2$) ACS reagent ≥99.0% (Sigma-Aldrich), cadmium sulfate anhydrous ($CdSO_4$) (Sigma-Aldrich), and ammonium dichromate ($(NH_4)_2$ Cr_2O_7) (Sigma-Aldrich), were the contaminants used in the multi-element trials. For multi-element experiments, the residual concentrations of each metal were determined using a Microwave Plasma-Atomic Emission Spectrometer (Agilent 4210 MP-AES).

6.6.2 Preparation of Phosphorylated cellulose fiber (PCF) substrate layer

CKF were phosphorylated using the procedure described in Brandes *et al.* [149], where the phosphorylation procedure was performed with a phosphate ester in the presence of molten urea. The fibers were mixed with the chemicals and taken to an oven at a temperature of 145 °C and held for 3 h. Then, the fibers were mixed with a solution containing sodium hydroxide and kept in agitation for 2 h. Finally, they were filtered and washed with acetone and distilled water and dried for 24 h at room temperature. Then, 100 g of PCF were dried in an oven at 80°C for 24 h. Then the dried material was ground for 5 min in a coffee grinder. 1 g of the ground PCF and 100 mL of distilled water were added in a 0.5L beaker, and mixed with a magnetic stirrer for 15 min. 6 mL of the resulting PCF dispersion was then casted in a 25 cm petri dish. It was kept at room temperature for

24 h until complete drying. The substrate was carefully removed from the petri dish with a metal spatula. The cast substrate was then accurately weighed.

6.6.3 Preparation of two-layer adsorption media

For the preparation of the electrospinning solution, at first, Chitosan powder (75-85% deacetylated, 50,000-13,000 Da, Sigma-Aldrich) was dissolved in a 90% acetic acid/10% distilled water (v/v) solution and then PEO powder (MW 900 000 Da, Sigma-Aldrich) was dissolved in distilled water. The solutions were dissolved in separate flasks at 4 wt% and kept in magnetic stirring for 24 h. In second, 60% by mass of chitosan solution and 40% by mass of PEO solution were then mixed for 4 h on a magnetic stirrer. The final solution was then taken to the ultrasonic sonificator (Branson) for 20 minutes. Before proceeding to the electrospinning equipment, the solution rested 3 h in static position. Electrospinning of the polymer solution was carried out using a bench-top device similar to the one described in Brandes *et al.* [149] The PCF substrate was first securely fixed with tapes on the aluminum foil collector. This set-up was selected to allow the deposition of a thin layer of nanofibers on top of the PCF. A voltage of 18 kV, a distance of 20 cm and a polymer flow rate of 0.5 mL/h were used. The electrospinning process was carried out during 2, 4 and 6 h, at 50% relative humidity. Then, the two-layer media was carefully removed from the foil. Finally, this composite material was heat-treated in an oven at 140°C for 30 min.

6.6.4 Characterization of the adsorbent media

The surface morphology of the two-layer media were examined by SEM (HITACHI SU 1510) after coating. The images were obtained from both sides. The SEM is equipped with an EDX microanalysis system (OXFORD Instruments, model Aztec x-max 20). It was used to identify and quantify chemical elements at different locations on the surface of the media. The average diameter of CS-PEO nanofibers and phosphorylated cellulose fibers and average porosity of the adsorbents were calculated using the ImageJ software with the particle analysis and measurement tools (https://imagej.net/ImageJ). The average pore diameter of the adsorbent was calculated according to the bubble point method using a

Sterlitech HP4750 stirred cell, USA. The average pore size was calculated using the Washburn method according to Equation 6.1.

$$D = \frac{-4\gamma \cos\theta}{P} \qquad \text{Eq. 6.1}$$

Where D is the pore diameter (μm); γ the surface tension of water (72 dyn/cm); θ the contact angle (32^0 and 0^0); and P is the pressure (psi).

Contact angles were measured using a FTA 400 (Software for Drop Shape Analysis) tensiometer. The equipment is composed of a CCD camera, a horizontal moving sample holder and a vertical and horizontal displacement syringe holder. Drops of 4 μl were deposited on the surface of the samples using a micro-syringe. The drop images were captured by cameras and processed by the instrument software to determine the contact angle value.

Mechanical properties of adsorbents were determined using an universal testing machine Z005 from Zwick Roell, USA, through uniaxial tensile strength test. All samples were tested in tensile mode with a 0.05 N preload at a displacement rate of 1 in/min at room temperature. Samples were cut in rectangular form (about 10 mm by length, 2 mm by width).

FTIR analysis (PerkinElmer Spectrum FTIR 2000) was performed in the range of 400-4000 cm^{-1}. DSC analysis was done with a DSC 2500 modulus (TA Instruments, USA) with samples containing a mass of 5 g at a heating rate of 10 C min^{-1}. The samples were heated from 25 to 400°C. XRD was performed for material's crystallography by means of a Focus D8 X-ray diffractometer (Bruker, USA).

Flow and permeability were defined using an outlet cell (HP 4750, Sterlitech, USA) with N_2 gas to keep constant pressure at 1 bar. The time of passage of 200 mL of distilled water through the membranes was recorded and used for the flux calculations. The flux, *J*, was calculated according to Equation 6.2.

$$J = \frac{Q_p}{A_m t P} \qquad \text{Eq. 6.2}$$

Where Q_p is the volume of filtrate across the adsorbent media at time (t), A_m is the area of the media and P is the pressure (bar). A_m (14.6 cm^2) is a constant value provided by Sterlitech. The permeability was calculated as flux (J) per unit pressure (bar) multiplied by the thickness of the media (mm).

6.6.5 Adsorption experiments

Batch adsorption tests were performed to evaluate the adsorption of Cd^{2+} by the two-layer media. For kinetic experiments, 30 mg of the media was added to 60 mL solution containing 100 ppm Cd^{2+} in a 250 mL Erlenmeyer flask. The flask was shaken with an orbital shaker (Lab-line Instrument) at a temperature of 25°C, pH 5.5 and 200 rpm. Stirring was provided until the equilibrium concentration was reached. The amount of adsorbed cadmium ions, q (mg/g), was calculated using Equation 2.1 at various contact times (10-300 min). Pseudo-first order and pseudo-second order models were applied according to the nonlinear formulas (Equation 4.2). The initial adsorption rate h (mg ($gmin^{-1}$)) was determined with the k_2 and q_e values of the pseudo-second order model, (Equation 4.3). For equilibrium experiments, the initial concentrations of Cd^{2+} concentrations were 50, 100, 200 and 300 mg/L, which were evaluated at temperatures of 25, 40 and 60°C. The non-linearized Langmuir (Equation 5.5 and Equation 4.3), Freundlich (Equation 2.3)) and Dubinin-Radushkevich (Equation 2.5 and 2.7)) isotherm models were applied to the results. Thermodynamic parameters, Enthalpy change, Entropy change and Gibbs free energy were calculated using Equation 4.11 and 4.12, respectively.

Batch tests were also performed to evaluate the adsorption of multi-heavy metals by the two-layer media. In Erlenmeyer flasks (250 mL), 2 g of the media and 20 mL (5 mL of Cu (II), 5 mL of Pb (II), 5 mL of Cd (II) and 5 mL of Cr (VI)) of 10 ppm solutions were added. Then, the Erlenmeyer flasks were shaken with an orbital shaker (Lab-line Instrument) at a temperature of 25°C, pH 5.5 and 200 rpm. The agitation was provided for 3 h. The maximum adsorption capacity was calculated using Equation 2.1.

6.6.6 Sorption-desorption study of Cd^{2+}

For the adsorption cycles, 10 mg of PCF/CS-PEO adsorbent media was added in a flask with 20 mL of Cd^{2+} (100 ppm) at 25°C, 200 rpm and a pH of 5.5. The content was agitated for 4 h. Then, the solid media was removed and washed three times with deionized water to remove any residual Cd^{2+} on the surface. For the regeneration and desorption evaluation, the media was placed in an Erlenmeyer flask containing 20 mL of HNO_3, HCl and EDTA (0.05 and 0.10 M, respectively) and NHO_3, Ca $(NO_3)_2$, EDTA (0.10 and 0.01 M, respectively). The flask was agitated with an orbital shaker for 3h at 25°C and 200 rpm. The amount of metal ions adsorbed on the media and the residual metal ion concentration in desorption were calculated according to Equation 5.11. The sorption/desorption experiments were performed in duplicate.

6.6.7 Methods of analysis of heavy metal bath concentrations

The concentrations of the baths containing only Cadmium ions were analyzed by the complexation titration method. 5 mL of Cd(II), 0.5 mL of ammonia and 0.5 g of eriochrome Black T were placed in a 25 mL beaker. This beaker was placed on a magnetic stirrer and the contents of the flask were kept under gentle stirring. An EDTA solution (0.001 M) was slowly added to the solution until the end point was achieved. The EDTA volume was recorded and used to calculate the concentration of Cd(II) remaining in the solution.

The analysis of the multi-bath of contaminants was performed using a Microwave Plasma-Atomic Emission Spectrometer. 500 mL of solutions for each heavy metal at 10 ppm were prepared separately in order to calibrate the equipment and the same volume of the dilution matrix (distilled water) was also prepared to calibrate the equipment. The calibration solutions were treated and recorded on the equipment. The standard calibrated wavelengths were of 228 nm for Cd, 425 nm for Cr, 324 nm for Cu, and 405 nm for Pb. 20 mL of the Multi-contaminant solutions at 10 ppm were then fed to the equipment and measurement were done in quintuplicate.

6.7 Results and discussion

6.7.1 Morphology of PCF/CS-PEO adsorbent media

In order to produce an adsorbent media with polyvalent characteristics, which could capture anionic and cationic contaminants, electrospun chitosan nanofibers were deposited on the surface of a phosphorylated cellulose fibers substrate, with different final percentages by weight of chitosan nanofibers, which were approximately 7, 25 and 40 wt%. These adsorbents media are composed of two layers. The first layer was produced by the casting and evaporation technique of phosphorylated cellulose fibers, which is the main substrate of the adsorbent media. This layer has a morphological objective of greater porosity and mechanical resistance. After the production of the first layer was finished, the second layer was deposited under the top of the cellulose fiber substrate via the electrospinning process. Figure 6.1 presents a scheme with real photographs of the CS-PEO nanofibers, PCF substrate and bi-layer adsorbent media. The diagram shows an adsorbent made of CS-PEO nanofibers via electrospinning, an adsorbent produced via casting/evaporation composed of phosphorylated cellulose fibers which is titled PCF substrate and finally the visual result of the bi-layer adsorbent media. It is possible to see in Figure 6.1 the photograph of the PCF substrate which visually looks like a fiber network with pores of different sizes and geometries distributed by the whole area of the material. The macro pores distributed unevenly over the surface of the adsorbent medium are attributed to the casting/evaporation process for the production of this substrate. Accelerated evaporation tended to create larger pores, a factor to which contributed a higher water permeability, however, probably reducing the mechanical properties. The CS-PEO adsorbent presents a more transparent appearance and a nanofiber network to which the porosity appears to be visually closed compared to the PCF substrate. The production of the bi-layer adsorbent media, which was composed by depositing electrospun CS-PEO nanofibers on the PCF substrate can be observed in this same diagram. The diagram shows the top layer of the adsorbent which is composed of CS-PEO nanofibers. The deposition of these nanofibers was adhered to the PCF substrate efficiently and visually the nanofibers appear to have covered and reduced the porosity of the PCF substrate. Deposited nanofibers represented approximately 40% of the total

weight of the bi-layer adsorbent media. Already the bottom layer of the adsorbent media, which is represented by PCF substrate, appears to have slightly reduced its initial porosity and maintained its permeability properties. One of the purposes of the development of a bi layer adsorbent media was to obtain a surface capable of capturing anionic contaminants (chitosan nanofibers) and the other cationic contaminants (PCF substrate). Another purpose was to obtain an adsorbent with water permeability. Thus, the objective was to cover the PCF substrate with chitosan nanofibers without losing its water permeability property, goals that appear to have been achieved.

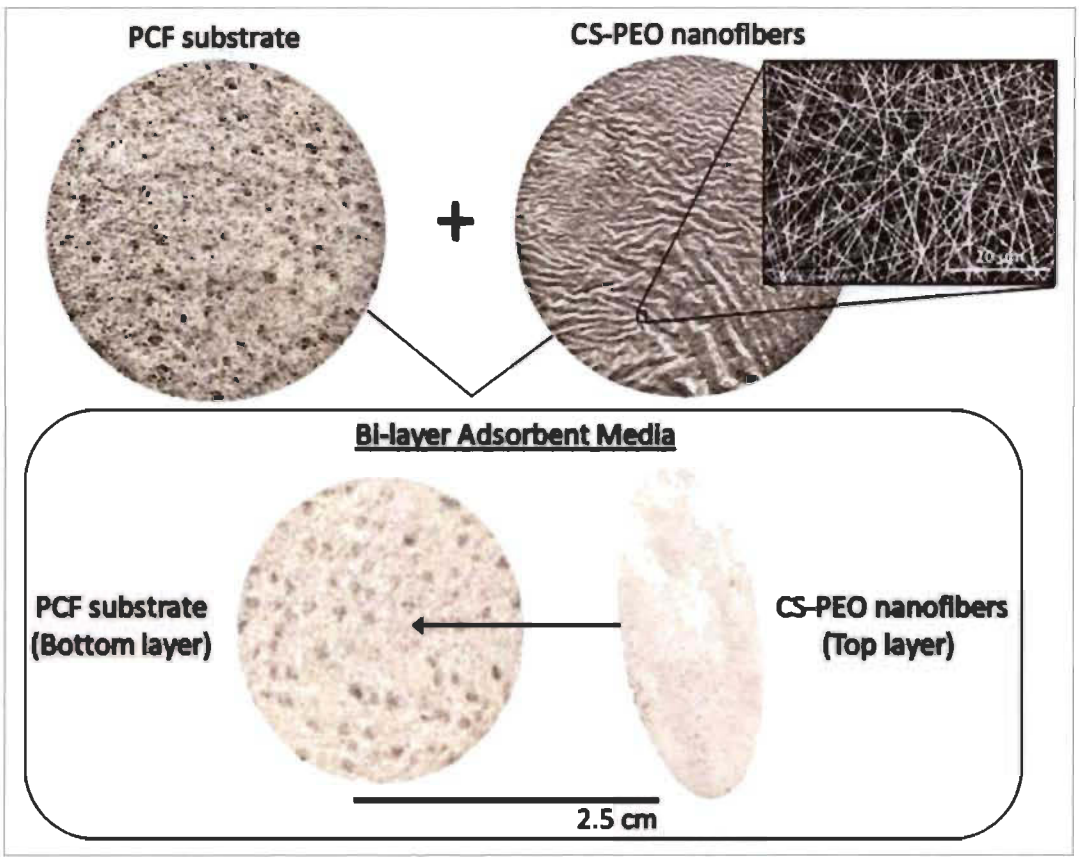

Figure 6.1 Photographic diagram showing the CS-PEO nanofibers, PCF substrate and the bi-layer adsorbent media.

A deeper study of the morphology of the adsorbent media was carried out by SEM. Figure 6.2 (a-e) shows SEM micrograph of the adsorbent media at different magnifications. Figure 6.2a shows a picture at 250x magnification of the top layer of the bi-layer adsorbent media, where chitosan nanofibers prevail. The CS-PEO nanofibers formed a well-distributed network over the entire surface of the PCF substrate. The darker, rounder

regions are the pores of the PCF substrate which seem to have a less dense network of nanofibers. Figure 6.2b shows a picture at 250x magnification of the bottom layer of the bi-layer adsorbent media, where the PCF substrate prevails. The picture clearly shows that the bottom side is mostly composed of PCF, which are on the microfiber scale. Through the pores of the PCF substrate it is possible to see the CS-PEO nanofibers that are part of the other adsorbent layer, which have not been able to enter the PCF substrate and come to your surface. The view from top of the corner of the adsorbent media can be seen in Figure 6.2c. This micrography clearly shows a dense nanofiber surface covering the phosphorylated cellulose fibers. Figure 6.2d and Figure 6.2e show the cross-section of the adsorbent media. This view shows more clearly the two layers that make up the adsorbent media. EDX is an analytical technique which was used for the chemical characterization of the adsorbent media. The phosphate groups that are present on the surface of PCF are composed of the chemical elements, phosphorus and oxygen. Since the EDX technique largely follows the fundamental principle that each element has a unique atomic structure, so that the X-rays emitted are characteristic of this structure, which identify the element, so the EDX analysis was performed to evaluate the amount of phosphorus in the adsorbent media. The Figure 6.2f shows the EDX spectrum of the media adsorbent, which contains a relevant phosphorus peak (6.6 wt%). This result proves the presence of phosphate groups in adsorbent media, groups which are fundamental in the adsorption of contaminants [161]. In the same spectrum it is possible to observe oxygen and carbon peaks, elements that are part of the chitosan structure and phosphorylated cellulose. It is still possible to notice a small peak of nitrogen, which is probably coming from the amine groups present in the chitosan chemical structure.

In order to better understand the adsorbent media, using the SEM images, analyses of the average fiber diameter and porosity content were performed with the support of the ImageJ software. This analysis could give us an indication of how much nanofiber we could deposit on the substrate without losing porosity considerably, which could result in a reduction in permeability. The water permeability is considered very important in the final result of the adsorbent since it can be applied in filtration, where this characteristic is essential. With the ImageJ software, using the particle analysis tool, which detects and quantifies particles, pores and other image features having boundaries, analyses were

performed on adsorbents with different amounts of chitosan nanofibers deposited on the cellulose substrate. Our goal was to obtain a coating of the substrate with the chitosan nanofibers which could reduce around 10% of the porosity content when compared to the original substrate. Thus, pore content analysis was first performed on a CS-PEO nanofibers adsorbent and a PCF substrate and the results were 40.6% and 53.1%, respectively. Then the pore content of the adsorbent media was measured, which resulted in 47.8%. The deposition of CS-PEO nanofibers on the PCF substrate has reduced its porosity, as the network formed by nanofibers is dense and closed. A higher percentage of pore content should facilitate the flow of water during filtration [163, 164]. Thus, as the percentage by weight of CS-PEO nanofibers in the average adsorbent media was 40wt%, and the porosity had reduced by 10% in relation to the PCF substrate, we consider this a good result. Using ImageJ, an analysis of the average fiber diameter of CS-PEO nanofibers and phosphorylated cellulose fibers, which make up the layers of the media adsorbent was measured. CPF substrate layer presents an average fiber diameter of 21.5 (±4) μm and the CS-PEO Nanofibers layer of 372 (±82) nm. Using the same analysis feature, and the SEM cross-section images of the adsorbent media, the average thickness of the layers composing the adsorbent media were measured. The results found were of 8.6 (±82) μm for the CS-PEO nanofibers layer and 56.7 (±8) μm for the PCF substrate layer, representing approximately 13% and 87% of the thickness respectively. The maximum pore size was calculated using the bubble point method. The results found were 3.5 μm for the CS-PEO nanofibers adsorbent, 27.8 μm for the PCF adsorbent and 20.9 μm for the adsorbent media. These results showed that the layer composed of CS-PEO nanofibers has a lower porosity, composed of nanofibers and smaller pore sizes. Already the CPF layer has a higher porosity, composed of microfibers and larger pore sizes. Although the nanofibers layer represents 40wt% of the media adsorbent, it did not severely impact the final porosity. Zahid *et al.* [165] presented and showed in its study adsorbents with porosities, medium particle size and fiber diameter similar to those obtained in this study. Yang *et al.* [72] functionalized chitosan electrospun nanofibers to remove heavy metals from aqueous solutions and found average fiber diameters and porosities that are close to those found in this study.

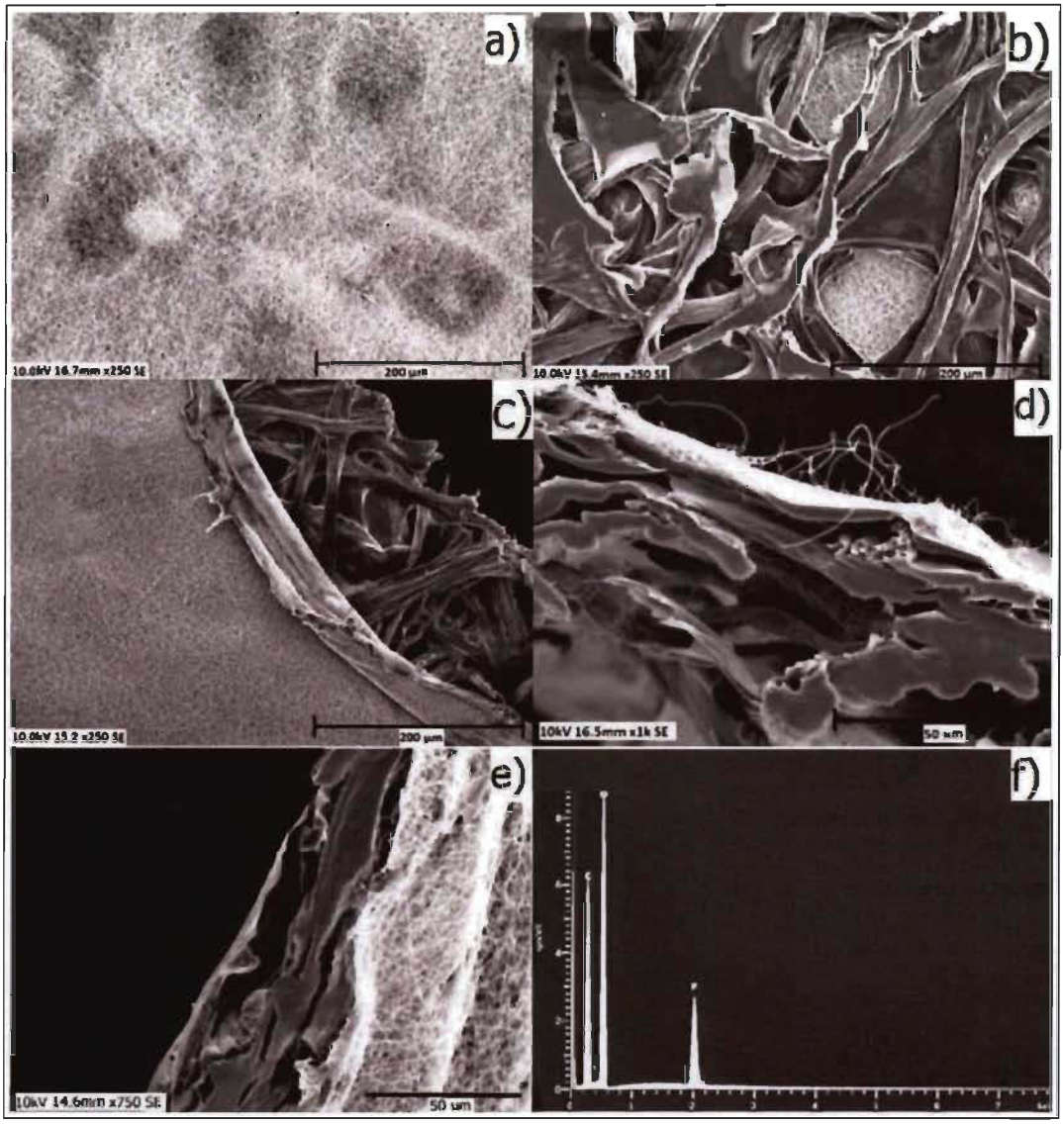

Figure 6.2 SEM micrographs and EDX spectrum of the two-layer adsorbent media. View of the top surface of adsorbent media, CS-PEO nanofiber layer (a), View of the bottom surface of the adsorbent media, PCF substrate layer (b), top edge view of the adsorbent media (c), adsorbent media cross-section view (d-e), EDX spectrum of the adsorbent media (f)

6.7.2 Characterization of adsorbent materials

Contact angle results for the CS-PEO nanofibers, PCF substrate and adsorbent media can be seen in Figure 6.3. This analysis was used to evaluate the wettability of the adsorbents. The CS-PEO adsorbent nanofibers had a stabilized contact angle at 40 degrees after 10s contact with the surface, which represents a hydrophilic surface. In relation to the PCF

substrate, the liquid water molecules were strongly attracted by the PCF adsorbent solid molecules, and the liquid drop spread completely after contact with the surface, corresponding to a contact angle of 0 degrees. The same effect was observed for the adsorbent media and this means that the surface energy of the adsorbent media is high due to complete wetting and this indicates a greater ease of adhesion on the surface, which should facilitate adsorption of metal contaminants.

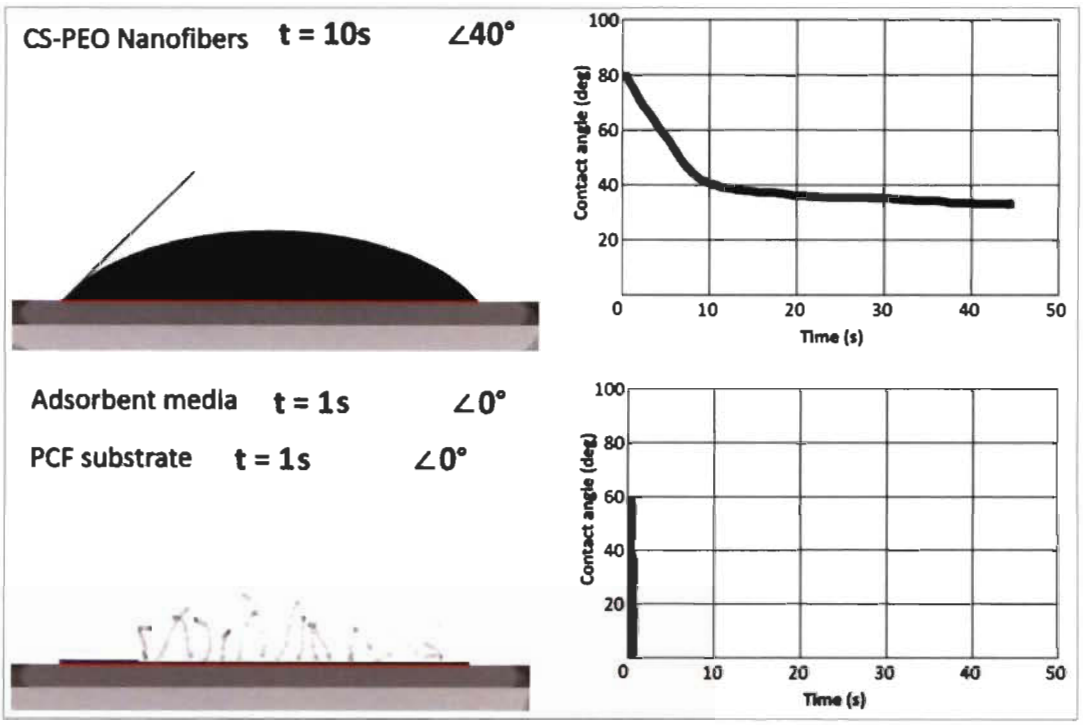

Figure 6.3 Contact angle results for the CS-PEO nanofibers, PCF substrate and adsorbent media.

The mechanical properties of the PCF substrate, adsorbent media and CS/PEO nanofibers were tested and the results are summarized in Figure 6.4 and Table 6.1.

Figure 6.4 and Table 6.1 show the curves and results for Young's modulus, tensile strength and maximum strain of the PCF substrate, Adsorbent media and CS-PEO nanofibers. CS-PEO nanofibers present lower results for all properties and PCF substrate the highest.

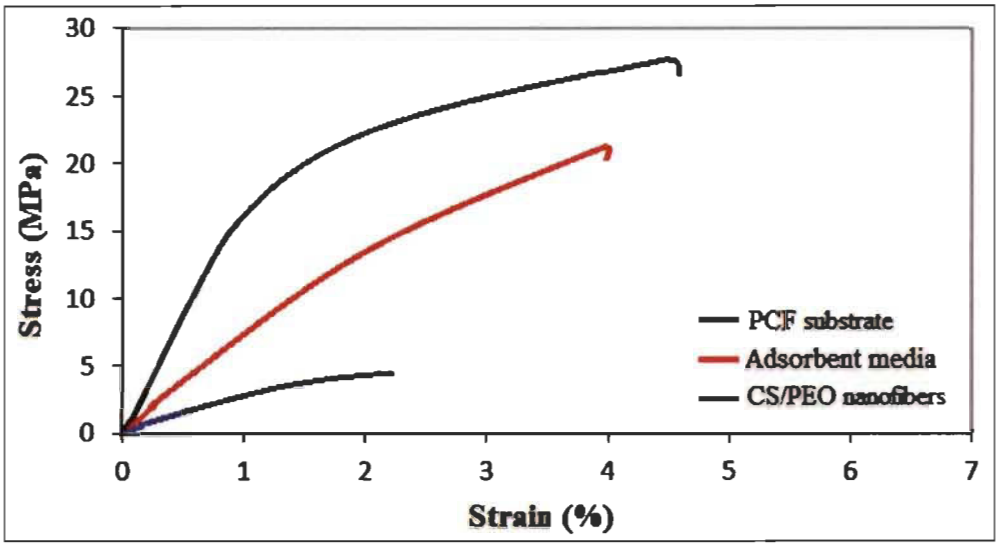

Figure 6.4 Stress-strain curves of the adsorbent materials.

Table 6.1 Young's modulus, Maximum stress and elongation at break of adsorbent materials.

Adsorbent	Young's modulus (GPa)	Tensile strength (MPa)	Max. strain (%)
PCF substrate	0.6 ± 0.2	27.5 ± 7.4	4.5 ± 1.4
Adsorbent media	0.5 ± 0.1	21.0 ± 5.4	4.0 ± 1.2
CS-PEO nanofibers	0.2 ± 0.1	4.6 ± 0.6	2.2 ± 0.6

The tensile strength of the adsorbents increased from 4.58 to 27.49 MPa and Young's modulus from 0.206 to 0.605 GPa. Even the strain increased from 2.22 to 4.54%. The bi-layer adsorbent media, which was formed from covering the PCF substrate with the CS-PEO nanofibers, reached values of 21.04 MPa (23% less than PCF substrate, but 78% more than CS-PEO nanofibers), 0.53 GPa (12% less than PCF substrate, but 61% more than CS-PEO nanofibers) and 3.95% (13% lower than PCF substrate, but 43% higher than CS/PEO nanofibers), which were among the values of the other two adsorbents. These results show that the coating of PCF substrate with CS-PEO nanofibers has slightly lowered the values compared to PCF substrate, however, these results are very high compared to CS-PEO nanofibers. The coating of the PCF substrate with the CS-PEO nanofibers and thus the creation of a multi-functional adsorbent media had a positive impact on the mechanical properties, since it virtually maintained the good mechanical

properties of PFC and significantly increased the low properties of CS-PEO nanofibers. It is also important to mention that the good results achieved with the developed media adsorbent may also be attributed the probable good interaction and anchorage between the PCF substrate and the CS-PEO nanofibers. PCF microfibers which are randomly formed are believed to have acted as a support for the CS-PEO nanofiber network, which was impregnated into the cellulose microfiber network during its deposition by the electrospinning process. The formation of this composite material united the good mechanical properties of cellulose microfibers, which reinforced the nanofiber web, where we can say that they acted as a matrix and reinforcement.

Thermal analysis of PCF substrate and two-layer media samples by DSC were carried out to study their thermal characteristics (see Figure 6.5).

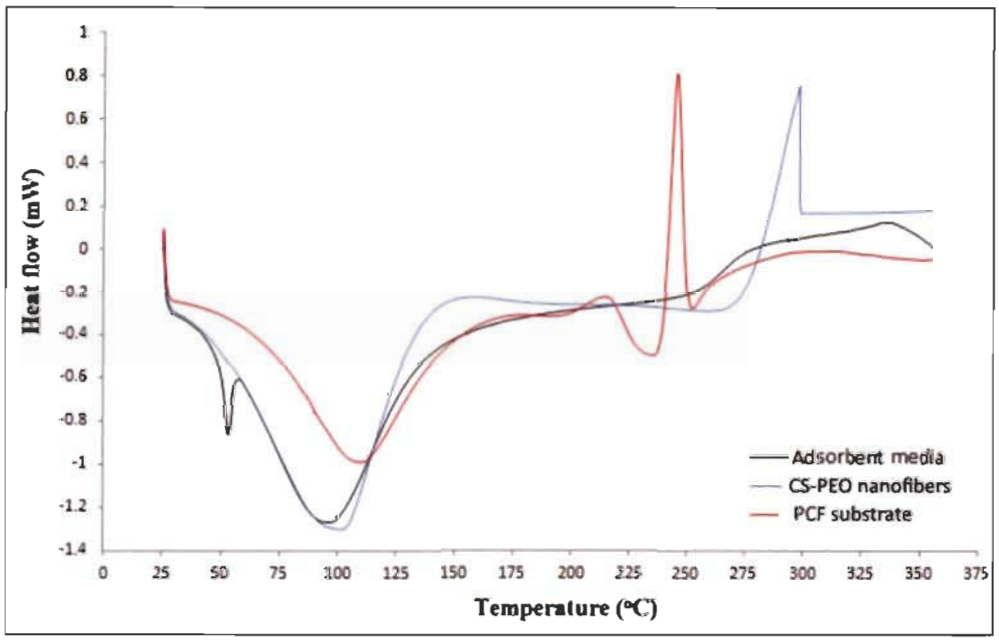

Figure 6.5 DSC spectrum of the PCF substrate and the two-layer PCF/CS-PEO adsorbent media.

The PCF substrate curve begins its thermal event at 58°C (onset temperature), with an endothermic peak or melting temperature at 108°C and an endset temperature at 150°C, which is in accordance with Bezerra *et al.* [166]. When the temperature rises, the material shows an exothermic peak with a starting temperature of 235°C, a peak at 248°C and a final temperature of 253°C. This peak can be characterised as a cross-linking event,

representing chemical reactions which molecules are binding together and forming three-dimensional networks. For the adsorbent media, the onset temperature starts at 49°C, a small endothermic peak is appearing at 53°C which is a typical pre-transition or glass-transition temperature point, and the melting temperature occurs at 93°C. The endset temperature was recorded at 135°C. It is also possible to observe the exothermic peak event at 343°C. The endothermic peak corresponds to the fusion transition or a first order transition due to the particle size distribution of the crystalline regions present in the macromolecules [167]. The results showed that the addition of chitosan nanofibers to the PCF substrate increased the endothermic area and reduced the melting temperature at 15°C.

The XRD spectra of the PCF (red curve) and PCF/CS-PEO (black curve) materials are shown in Figure 6.6.

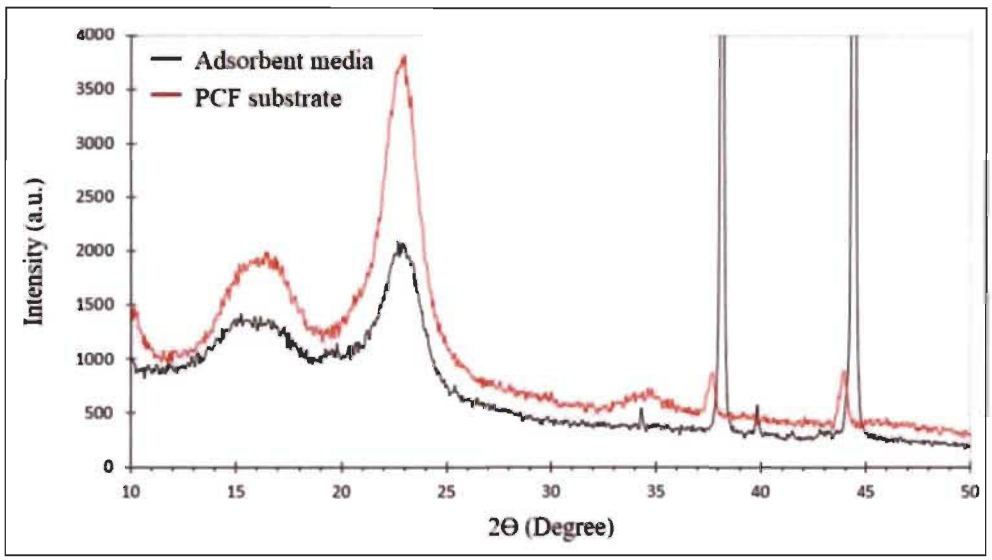

Figure 6.6 XRD spectrum of the PCF substrate and two-layer PCF/CS-PEO adsorbent media.

The PCF substrate shows an intense peak of diffraction at (020) at 22.4°, as well as intensities of (101) and ($10\bar{1}$) lattice diffractions at 14.8° and 16.1°, being typical diffraction patterns of cellulose I. For the spectrum of the two-layer PCF/CS-PEO media, the presence of typical chitosan peaks is expected. The chitosan spectrum normally presents peaks at 10.67° which did not appear in the spectra and peaks at 19.92° which appeared discreetly in the spectrum. Peaks related to PCF appear, however, with lower

intensities when compared to the previous spectrum. The calculated percentage crystallinity index was found around 37% for adsorbent media and 47% for PCF substrate [44, 168].

Figure 6.7 shows FTIR spectra of the PCF substrate (red curve), adsorbent media (black curve) and CS/PEO nanofibers (blue curve) materials. CS/PEO mat shows peaks at 3430 cm^{-1} representing the OH and NH stretch, at 1662 and 1584 cm^{-1} representing amide I and II, at 2930 and 2850 cm^{-1} representing CH stretch and at 1380 cm^{-1} showing the deformation of C-CH_3. Regarding the PCF/CS-PEO media, chitosan absorption peaks were found at 3450 cm^{-1} (hydroxyl group OH), 3360 cm^{-1} (NH group - elongation vibration), 1590 cm^{-1} (amine group NH_2) and 1560 cm^{-1} (flexion vibration NH - amide group). Peaks corresponding to phosphorylated cellulose fibers (PFC) are still appearing at 2385 cm^{-1}, 1050 cm^{-1} and 920 cm^{-1}. For the PCF substrate, the absorption peaks appeared at 920 cm^{-1} (P-OH elongation vibration of the phosphoric group), at 1215 cm^{-1} (P=O stretching), at 1050 and 785 cm^{-1} (P-O-C bands) and at 2385 cm^{-1} (P-H band), both corresponding to phosphorus cellulose fibers, thus confirming the presence of phosphorus groups [169].

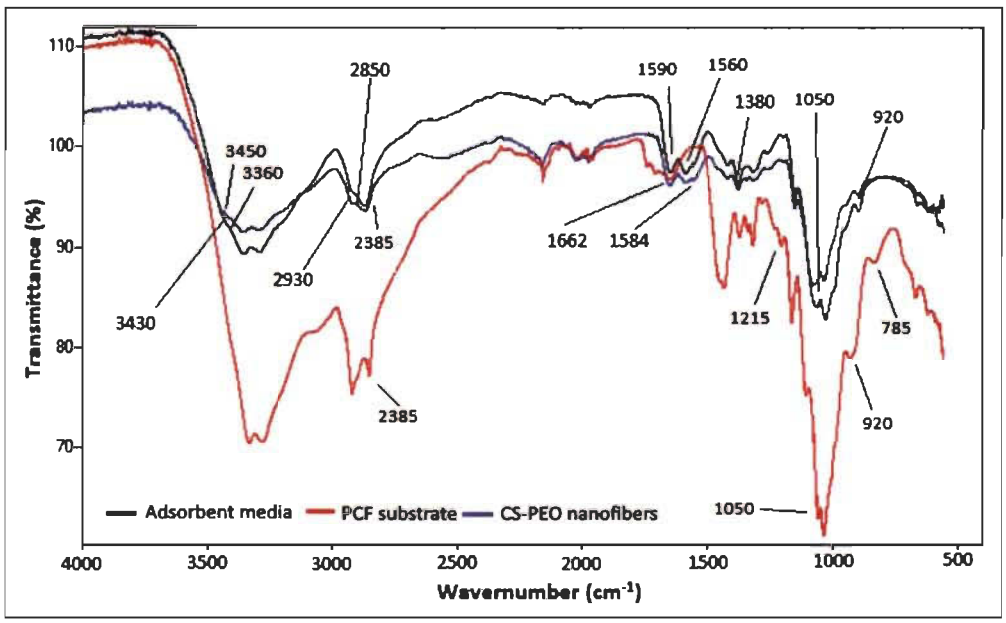

Figure 6.7 FTIR spectrum of the PCF substrate and two-layer PCF/CS-PEO adsorbent media.

As previously mentioned, one of the main purposes of developing an adsorbent based on a PCF substrate coated with chitosan nanofibers was to obtain a final adsorbent with good permeability properties. However, it is known that chitosan nanofibers generally have low water permeability and require substantial energy to overcome flow resistance due to the small pore size. Although the pressure drops, they develop is much smaller than that of ultrafiltration, nanofiltration or reverse osmosis membranes, their applications for filtration/adsorption applications are still limited. So, since the PCF substrate has good permeability characteristics, the intention was to cover it with chitosan nanofibers without significantly losing its initial permeability. Our goal was to develop a final adsorbent that would present a change in flow and water permeability of approximately 10% when compared to the initial substrate. Water permeability tests were thus carried out with the two-layer adsorbent media to study the effect of the structural configuration on water flux and permeability. Results were made at a constant pressure of 1 bar. For this purpose, the adsorbents were evaluated in relation to flux and permeability. The adsorbent media that achieved our goal was composed of 60 wt% PCF and 40 wt% CS nanofibers. The results calculated in relation to the water flow were 12.65 $Lm^{-2}h^{-1}bar^{-1}$ and 10.96 $Lm^{-2}h^{-1}bar^{-1}$ for PCF substrate and adsorbent media, respectively. For the calculation of permeability, the thicknesses of 0.29 and 0.425 mm were considered, calculating 3.66 $Lm^{-2}h^{-1}bar^{-1}mm$ and 4.65 $Lm^{-2}h^{-1}bar^{-1}mm$ for the PCF substrate and adsorbent media, respectively. These results show that the water flow was slightly reduced after covering the PCF substrate with the chitosan nanofibers, however, due to the thickness of the membrane, it presented a higher permeability. Thus, despite the formation of a layer of nanofibers under the cellulose fibers, the membrane is still suitable for application in a possible filtration/adsorption system [170, 171].

6.7.3 Contact time and adsorption kinetics for Cd (II)

Figure 6.8 shows the effect of contact time on cadmium ions adsorption for a CS/PEO nonwoven mat, a PCF substrate, and a two-layer PCF/CS-PEO media. Results show that the best adsorption is achieved with the PCF substrate, followed by the two-layer media, and finally by the single CS/PEO mat. The functional groups present on the surface of the adsorbents act by connecting with the free ions in the aqueous solutions. In the case of

this study, cadmium ions tend to connect more easily and firmly with the phosphate functional groups present on the surface of PCF, compared to the amine groups present on the surface of chitosan nanofibers. The adsorption curve for which the PCF/CS-PEO adsorbent media is shown in Figure 6.8 represents a curve arranged below the curve represented by the PCF substrate and above the curve represented by the CS/PEO nanofibers. Thus, since the adsorbent media is composed of two layers, which are the PFC substrate and the chitosan nanofibers, we can interpret and reaffirm that the phosphate functional groups give a higher adsorption capacity compared to the amine groups. The three adsorbents evaluated presented an equilibrium time approximately 3 h after the beginning of the test. The CS/PEO nanofibers, PCF/CS-PEO adsorbent media, and PCF substrate materials reached a maximum Cd^{2+} adsorption capacity of 58.91 mg/g, 101.39 mg/g, and 115.62 mg/g, respectively.

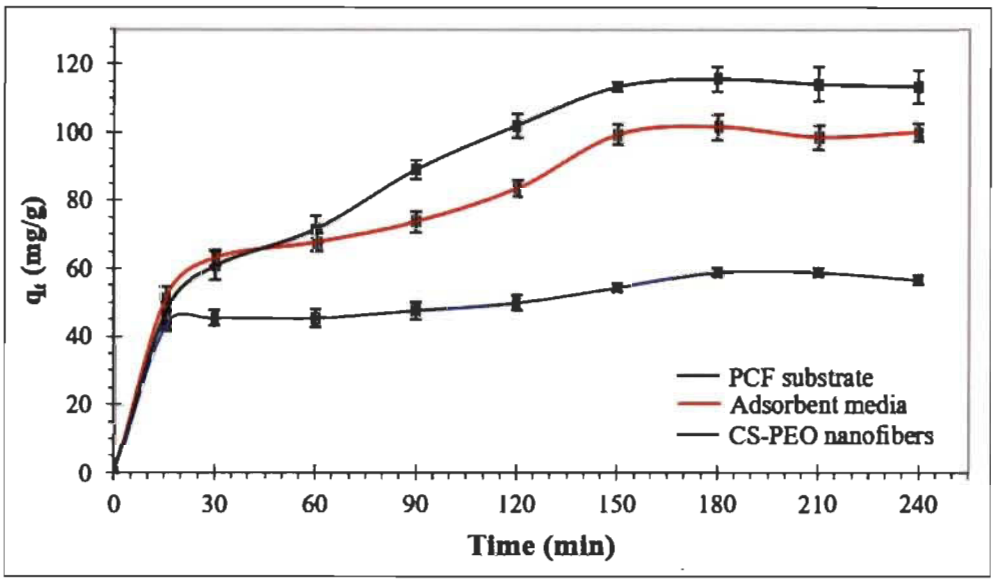

Figure 6.8 Effect of contact time on cadmium ions adsorption by CS/PEO nanofibers, PCF substrate, and PCF/CS-PEO media adsorbent materials.

To investigate the control mechanism of the adsorption process and provide the kinetic parameters, nonlinear pseudo-first and pseudo-second order models were applied to the experimental data. The kinetic parameters are presented in Table 6.2. A comparative data analysis for CS/PEO, PCF and PCF/CS-PEO materials was carried out. For all cases, R^2 values were higher for the pseudo-second model. That is, this model better fit with the

experimental data. It also suggests that the most likely adsorption mechanism is chemisorption [70, 172]. Basically, the cadmium adsorption for the PCF substrate proceeds by ions exchange between the phosphate groups and cadmium cations, while for the two-layer PCF/CS-PEO media, the composition is divided into 60% of phosphate functional groups from PCF substrate and 40% of amine groups from protonated CS nanofibers. The standard CS/PEO nanofibers mat adsorb cations through the amine groups. The calculated equilibrium adsorption capacity using the pseudo-second order model was of 56.15 mg/g, 106.51 mg/g, and 134.16 mg/g for the CS/PEO, PCF/CS-PEO and PCF adsorbent materials, respectively. The increase in equilibrium adsorption capacity of approximately 139% for PCF substrate compared to CS/PEO nanofibers can be attributed to phosphate groups which can interact more easily with cadmium ions due to probably requiring less energy. The two-layer PCF/CS-PEO media has approximately 21% lower adsorption capacity compared to the PCF substrate. However, it has an adsorption capacity 90% higher than CS/PEO, which again can be attributed to the functional groups present in the surface of this adsorbent, as previously highlighted.

Table 6.2 Kinetic parameters for cadmium ions adsorption by CS/PEO, PCF and Bi-layer adsorbent materials.

Kinetic model	CS/PEO	PCF	Bi-layer Adsorbent
Pseudo-first order model			
R^2	0.912	0.954	0.890
K_1 (min^{-1})	0.098	0.021	0.032
q_e (mg/g)	52.80	113.46	93.69
Pseudo-second order model			
R^2	0.947	0.974	0.943
K_2 (mg/mg min^{-1})	0.0028	0.0019	0.0041
q_e (mg/g)	56.14	134.16	106.51

6.7.4 Thermodynamic and isotherm models for Cd (II) adsorption

Figure 6.9 shows the non-linear forms of the Langmuir, Freundlich and Dubinin-Radushkevich cadmium adsorption isotherms for the two-layer adsorbent media at 25°C, 40°C and 60°C. R^2 fitting values and isotherm parameters are also presented in Table 6.3. Results indicate that all isotherm curves are favourable. Analysis based on R^2 values indicate that the Langmuir model best fitted the experimental data. Therefore, the adsorption of Cd^{2+} occurs in an ideal monolayer on the homogeneous media surface,

where the surface of the PCF which contains the phosphate groups is probably the most involved, because the negative phosphate groups formed on the surface are highly reactive and can bind with cationic elements. The maximum adsorption capacity found was 591 mg/g at 60°C. The K_L values increased with increasing temperature, confirming the endothermic nature of adsorption. The calculated R_L were less than 1, which confirms that the adsorbate prefers the solid phase to the liquid phase and the adsorption is considered favourable.

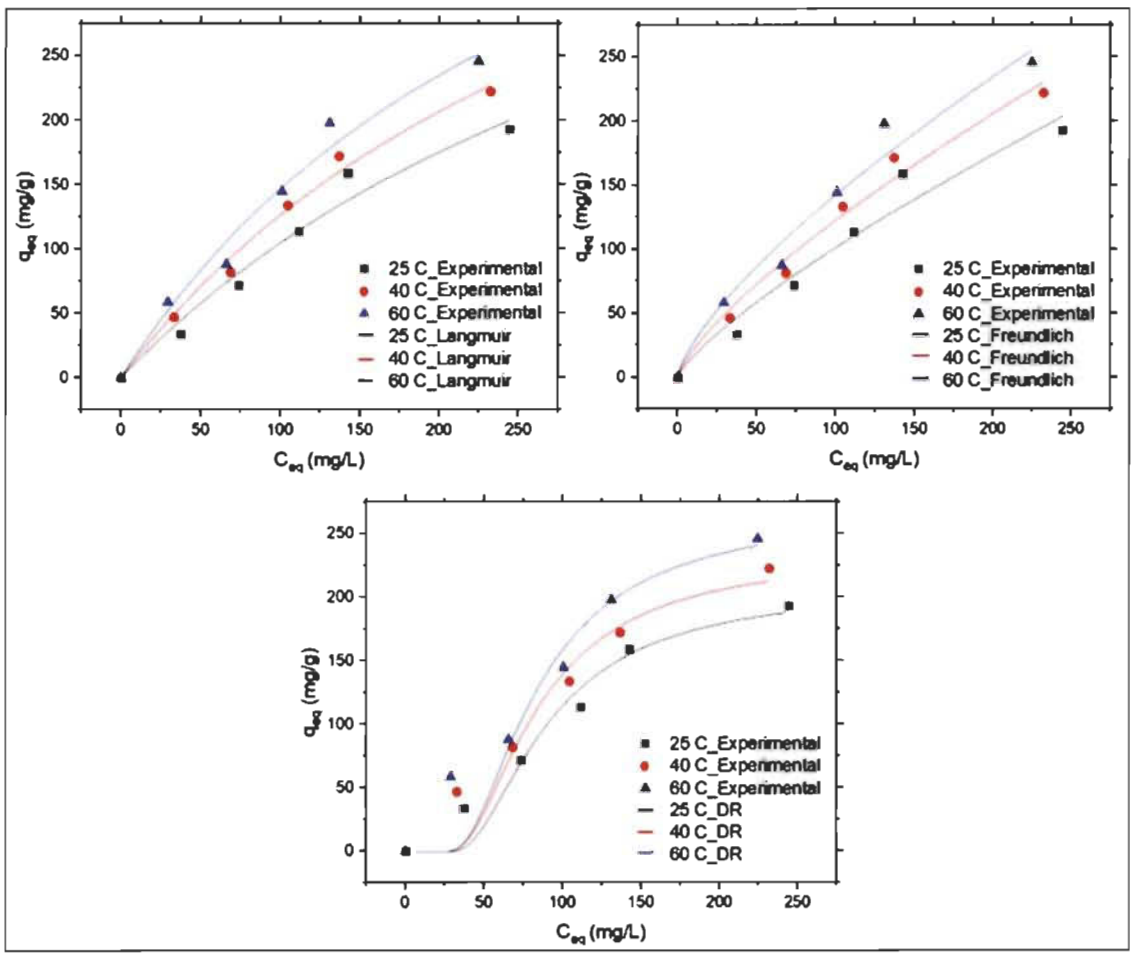

Figure 6.9 Cd^{2+}isotherm adsorption models for the bi-layer media adsorbent.

Table 6.3 Parameters obtained from the plots of Langmuir, Freundlich and Dubinin-Radushkevich models for Cd^{2+} adsorption on bi-layer adsorbent media.

Isotherm model	T = 25 °C	T = 40 °C	T = 60 °C
Langmuir			
R^2	0.967	0.988	0.976
K_L *(L/mg)*	0.0023	0.0028	0.0032
q_{max} *(mg/g)*	547.45	575.23	591.62
R_L	0.788	0.758	0.736
Freundlich			
R^2	0.950	0.979	0.969
K_f *[(mg/g) (mg/L)$^{1/n}$]*	2.78	3.92	5.22
1/n	0.78	0.74	0.71
Dubinin-Radushkevich			
R^2	0.945	0.915	0.889
K (mol^2/J^2)	88.43	76.73	76.93
$q_{D\text{-}R}$ (mol/g)	208.39	234.20	266.73
E (kJ/mol)	0.106	0.114	0.114

Regarding thermodynamic parameters, the energy flow between the system and the neighborhood can be employed with the criterion of spontaneity. Those where energy leaves the system are called exergonic ($\Delta G < 0$) and therefore spontaneous. On the other hand, when energy enters the system ($\Delta G > 0$), it is said that the process is endergonic and not spontaneous. Results are shown in Table 6.4. ΔG were negative at each temperature studied, which suggests a spontaneous adsorption of Cd^{2+} by the media. The positive values of enthalpy (ΔH) and entropy (ΔS) are attributed to the endothermic nature of the process and show an increase in the degree of randomness of the adsorbent-adsorbate system, respectively.

Table 6.4 Thermodynamic parameters for Cd^{2+} adsorption on bi-layer adsorbent media.

Temperature (°C)	R^2	ΔH (kJ)	ΔS (kJ/K)	ΔG (kJ)
25	0.967	6882.51	24.54	-436.47
40	-	-	-	-804.69
60	-	-	-	-1295.65

6.7.5 Cd^{2+} sorption-desorption cycle for the two-layer PCF/CS-PEO media

Figure 6.10 presents the effect of adsorption-desorption of Cd^{2+} by the two-layer PCF/CS-PEO media for three consecutive cycles. Results show that after three cycles, the sorbent media loses approximately 16% of its adsorption capacity, which is considered acceptable. This can be explained by the slight degradation of functional groups caused by the regeneration step performed with EDTA after each cycle. That, degradation can be resulted from the destruction of binding sites on the surface or the alteration of the configuration of binding states by EDTA. We can also assume that EDTA could form highly stable complexes with binding site elements [173].

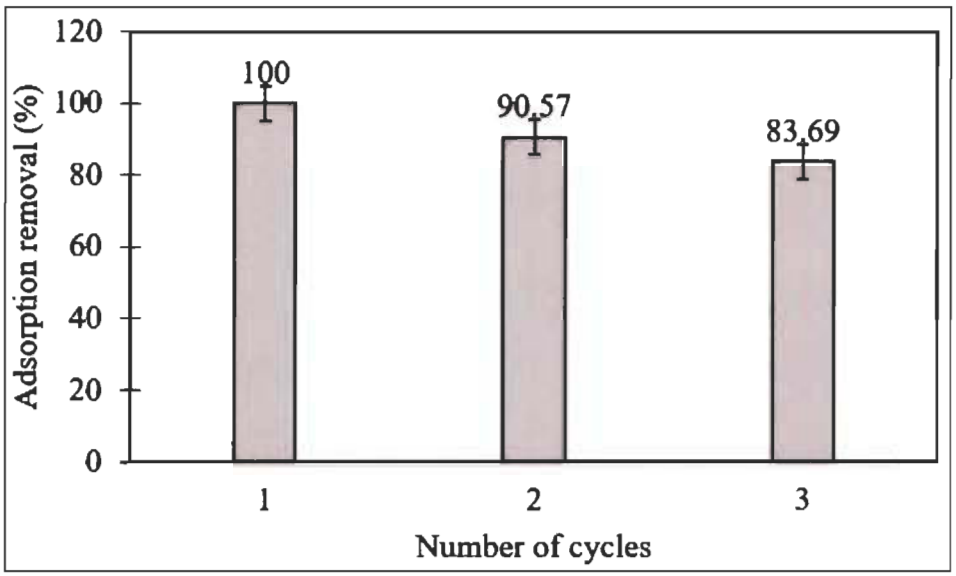

Figure 6.10 Adsorption-desorption cycle for the bi-layer adsorbent media

6.7.6 Adsorption capacity comparison with other sorbents

Table 6.5 compares Cd^{2+} adsorption capacity of the two-layer Bi-layer media adsorbent to data from the literature obtained with various adsorbents at 25°C. Results show that the bi-layer adsorbent media has a higher adsorption capacity than any of the compared materials used under similar conditions. A CS-based electrospun mat produced by Aliabadi *et al.* [70] is about 2.3 times less efficient, while activated carbon experiments carried out by Karnib *et al.* [174] is approximately 4 times less efficient. Interestingly, there was an increase in adsorption capacity in the adsorbents developed in this thesis. Starting with the CS/PEO/PNC adsorbent (10% PNC and approximately 0.7% phosphate

groups), the adsorption reached 232 mg/g. Then, the CS/PEO/PMC (50% PMC and approximately 1.7% phosphate groups), the adsorption increased to 275 mg/g. Finally, the bi-layer adsorbent (approximately 4.2% phosphate groups), adsorption reached 547 mg/g of maximum adsorption capacity. These results indicate and suggest that the sites and phosphate groups present in the adsorbent surfaces were the main functional groups responsible for the increase in the maximum adsorption capacity.

Table 6.5 Maximum adsorption capacity of Cd^{2+} for various adsorbents at 25°C.

Adsorbent	q_{max} (mg/g)	pH	Stirring (rpm)	Reference
Biochar (rice straw)	139.9	6.0	150	Gao *et al.* [175]
Carbon nanotubes	10.8	5.0	-	Li *et al.* [176]
Blue-green algae	2.8	5.0	150	Chojnacka *et al.* [177]
Nanohydroxyapatite	142.8	5.5	300	Mobasherpour *et al.* [178]
Natural zeolite	130.4	5.5	-	Castaldi *et al.* [179]
Kraft lignin	137.1	6.0	-	Mohan *et al.* [173]
Activated carbon	178.5	2.0	100	Karnib *et al.* [174]
CS/PEO adsorbent	230.3	5.0	-	Aliabadi *et al.* [70]
CS/PEO/PNC adsorbent	232.5	5.5	200	This study (Chapter 4)
CS/PEO/PMC adsorbent	275.8	5.5	200	This study (Chapter 5)
Bi-layer media adsorbent	547.4	5.5	200	This study (Chapter 6)

6.7.7 Adsorption tests with multi-heavy metals water content

2 g of individual bi-layer adsorbent media were placed separately in 125 mL Erlenmeyer's flasks containing solutions with 20 mL at 10 ppm (5 mL of each: Pb (II), Cu (II), Cd (II), Cr (VI). It is important to note that the solution contains heavy metals with positive charges (Cd^{2+}, Cu^{2+} and Pb^{2+}) and negative charges (Cr^{2-}). The flasks were kept in an

orbital agitator at a temperature of 25°C, agitation of 200 rpm and pH 5.5, for 3 h. The samples were evaluated in terms of adsorption capacity and metal ion removal (Table 6.6).

Table 6.6 Adsorption capacity and metal ion removal by the bi-layer adsorbent media for multi-heavy metal solution.

Adsorption parameter	Cd (II)	Cr (VI)	Cu (II)	Pb (II)
Adsorption capacity	60 mg/g ± 12	30 mg/g ± 12	75 mg/g ± 3	31 mg/g ± 3
Metal ion removal	58 % ± 11	28 % ± 12	71 % ± 2	29 % ± 4

The PCF/CS-PEO media can adsorb all heavy metals present initially in the solution, however, in different amounts. This result proves the capacity of the membrane to adsorb both cationic and anionic heavy metals ions at the same time. This result can be explained by two reason. First, the two-layer PCF/CS-PEO media contains mostly phosphate groups with negative charges on the PCF substrate layer (bottom part of the media), which can easily bind with metallic cations. Then, the thin nonwoven CS/PEO layer (when not neutralized) contains positively charged amine groups, which can bind negative anions of hexavalent chromium. Results also show that adsorption selectivity is achieved according to the following order: Cu (II) > Cd (II) > Pb (II) > Cr (VI). Neto *et al.* [180] using a Cr (VI) solution achieved an experimental result of 48.08 mg/g on the surface of a Lignocellulosic derivative and chitosan bio-adsorbent. In another study Zhang *et al.* [181] incorporated Citric acid into nanofibrous cellulose to create mats and adsorb Cr (VI) in aqueous solutions. In the contact time test, after 120 min an adsorption capacity of approximately 12 mg/g was obtained with these mats. Results obtained in this work are in accordance with the literature, with a Cr (VI) adsorption capacity of 29.6 mg/g after 180 min. Lakhdhar *et al.* [68] used CS/PEO nanofibers to adsorb Cu (II) and obtained an experimental adsorption capacity of approximately 100 mg/g, which is not far from the result of this study (74.5 mg/g). A novel g-C_3N_4/MnO_2 composite was prepared by Guo *et al.* [182] by *in situ* deposition of MnO_2 on graphitic carbon nitride (g-C_3N_4) nanosheets and Fan *et al.* [183] prepared an alkali-treated persimmon fallen leaves for removal of Pb (II) in aqueous solutions. Arshadi *et al.* [184], Kataria *et al.* [185] and Melo *et al.* [186] used barley straw ash, ZnO nanoflowers and tururi fibers, respectively, for adsorption of

Cd (II) aqueous solutions. The literature results regarding the adsorption of Cd (II) and Pb (II) are also in accordance with the results obtained in this study.

The bi-layer adsorbent media proved to be efficient for the removal of multi elements, non-selective, and polyvalent, i.e., capable of adsorbing anions and cations. Some examples of materials capable of adsorbing multi contaminants have already been developed and evaluated, such as those presented by Mohan *et al.* [187], Visa *et al.* [188], Hanzlik *et al.* [189], Dong *et al.* [190] and Melo *et al.* [186]. The results obtained by this adsorbent media were considered excellent, since it was able to adsorb different metal cations and a metallic anion. This means that this material is promising for the treatment of effluents with different types of contaminants.

6.8 Conclusions

The objective of the work was to develop a media adsorbent capable of multi-contaminant adsorption. The morphological analysis revealed the microstructure of an adsorbent formed by a layer of phosphorylated cellulose microfibers and another of CS-PEO nanofibers. Extremely hydrophilic surface which is completely wetted, with porosity and pore size considered as micropores and crystallinity of approximately 37%. The chemical analyses performed on the adsorbent media showed the presence of phosphorus, nitrogen, carbon and oxygen, as well as phosphate and amine functional groups on the surface of the material. The deposition of CS-PEO nanofibers on the phosphorylated cellulose substrate formed a composite material, and the nanofibers acted as a matrix that was reinforced by the cellulose microfibers. The result was a composite with better mechanical properties compared to CS-PEO nanofibers. The results obtained for permeability and water flow were considered adequate for the application of this adsorbent in filtering systems, since it was considered permeable. The adsorption tests showed that the adsorbent media developed when used in the adsorption of Cd (II) was higher in comparison to the references and also obtained acceptable values when used in the adsorption of a bath with multi-contaminates. It also proved to adsorb non-selective cationic and anionic metallic contaminants. Due to the results obtained in this study, this adsorbent has a great potential to be used in filter systems for the adsorption of metallic

contaminants. Since the adsorbent is composed of natural and abundant polymers, which makes it accessible, the authors believe it could effectively contribute to the efficiency of current systems and contribute to the conservation of the environment.

Chapitre 7 - Conclusions

In this work, we succeeded, first, in producing "based chitosan-phosphorylated nanocellulose" media by electrospinning technique and in examining the different physical and chemical properties of these nanofibrous membranes using characterization techniques such as SEM, AFM, EDX, FTIR, cationic charge demand, etc. We evaluated the adsorption performance of the adsorbent with respect to cadmium ions. In this step, we conducted a study of the kinetics, equilibrium and thermodynamics of adsorption.

Secondly, we succeeded in producing "based chitosan-phosphorylated microcellulose" sorbent media by electrospinning technique and in examining the different physical, chemical and thermal properties of these nanofibrous mats using characterization techniques such as SEM, AFM, EDX, FTIR, XRD, DSC, etc. We evaluated the adsorption performance of the adsorbent with respect to cadmium ions. In this step, we conducted a study of the kinetics, equilibrium and thermodynamics of adsorption. Similarly, the possibility of their reuse and regeneration were examined.

Thirdly, we were able to produce a two-layer sorbent media based on phosphorylated cellulose fibers produced via casting covered by chitosan nanofibers produced via electrospinning. These were examined using characterization techniques such as SEM, AFM, EDX, FTIR, XRD, DSC and tensile strength test. It is important to note that the membranes were also evaluated for their water pressure permeability. We also evaluated the adsorption performance of the adsorbent in relation to cadmium ions (kinetics, equilibrium and thermodynamics of the adsorption). A multi-heavy metal solution content of contaminants (Cd (II), Cu (II), Pb (II) and Cr (VI)) was tested in order to evaluate the selectivity of the sorbent and its ability to capture cationic and anionic ions.

The first article was based on the production of a nonwoven mat made of chitosan and phosphorylated nanocellulose. The difficulty found was related to the limitation of homogeneously mixing the two materials and producing quality nanofibers, in percentages in weight greater than 10% for nanocellulose. Due to this limitation, the cadmium adsorption results were not very promising.

In the second article, we tried to overcome the problem of the first by trying to mix phosphorylated microcellulose (smaller surface area) with chitosan in order to develop a sorbent media with larger phosphorylated cellulose particles. In this case, we were able to incorporate up to 50% by weight of cellulose, however, we found an almost zero permeability of the material, which would make it impossible to use them in filtration/adsorption applications.

Finally, in the third article, in order to overcome the problems found previously, a adsorbent media based on phosphorylated cellulose fibers was produced via casting. This membrane presented a high adsorption capacity for the cadmium and high permeability. Then we covered the same substrate with non-neutralised electrospun chitosan nanofibers in order to have a bi-layer composite sorbent media capable of capturing cations and anions. Adsorption tests have proved the efficiency of this adsorbent media in capturing in a selective way multi contaminant, having better mechanical properties and good water permeability.

In conclusion, the results of this thesis will be used, in a next step, to establish the important parameters for the design and development of tertiary treatment equipment on an industrial scale. In order to contribute to the achievement of this long-term objective, the following recommendations can be considered for future work:

a. Explore the adsorption efficiency of sorbent media produced in this study, with respect to other types of contaminants (organic and inorganic in nature).
b. Test and evaluate the adsorption efficiency of sorbent media developed in this study on real effluents generated by typical industries, such as mining and pharmaceuticals.
c. Design a macro-porous, three-dimensional and multifunctional filter system based on these media and then evaluate their efficiency, adsorption performance and permeability properties (flow rate, pressure drop).

Chapitre 8 - Bibliography

[1] W.J. Cosgrove, D.P. Loucks, Water management: Current and future challenges and research directions, Water Resources Research 51(6) (2015) 4823-4839.

[2] J. Allan, Water in the Environment/Socio-Economic Development Discourse: Sustainability, Changing Management Paradigms and Policy Responses in a Global System, Government and Opposition 40 (2005) 181-199.

[3] A. Mudhoo, V.A. Garg, S. Wang, Removal of heavy metals by biosorption, Environmental Chemistry Letters 10 (2012) 109-117.

[4] T. Sato, M. Qadir, S. Yamamoto, T. Endo, Z. Ahmad, Global, regional, and country level need for data on wastewater generation, treatment, and use, Agricultural Water Management 130 (2013) 1–13.

[5] M. Hashim, S. Mukhopadhyay, J. Sahu, B. Sen Gupta, Remediation Technologies for Heavy Metal Contaminated Groundwater, Journal of environmental management 92 (2011) 2355-88.

[6] F. Fu, Q. Wang, Removal of Heavy Metal Ions from Wastewaters: A Review, Journal of environmental management 92 (2011) 407-18.

[7] C. Vidal, R. Nascimento, G. Raulino, A. Clecius, D. Melo, Adsorção: aspectos teóricos e aplicações ambientais, Editora UFC, Fortaleza 1 (2014) 221.

[8] WHO, Cadmium in drinking-water. Background document for development of WHO guidelines for drinking-water quality, Geneva, Switzerland (2011) 1-21.

[9] C.W. Network, Canada's challenges and opportunities to address contaminants in wastewater, Environment and Climate Change Canada, Ottawa, Canada (2018) 1-27.

[10] N.M. Saifuddin, K. Palanisamy, Removal of heavy metal from industrial wastewater using chitosan coated oil palm shell charcoal, Electronic Journal of Biotechnology 8 (2005) 805.

[11] I. Lakhdhar, B. Chabot, P. Mangin, Optimization of nickel ions removal from aqueous solutions by chitosan-polyethylene oxide electrospun nanofibers, WIT Transactions on Ecology and the Environment 196 (2015) 387 - 398.

[12] E. Guibal, Interactions of metal ions with chitosan-based sorbents: A review, Separation and Purification Technology 38 (2004) 43-74.

[13] P. Liu, P. Borrell, M. Božič, V. Kokol, K. Oksman, A. P Mathew, Nanocelluloses and their phosphorylated derivatives for selective adsorption of Ag+, Cu2+ and

Fe3+ from industrial effluents, Journal of Hazardous Materials 294 (2015) 177-185.

[14] N. Bhardwaj, S. Kundu, Electrospinning: A fascinating fiber fabrication technique, Biotechnology Advances 28 (2010) 325-347.

[15] J. Schnoor, Water Sustainability in a Changing World, Civil and Environmental Engineering Publications (2020).

[16] R. Andreozzi, V. Caprio, A. Insola, R. Marotta, Advanced Oxidation Processes (AOP) for Water Purification and Recovery, Catalysis Today 53 (1999) 51-59.

[17] D. Ruthven, Principles of Adsorption & Adsorption Processes, 1 (1984).

[18] D.D. Duong, Adsorption Analysis: Equilibria and Kinetics, Chemical Engineer Series, 2, London, 2 (1998) 49-77.

[19] I. Lakhdhar, D. Belosinschi, P. Mangin, B. Chabot, Development of a bio-based sorbent media for the removal of nickel ions from aqueous solutions, Journal of Environmental Chemical Engineering 4 (2016) 3159-3169.

[20] S. Bailey, T. Estes, R. Bricka, D. Adrian, A Review of Potentially Low-Cost Sorbents for Heavy Metal, Water Research 33 (1999) 2469-2479.

[21] D. Kołodyńska, J. Krukowska, P. Thomas, Comparison of Sorption and Desorption Studies of Heavy Metal Ions From Biochar and Commercial Active Carbon, Chemical Engineering Journal 307 (2016) 353-363.

[22] A. Wu, J. Jia, S. Luan, Amphiphilic PMMA/PEI core–shell nanoparticles as polymeric adsorbents to remove heavy metal pollutants, Colloids and Surfaces A: Physicochemical and Engineering Aspects 384 (2011) 180-185.

[23] M. Padervand, M. Gholami, Removal of toxic heavy metal ions from waste water by functionalized magnetic core-zeolitic shell nanocomposites as adsorbents, Environmental science and pollution research international 20 (2012) 3900–3909.

[24] V. Zargar, M. Asghari, A. Dashti, A Review on Chitin and Chitosan Polymers: Structure, Chemistry, Solubility, Derivatives, and Applications, ChemBioEng Reviews 2 (2015) 204-226.

[25] V.V.C. Azevedo, S.A. Chaves, D.C. Bezerra, M. Lia Fook, A.C.F.M. Costa, Quitina e quitosana: Aplicações como biomateriais, Revista Eletrônica De Materiais E Processos 2 (2007) 27-34.

[26] M. Elnashar, Characterization and Properties of Chitosan, Biotechnology of Biopolymers 5 (2011) 91-108.

[27] W. Argüelles-Monal, F. Goycoolea, Chitin and Chitosan: Major Sources, Properties and Applications, Monomers, Polymers and Composites from Renewable Resources 25 (2008) 517-542.

[28] M. Bizarria, M. d'Ávila, L. Innocentini-Mei, Non-woven nanofiber chitosan/PEO membranes obtained by electrospinning, Brazilian Journal of Chemical Engineering 31 (2014) 57-68.

[29] N. Ardila, N. Medina, M. Arkoun, M.-C. Heuzey, A. Ajji, C. Panchal, Chitosan–bacterial nanocellulose nanofibrous structures for potential wound dressing applications, Cellulose 23 (2016) 3089-3104.

[30] P. Dutta, J. Dutta, V. Tripathi, Chitin and chitosan: Chemistry, properties and applications, J Sci Indus Res 63 (2003) 20-31.

[31] N. Naseri, A. P Mathew, L. Girandon, M. Fröhlich, K. Oksman, Porous electrospun nanocomposite mats based on chitosan–cellulose nanocrystals for wound dressing: Effect of surface characteristics of nanocrystals, Cellulose 22 (2014) 521-534.

[32] M. Benavente, Adsorption of Metallic Ions onto Chitosan: Equilibrium and Kinetic Studies, Department of Chemical Engineering and Technology, Royal Institute of Technology Stockholm, Sweden, 2008, 61.

[33] W. Ngah, L.C. Teong, M.A.K. Megat Hanafiah, Adsorption of Dyes and Heavy Metal Ions by Chitosan Composites: A Review, Carbohydrate Polymers 83 (2011) 1446-1456.

[34] X. Sun, B. Peng, Y. Ji, J. Chen, D. Li, Chitosan(Chitin)/Cellulose Composite Biosorbents Prepared Using Ionic Liquid for Heavy Metal Ions Adsorption, AIChE Journal 55 (2009) 2062-2069.

[35] E. Salehi, P. Daraei, A. Shamsabadi, A review on chitosan-based adsorptive membranes, Carbohydrate Polymers 152 (2016) 419-432.

[36] R. Moon, A. Martini, J. Nairn, J. Simonsen, J. Youngblood, ChemInform Abstract: Cellulose Nanomaterials Review: Structure, Properties and Nanocomposites, Chemical Society reviews 40 (2011) 3941-94.

[37] D. Klemm, B. Heublein, H.-P. Fink, A. Bohn, Cellulose: Fascinating Biopolymer and Sustainable Raw Material, Angewandte Chemie (International ed. in English) 44 (2005) 3358-93.

[38] S. Kalia, A. Dufresne, B. Cherian, B.S. Kaith, L. Avérous, J. Njuguna, E. Nassiopoulos, Cellulose-Based Bio- and Nanocomposites: A Review, International Journal of Polymer Science 2011 (2011) 1-35.

[39] A. Dufresne, Nanocellulose: A new ageless bionanomaterial, Materials Today 16 (2013) 220-227.

[40] W. Czaja, D. Romanovicz, R.M. Brown, Structural investigation of microbial cellulose produced in stationary and agitated culture, Cellulose 11 (2004) 113-114.

[41] S. Eyley, W. Thielemans, Surface modification of cellulose nanocrystals, Nanoscale 6 (2014) 7764-7779.

[42] V. Santos, K. Monteiro, D. Sousa, S. Rodrigues, C. Donnici, Síntese e caracterização de novos copolímeros fosforilados, Polímeros 25 (2015) 19-24.

[43] Y. Shi, D. Belosinschi, F. Brouillette, A. Belfkira, B. Chabot, Phosphorylation of Kraft fibers with phosphate esters, Carbohydrate Polymers 106 (2014) 121–127.

[44] V. Kokol, M. Božič, R. Vogrinčič, A. P Mathew, Characterization and properties of homo- and heterogenously phosphorylated nanocellulose, Carbohydrate Polymers 125 (2015) 301-313.

[45] Y. Shi, D. Belosinschi, F. Brouillette, A. Belfkira, B. Chabot, The Properties of Phosphorylated Kraft Fibers, BioResources 10 (2015) 4375-4390.

[46] Y. Noguchi, I. Homma, Y. Matsubara, Complete nanofibrillation of cellulose prepared by phosphorylation, Cellulose 24 (2017) 1295–1305.

[47] P. Granja, L. Pouysegu, M. Pétraud, B. Jéso, C. Baquey, M. Barbosa, Cellulose phosphates as biomaterials. I. Synthesis and characterization of highly phosphorylated cellulose gels, Journal of Applied Polymer Science 82 (2001) 3341-3353.

[48] Y. Mizusawa, J. Burke, Prednisolone and cellulose phosphate treatment in idiopathic infantile hypercalcaemia with nephrocalcinosis, Journal of paediatrics and child health 32 (1996) 350-2.

[49] T. Oshima, K. Kondo, K. Ohto, K. Inoue, Y. Baba, Preparation of phosphorylated bacterial cellulose as an adsorbent for metal ions, Reactive and Functional Polymers 68 (2008) 376-383.

[50] F. Ahmed, B. Lalia, R. Hashaikeh, A review on electrospinning for membrane fabrication: Challenges and applications, Desalination 356 (2015) 15-30.

[51] J. Vonch, A. Yarin, C. Megaridis, Electrospinning: A study in the formation of nanofibers, The Journal of Undergraduate Research at the University of Illinois at Chicago 1 (2007) 1-6.

[52] X. Shi, W. Zhou, D. Ma, Q. Ma, D. Bridges, Y. Ma, A. Hu, Review Article Electrospinning of Nanofibers and Their Applications for Energy Devices, Journal of Nanomaterials 2015 (2015) 1-20.

[53] M. Elsabee, H. Naguib, R. Morsi, Chitosan based nanofibers, review, Materials Science and Engineering: C 32 (2012) 1711–1726.

[54] M. Spasova, N. Manolova, D. Paneva, I. Rashkov, Preparation of chitosan-containing nanofibres by electrospinning of chitosan/poly(ethylene oxide) blend solutions, e-Polymers 4 (2004) 056.

[55] M. Pakravan, M.-C. Heuzey, A. Ajji, A fundamental study of chitosan/PEO electrospinning, Polymer 52 (2011) 4813.

[56] K. Rieger, N. Birch, J. Schiffman, SI Electrospinning Chitosan/Poly(ethylene oxide) Solutions with Essential Oils: Correlating Solution Rheology to Nanofiber Formation, Carbohydrate Polymers 139 (2016) 131-138.

[57] R. Rošic, P. Kocbek, S. Baumgartner, J. Kristl, Electrospun Chitosan/Peo Nanofibers and Their Relevance in Biomedical Application, 2011, 1296-1299.

[58] L. Martinová, D. Lubasova, Electrospun Chitosan Based Nanofibers, RJTA 12 (2008) 72-79.

[59] B. Omidiji, Evaporative Pattern Casting (EPC) Process, (2018) DOI: 10.5772/intechopen.73526.

[60] H. Lee, S. Ray Chaudhuri, W. Krantz, S.-T. Hwang, A model for evaporative casting of polymeric membranes incorporating convection due to density changes, Journal of Membrane Science 284 (2006) 161-172.

[61] T. Bucher, V. Filiz, C. Abetz, V. Abetz, Formation of Thin, Isoporous Block Copolymer Membranes by an Upscalable Profile Roller Coating Process - A Promising Way to Save Block Copolymer, Membranes 8 (2018) 57.

[62] P.I. Ali, V. Gupta, Advances in Water Treatment by Adsorption Technology, Nature protocols 1 (2006) 2661-7.

[63] X. Qu, P. Alvarez, Q. Li, Applications of nanotechnology in water and wastewater treatment, Water research 47 (2013) 3931-3946.

[64] M. Ahmad, S. Ahmed, B. Swami, S. Ikram, Adsorption of heavy metal ions: Role of chitosan and cellulose for water treatment, Int. J. Pharmacogn. 2 (2015) 280-289.

[65] B. Mathew, Toxicity, mechanism and health effects of some heavy metals, Interdis toxicology 7 (2014) 60-72.

[66] G. Nordberg, A. Bernard, G.L. Diamond, J. Duffus, P. Illing, M. Nordberg, I. Bergdahl, T. Jin, S. Skerfving, Risk assessment of effects of cadmium on human health (IUPAC Technical Report), Pure and Applied Chemistry 90 (2018) 757-802.

[67] H. Zhang, M. Reynolds, Cadmium exposure in living organisms: A short review, Science of The Total Environment 678 (2019) 761-767.

[68] I. Lakhdhar, P. Mangin, B. Chabot, Copper (II) ions adsorption from aqueous solutions using electrospun chitosan/peo nanofibres: Effects of process variables and process optimization, Journal of Water Process Engineering 7 (2015) 295-305.

[69] J. González, S. Román Suero, J.M. Encinar, G. Martínez, Pyrolysis of various biomass residues and char utilization for the production of activated carbons, Journal of Analytical and Applied Pyrolysis In Press 85 (2009) 134–141.

[70] M. Aliabadi, M. Irani, j. İsmaeili, H. Piri, M.J. Parnian, Electrospun nanofiber membrane of PEO/Chitosan for the adsorption of nickel, cadmium, lead and copper ions from aqueous solution, Chemical Engineering Journal 220 (2013) 237-243.

[71] M. Vakili, S. Deng, G. Cagnetta, W. Wang, P. Meng, D. Liu, G. Yu, Regeneration of chitosan-based adsorbents used in heavy metal adsorption: A review, Separation and Purification Technology 224 (2019) 373-387.

[72] D. Yang, L. Li, B. Chen, S. Shi, J. Nie, G. Ma, Functionalized chitosan electrospun nanofiber membranes for heavy-metal removal, Polymer 163 (2018) 74-85.

[73] A. Mautner, H. Maples, T. Kobkeatthawin, V. Kokol, Z. Karim, K. Li, A. Bismarck, Phosphorylated nanocellulose papers for copper adsorption from aqueous solutions, International Journal of Environmental Science and Technology 13 (2016) 1861–1872.

[74] K. Prasad, Evaluation of colour changes of indicators in the titration of cadmium with EDTA, Analytica Chimica Acta 264 (1992) 137-140.

[75] N. Naseri, C. Algan, V. Jacobs, M. John, K. Oksman, A. P Mathew, Electrospun chitosan-based nanocomposite mats reinforced with chitin nanocrystals for wound dressing, Carbohydrate Polymers 109 (2014) 7-15.

[76] H. Oguzlu, Y. Boluk, Interactions between cellulose nanocrystals and anionic and neutral polymers in aqueous solutions, Cellulose 24 (2016) 131-146.

[77] C. Salas, T. Nypelö, C. Rodriguez-Abreu, C. Carrillo, O. Rojas, Nanocellulose properties and applications in colloids and interfaces, Current Opinion in Colloid & Interface Science 19 (2014) 383-396.

[78] J. Schiffman, C. Schauer, A Review: Electrospinning of Biopolymer Nanofibers and their Applications, Polymer Reviews 48 (2008) 317-352.

[79] N. Naseri, A. P Mathew, K. Oksman, Electrospinnability of bionanocomposites with high nanocrystal loadings: The effect of nanocrystal surface characteristics, Carbohydrate Polymers 147 (2016) 464-472.

[80] R. Nezarati, M. Eifert, E. Cosgriff-Hernandez, Effects of Humidity and Solution Viscosity on Electrospun Fiber Morphology, Tissue engineering. Part C, Methods 19 (2013) 810–819.

[81] J. Pelipenko, J. Kristl, B. Janković, S. Baumgartner, P. Kocbek, The impact of relative humidity during electrospinning on the morphology and mechanical properties of nanofibers, International journal of pharmaceutics 456 (2013) 125-134.

[82] V. Pillay, C. Dott, Y. Choonara, C. Tyagi, L. Tomar, P. Kumar, L. Toit, P.D.V. Ndesendo, A Review of the Effect of Processing Variables on the Fabrication of Electrospun Nanofibers for Drug Delivery Applications, Journal of Nanomaterials 2013 (2013) 1-22.

[83] Q. Zhou, B. Liao, L. Lin, W. Qiu, Z. Song, Adsorption of Cu(II) and Cd(II) from aqueous solutions by ferromanganese binary oxide-biochar composites, The Science of the total environment 615 (2017) 115-122.

[84] G. Tan, Y. Xu, H. Wang, W. Sun, Sorption of mercury (II) and atrazine by biochar, modified biochars and biochar based activated carbon in aqueous solution, Bioresource Technology 211 (2016) 727-735.

[85] M. Sekar, V. Sakthi, R. Selvaraj, Kinetics and Equilibrium Adsorption Study of Lead (II) Onto Activated Carbon Prepared From Cocounut Shell, Journal of colloid and interface science 279 (2004) 307-13.

[86] J. Deng, Y. Liu, S. Liu, G. Zeng, X. Tan, B. Huang, X. Tang, S. Wang, Q. Hua, Z. Yan, Competitive adsorption of Pb(II), Cd(II) and Cu(II) onto chitosan-pyromellitic dianhydride modified biochar, Journal of Colloid and Interface Science 506 (2017) 355-364.

[87] N. Azouaou, Z. Sadaoui, A. Djaafri, H. Mokaddem, Adsorption of cadmium from aqueous solution onto untreated coffee grounds: Equilibrium, kinetics and thermodynamics, Journal of hazardous materials 184 (2010) 126-34.

[88] N. Balkaya, H. Cesur, Adsorption of cadmium from aqueous solution by phosphogypsum, Chemical Engineering Journal 140 (2008) 247-254.

[89] M. Mahmoud, Adsorption of Cadmium onto Orange Peels: Isotherms, Kinetics, and Thermodynamics, Journal of Chromatography & Separation Techniques 05 (2014) 1000238.

[90] T. Salah, A. Mohammad, M. Hassan, B. El Anadouli, Development of nano-hydroxyapatite/chitosan composite for cadmium ions removal in wastewater treatment, Journal of the Taiwan Institute of Chemical Engineers 45 (2013) 683-690.

[91] S.K. Ponnusamy, K. Ramakrishnan, S. Kirupha, Thermodynamic and kinetic studies of cadmium adsorption from aqueous solution onto rice husk, Brazilian Journal of Chemical Engineering 27 (2010) 347-355.

[92] X. Yu, S. Tong, M.-F. Ge, L. Wu, J. Zuo, C.-Y. Cao, W. Song, Adsorption of heavy metal ions from aqueous solution by carboxylated cellulose nanocrystals, Journal of environmental sciences (China) 25 (2013) 933-43.

[93] A. Tajar, T. Kaghazchi, M. Soleimani, Adsorption of Cadmium from Aqueous Solutions on Sulfurized Activated Carbon Prepared from Nut Shells, Journal of hazardous materials 165 (2008) 1159-64.

[94] D. Obregón, M. Sun-Kou, Comparative cadmium adsorption study on activated carbon prepared from aguaje (Mauritia flexuosa) and olive fruit stones (Olea europaea L.), Journal of Environmental Chemical Engineering 2 (2014) 2280-2288.

[95] X. Cui, S. Fang, Y. Yao, T. Li, Q. Ni, X. Yang, Z. He, Potential mechanisms of cadmium removal from aqueous solution by Canna indica derived biochar, The Science of the total environment 562 (2016) 517-525.

[96] M. Sayed, N. Burham, Adsorption Behavior of Cd2+ and Zn2+onto Natural Egyptian Bentonitic Clay, Minerals 6 (2016) 114-129.

[97] L. Zeng, Y. Chen, Q. Zhang, X. Guo, Y. Peng, H. Xiao, X. Chen, J. Luo, Adsorption of Cd(II), Cu(II) and Ni(II) ions by cross-linking chitosan/rectorite nano-hybrid composite microspheres, Carbohydrate Polymers 130 (2015) 333-343.

[98] C. Hu, P. Zhu, M. Cai, H. Hu, Q. Fu, Comparative adsorption of Pb(II), Cu(II) and Cd(II) on chitosan saturated montmorillonite: Kinetic, thermodynamic and equilibrium studies, Applied Clay Science 143 (2017) 320-326.

[99] D. Liu, Z. Li, Y. Zhu, Z. Li, R. Kumar, Recycled chitosan nanofibril as an effective Cu(II), Pb(II) and Cd(II) ionic chelating agent: Adsorption and desorption performance, Carbohydrate polymers 111C (2014) 469-476.

[100] P. Chowdhary, A. Raj, R. Bharagava, Environmental pollution and health hazards from distillery wastewater and treatment approaches to combat the environmental threats: A review, Chemosphere 194 (2017) 229-246.

[101] G. Saxena, R. Chandra, R. Bharagava, Environmental Pollution, Toxicity Profile and Treatment Approaches for Tannery Wastewater and Its Chemical Pollutants, Reviews of environmental contamination and toxicology 240 (2016) 31-59.

[102] A. Meneghel, A. Gonçalves Jr, L. Strey, F. Rubio, D. Schwantes, J. Casarin, Biosorption and removal of chromium from water by using moringa seed cake (Moringa oleifera Lam.), Química Nova 36 (2012) 1104-1110.

[103] M. Rahimzadeh, S. Kazemi, A. Moghadamnia, Cadmium toxicity and treatment: An update, Caspian Journal of Internal Medicine 8 (2017) 135-145.

[104] X. Xu, S. Nie, H. Ding, F. Hou, Environmental pollution and kidney diseases, Nature Reviews Nephrology 14 (2018) 313–324.

[105] A. Abdolali, H.H. Ngo, W.S. Guo, D.J. Lee, K.-L. Tung, Development and evaluation of a new multi-metal binding biosorbent, Bioresource technology 160 (2013) 98-106.

[106] J. Ali Shah, T. Ashfaq, S.M. Hussain Gardazi, A. Tahir, A. Pervez, H. Haroon, Q. Mahmood, Waste biomass adsorbents for copper removal from industrial wastewater-A review, Journal of hazardous materials 263 (2013) 322-333.

[107] G. Ungureanu, S. Santos, R. Boaventura, C. Botelho, Arsenic and antimony in water and wastewater: Overview of removal techniques with special reference to latest advances in adsorption, Journal of environmental management 151C (2015) 326-342.

[108] A. Adeleye, J. Conway, K. Garner, Y. Huang, Y. Su, A. Keller, Engineered nanomaterials for water treatment and remediation: Costs, benefits, and applicability, Chemical Engineering Journal 286 (2015) 640-662.

[109] L. Broek, R. Knoop, F. Kappen, C. Boeriu, Chitosan films and blends for packaging material, Carbohydrate Polymers 116 (2015) 237-242.

[110] I. Younes, M. Rinaudo, Chitin and Chitosan Preparation from Marine Sources. Structure, Properties and Applications, Marine Drugs 13 (2015) 1133-1174.

[111] L. Zhang, Y. Zeng, Z. Cheng, Removal of heavy metal ions using chitosan and modified chitosan: A review, Journal of Molecular Liquids 214 (2016) 175-191.

[112] A. Carpenter, C.-F. de Lannoy, M. Wiesner, Cellulose Nanomaterials in Water Treatment Technologies, Environmental science & technology 49 (2015) 5277–5287.

[113] J. George, S. N, Cellulose nanocrystals: Synthesis, functional properties, and applications, Nanotechnology, Science and Applications 8 (2015) 45.

[114] M.-C. Li, Q. Wu, K. Song, S. Lee, Y. Qing, Y. Wu, Cellulose Nanoparticles: Structure–Morphology–Rheology Relationships, ACS Sustainable Chemistry & Engineering 3 (2015) 150407061249007.

[115] W. Jang, J. Yun, K. Jeon, H.-S. Byun, PVdF/graphene oxide hybrid membranes via electrospinning for water treatment applications, RSC Adv. 5 (2015) 46711-46717.

[116] S. Ray, S.-S. Chen, C.-W. Li, N.C. Nguyen, H. Nguyen, A comprehensive review: Electrospinning technique for fabrication and surface modification of membranes for water treatment application, RSC Adv. 6 (2016) 85495-85514.

[117] Y. Tian, M. Wu, R. Liu, Y. Li, D. Wang, J. Tan, R. Wu, Y. Huang, Electrospun membrane of cellulose acetate for heavy metal ion adsorption in water treatment, Carbohydrate Polymers 83 (2011) 743-748.

[118] U. Habiba, A. Afifi, N.A. Mohd Salleh, B. Ang, Chitosan/(Polyvinyl Alcohol)/Zeolite Electrospun Composite Nanofibrous Membrane for Adsorption of Cr6+, Fe3+ and Ni2+, Journal of Hazardous Materials 322 (2016) 182-194.

[119] L. Li, Y. Li, L. Cao, C. Yang, Enhanced chromium (VI) adsorption using nanosized chitosan fibers tailored by electrospinning, Carbohydrate Polymers 125 (2015) 206-213.

[120] Y. Shi, D. Belosinschi, F. Brouillette, A. Belfikira, The Properties of Phosphorylated Kraft Fibers, BioResources 10(3) (2015) 4375-4390.

[121] B. Martins, C. Cruz, A. Luna, C. Henriques, Sorption and desorption of Pb2+ ions by dead Sargassum sp. Biomass, Biochemical Engineering Journal 27 (2006) 310-314.

[122] l. Deng, Y. Su, H. Su, X. Wang, X. Zhu, Sorption and Desorption of Lead(II) from Wastewater by Green Algae Cladopha fasciularis, Journal of hazardous materials 143 (2007) 220-5.

[123] H. Pan, L. Song, L. Ma, Y. Pan, K. Liew, Y. Hu, Layer-by-layer assembled thin films based on fully biobased polysaccharides: Chitosan and phosphorylated cellulose for flame-retardant cotton fabric, Cellulose 21 (2014) 2995-3006.

[124] S. Lemma, F. Bossard, M. Rinaudo, Preparation of Pure and Stable Chitosan Nanofibers by Electrospinning in the Presence of Poly(ethylene oxide), International Journal of Molecular Sciences 17 (2016) 1790.

[125] P. Sangsanoh, P. Supaphol, Stability Improvement of Electrospun Chitosan Nanofibrous Membranes in Neutral or Weak Basic Aqueous Solutions, Biomacromolecules 7 (2006) 2710-4.

[126] C. Bergeron, E. Perrier, A. Potier, G. Delmas, A Study of the Deformation, Network, and Aging of Polyethylene Oxide Films by Infrared Spectroscopy and Calorimetric Measurements, International Journal of Spectroscopy 2012 (2012) 1-13.

[127] A. Pawlak, M. Mucha, Thermogravimetric and FTIR studies of chitosan blends, Thermochimica Acta 396 (2003) 153-166.

[128] P. Xiao, J. Zhang, Y. Feng, J. Wu, J. He, J. Zhang, Synthesis, characterization and properties of novel cellulose derivatives containing phosphorus: Cellulose diphenyl phosphate and its mixed esters, Cellulose 21 (2014) :2369–2378.

[129] D. Suflet, I. Popescu, I. Pelin, Preparation and adsorption studies of phosphorylated cellulose microspheres Cellulose Chemistry and Technology 51(1-2) (2017) 23-34.

[130] J. Namieśnik, A. Rabajczyk, The Speciation of Aluminum in Environmental Samples, Critical Reviews in Analytical Chemistry 40 (2010) 68-88.

[131] Y.-S. Ho, G. McKay, A Kinetic Study of Dye Sorption by Biosorbent Waste Product Pith, Resources Conservation and Recycling 25 (1999) 171-193.

[132] Y.-S. Ho, J. Porter, G. McKay, Equilibrium Isotherm Studies for the Sorption of Divalent Metal Ions onto Peat: Copper, Nickel and Lead Single Component Systems, Water Air and Soil Pollution 141 (2002) 1-33.

[133] S. Moreira, F. Sousa, A. Oliveira, R. Nascimento, E. Brito, Remoção de metais de solução aquosa usando bagaço de caju, Quimica Nova 32 (2009) 1717-1722.

[134] S. erdoğan, Y. Önal, C. Akmil-Başar, S. Erdemoglu, Ç. Sarici-Özdemir, E. Koseoglu, G. Içduygu, Optimization of nickel adsorption from aqueous solution by using activated carbon prepared from waste apricot by chemical activation, Applied Surface Science 252 (2005) 1324-1331.

[135] N. Ben Amar, N. Kechaou, J. Palmeri, A. Deratani, A. Sghaier, Comparison of tertiary treatment by nanofiltration and reverse osmosis for water reuse in denim textile industry, Journal of hazardous materials 170 (2009) 111-7.

[136] S. Garcia-Segura, J. Keller, E. Brillas, J. Radjenovic, Removal of organic contaminants from secondary effluent by anodic oxidation with a boron-doped diamond anode as tertiary treatment, Journal of Hazardous Materials 283 (2014) 551-557.

[137] V.K. Garg, R. Gupta, R. Hooda, R. Gupta, Adsorption of Chromium From Aqueous Solution on Treated Sawdust, Bioresource technology 92 (2004) 79-81.

[138] G. Pérez, A. Fernández-Alba, A. Urtiaga, I. Ortiz, Electro-oxidation of reverse osmosis concentrates generated in tertiary water treatment, Water research 44 (2010) 2763-72.

[139] A. Touffet, J. Baron, B. Welte, M. Joyeux, B. Teychene, H. Gallard, Impact of pretreatment conditions and chemical ageing on ultrafiltration membrane performances. Diagnostic of a coagulation/adsorption/filtration process, Journal of Membrane Science 489 (2015) 284-291.

[140] M. Alhumaimess, I. Alsohaimi, A. Alqadami, M. abou baker, M. Naushad, T. Ahamad, Synthesis of phosphorylated raw sawdust for the removal of toxic metal ions from aqueous medium: Adsorption mechanism for clean approach, Journal of Sol-Gel Science and Technology 89 (2018) 602–615.

[141] L. Lin, Z. Li, X. Song, Y. Jiao, C. Zhou, Preparation of Chitosan/Lanthanum Hydroxide Composite Aerogel Beads for Higher Phosphorus Adsorption, Materials Letters 218 (2018) 201-204.

[142] R. Brandes, D. Belosinschi, F. Brouillette, B. Chabot, A new electrospun chitosan/phosphorylated nanocellulose biosorbent for the removal of cadmium ions from aqueous solutions, Journal of Environmental Chemical Engineering 7(6) (2019) 103477.

[143] A. Zanoletti, I. Vassura, E. Venturini, M. Monai, T. Montini, S. Federici, A. Zacco, L. Treccani, E. Bontempi, A New Porous Hybrid Material Derived From Silica Fume and Alginate for Sustainable Pollutants Reduction, Frontiers in Chemistry 6 (2018) 1-13.

[144] A. Haider, S. Haider, I.-K. Kang, A comprehensive review summarizing the effect of electrospinning parameters and potential applications of nanofibers in biomedical and biotechnology, Arabian Journal of Chemistry (2015) 1165-1188.

[145] S. Sankaran, K. Deshmukh, B. Ahamed, S. Pasha, Electrospun Polymeric Nanofibers: Fundamental Aspects of Electrospinning Processes, Optimization of Electrospinning Parameters, Properties, and Applications, 2019, 375-409.

[146] S. Saha, M. Zubair, M. Khosa, S. Song, A. Ullah, Keratin and Chitosan Biosorbents for Wastewater Treatment: A Review, Journal of Polymers and the Environment 27 (2019) 1389–1403.

[147] M. Wołowiec, M. Komorowska-Kaufman, A. Pruss, G. Rzepa, T. Bajda, Removal of Heavy Metals and Metalloids from Water Using Drinking Water Treatment Residuals as Adsorbents: A Review, Minerals 9 (2019) 487.

[148] F. de la Torre, A. Salibian, L. Ferrari, Assessment of the pollution impact on biomarkers of effect of a freshwater fish, Chemosphere 68 (2007) 1582-90.

[149] X. Li, C. Poon, P.S. Liu, Heavy metal contamination of urban soils and street dusts in Hong Kong, Applied Geochemistry 16(11-12) (2001) 1361-1368.

[150] K. Murray, S. Thomas, A. Bodour, Prioritizing Research for Trace Pollutants And Emerging Contaminants In The Freshwater Environment, Environmental Pollution 158 (2010) 3462-3471.

[151] M. Dural Eken, M. Göksu, A. Özak, Investigation of heavy metal levels in economically important fish species captured from the Tuzla lagoon, Food Chemistry 102 (2007) 415-421.

[152] S. Khan, R. Farooq, S. Shahbaz, M. Khan, M. Siddique, Health Risk Assessment of Heavy Metals for Population via Consumption of Vegetables, World Applied Science Journal 6 (2009) 1602-1606.

[153] S. Davydova, Heavy metals as toxicants in big cities, Microchemical Journal 79 (2005) 133-136.

[154] V. Gitis, N. Hankins, Water treatment chemicals: Trends and challenges, Journal of Water Process Engineering 25 (2018) 34-38.

[155] F. Licciardello, M. Milani, S. Consoli, N. Pappalardo, S. Barbagallo, G. Cirelli, Wastewater tertiary treatment options to match reuse standards in agriculture, Agricultural Water Management 210 (2018) 232-242.

[156] J. Xue, T. Wu, Y. Dai, Y. Xia, Electrospinning and Electrospun Nanofibers: Methods, Materials, and Applications, Chemical Reviews 119 (2019) 5298–5415.

[157] F. Bouhamed, Z. Elouaer, J. Bouzid, B. Ouddane, Multi-component adsorption of copper, nickel and zinc from aqueous solutions onto activated carbon prepared from date stones, Environmental science and pollution research international 23 (2015) 15801–15806.

[158] A.A. Taha, M. Shreadah, A.M. Ahmed, H. Heiba, Multi-component Adsorption of Pb(II), Cd(II), and Ni(II) onto Egyptian Na-activated Bentonite; Equilibrium, Kinetics, Thermodynamics, and Application for Seawater Desalination, Journal of Environmental Chemical Engineering 4 (2016) 1166-1180.

[159] S. Sessarego, S. Rodrigues, X. ye, Q. Lu, J. Hill, Phosphonium-Enhanced Chitosan for Cr(VI) Adsorption in Wastewater Treatment, Carbohydrate Polymers 211 (2019) 249-256.

[160] X. Luo, J. Yuan, Y. Liu, C. Liu, X. Zhu, X. Dai, Z. Ma, F. Wang, Improved solid-phase synthesis of the phosphorylated cellulose microsphere adsorbents for highly effective Pb 2+ removal from water: the batch and fixed-bed column performance and the adsorption mechanism, ACS Sustainable Chemistry & Engineering 5 (2017) 5108–5117.

[161] Y. Ojima, S. Kosako, M. Kihara, N. Miyoshi, K. Igarashi, M. Azuma, Recovering metals from aqueous solutions by biosorption onto phosphorylated dry baker's yeast, Scientific Reports 9 (2019) 1-9.

[162] W. Zhang, H. Wang, X. Hu, H. Feng, W. Xiong, W. Guo, J. Zhou, A. Mosa, Y. Peng, Multicavity triethylenetetramine-chitosan/alginate composite beads for enhanced Cr(VI) removal, Journal of Cleaner Production 231 (2019) 733-745.

[163] L. Li, R.-H. Liu, B. Yang, Z.-H. Zhou, L. Xu, H.-D. Huang, G. Zhong, Interconnected microdomain structure of crosslinked cellulose nanocomposite

revealed by micro-Raman imaging and its influence on water permeability of film, Biomacromolecules 20 (2019) 2754–2762.

[164] X. Li, A. Janke, P. Formanek, A. Fery, M. Stamm, B.P. Tripathi, High permeation and antifouling polysulfone ultrafiltration membranes with in situ synthesized silica nanoparticles, Materials Today Communications 22 (2019) 100784.

[165] M. Zahid, A. Rashid, S. Akram, Z. Rehan, W. Razzaq, A Comprehensive Review on Polymeric Nano-Composite Membranes for Water Treatment, Journal of Membrane Science & Technology 08 (2018) 1-20.

[166] R. Bezerra, R. Casimiro Leal, M. Silva, A. Morais, T. Marques, J. Osajima, A. Meneguin, H. Barud, E. Filho, Direct Modification of Microcrystalline Cellulose with Ethylenediamine for Use as Adsorbent for Removal Amitriptyline Drug from Environment, Molecules 22 (2017) 2039.

[167] M. Ghanadpour, F. Carosio, P.T. Larsson, L. Wågberg, Phosphorylated Cellulose Nanofibrils: A Renewable Nanomaterial for the Preparation of Intrinsically Flame-Retardant Materials, Biomacromolecules 16(10) (2015) 3399-3410.

[168] S. Blilid, N. Katir, J. Bennagi, M. Lachini, S. Royer, A. El Kadib, Phosphorylated micro- vs nano-cellulose: A comparative study on their surface functionalisation, growth of titanium-oxo-phosphate clusters and removal of chemical pollutants, New Journal of Chemistry 43 (2019) 15555-15562.

[169] W.R. Wan Daud, M.K. Haafiz, A. Seeni, Cellulose phosphate from oil palm biomass as potential biomaterials, BioResources 6 (2011) 1719-1740.

[170] Z. Karim, A. P Mathew, M. Grahn, J. Mouzon, K. Oksman, Nanoporous membranes with cellulose nanocrystals as functional entity in chitosan: Removal of dyes from water, Carbohydrate polymers 112C (2014) 668-676.

[171] Z. Karim, A. P Mathew, V. Kokol, J. Wei, M. Grahn, High-flux affinity membranes based on cellulose nanocomposites for removal of heavy metal ions from industrial effluents, RSC Adv. 6 (2016) 20644-20653.

[172] M. Igura, M. Okazaki, Cadmium sorption characteristics of phosphorylated sago starch-extraction residue, Journal of hazardous materials 178 (2010) 686-92.

[173] D. Mohan, C. Pittman, P. Steele, Single, binary and multi-component adsorption of copper and cadmium from aqueous solutions on Kraft lignin - a biosorbent, Journal of colloid and interface science 297 (2006) 489-504.

[174] M. Karnib, A. Kabbani, H. Holail, Z. Olama, Heavy Metals Removal Using Activated Carbon, Silica and Silica Activated Carbon Composite, Energy Procedia 50 (2014) 113–120.

[175] L.-Y. Gao, J.-H. Deng, G.-F. Huang, K. Li, K.-Z. Cai, Y. Liu, F. Huang, Relative distribution of Cd2+ adsorption mechanisms on biochars derived from rice straw and sewage sludge, Bioresource Technology 272 (2018) 114-122.

[176] Y.-H. Li, J. Ding, Z. Luan, D. Zechao, Y. Zhu, C. Xu, D. Wu, B. Wei, Competitive adsorption of Pb2+, Cu2+ and Cd2+ ions from aqueous solutions by multiwalled carbon nanotubes, Carbon 41 (2003) 2787-2792.

[177] K. Chojnacka, A. Chojnacki, H. Górecka, Biosorption of Cr3+, Cd2+ and Cu2+ ions by blue-green algae Spirulina sp.: Kinetics, equilibrium and the mechanism of the process, Chemosphere 59 (2005) 75-84.

[178] I. Mobasherpour, E. Salahi, M. Pazouki, Comparative of the removal of Pb2+, Cd2+ and Ni2+ by nano crystallite hydroxyapatite from aqueous solutions: Adsorption isotherm study, Arabian Journal of Chemistry 5 (2012) 439–446.

[179] P. Castaldi, L. Santona, S. Enzo, Sorption processes and XRD analysis of a natural zeolite exchanged with Pb2+, Cd2+ and Zn2+ cations, Journal of hazardous materials 156 (2008) 428-34.

[180] J.C. de Andrade Neto, G.J. Pereira, A. de Araújo Morandim-Giannetti, Lignocellulosic derivative and chitosan bioadsorbent: Synthesis, characterization, and performance in chromium adsorption, Journal of Applied Polymer Science 137(40) (2020) 49208.

[181] D. Zhang, W. Xu, J. Cai, S.-Y. Cheng, W.-P. Ding, Citric acid-incorporated cellulose nanofibrous mats as food materials-based biosorbent for removal of hexavalent chromium from aqueous solutions, International Journal of Biological Macromolecules 149 (2020) 459-466.

[182] J. Guo, T. Chen, X. Zhou, T. Zheng, W. Xia, C. Zhong, Y. Liu, Preparation and Pb (II) adsorption in aqueous of 2D/2D g-C3N4/MnO2 composite, Applied Organometallic Chemistry 33(10) (2019) e5119.

[183] R. Fan, Q. Yi, Y. Xie, F. Xie, Q. Zhang, Z. Luo, Enhanced adsorption and recovery of Pb(II) from aqueous solution by alkali-treated persimmon fallen leaves, Journal of Applied Polymer Science 133(28) (2016) 43656.

[184] M. Arshadi, M.J. Amiri, S. Mousavi, Kinetic, equilibrium and thermodynamic investigations of Ni(II), Cd(II), Cu(II) and Co(II) adsorption on barley straw ash, Water Resources and Industry 6 (2014) 1-17.

[185] N. Kataria, V.K. Garg, Optimization of Pb (II) and Cd (II) adsorption onto ZnO nanoflowers using central composite design: isotherms and kinetics modelling, Journal of Molecular Liquids 271 (2018) 228-239.

[186] D.Q. Melo, C.B. Vidal, A.L. da Silva, R.N.P. Teixeira, G.S.C. Raulino, T.C. Medeiros, P.B.A. Fechine, S.E. Mazzeto, D. De Keukeleire, R.F. Nascimento,

Removal of Cd2+, Cu2+, Ni2+, and Pb2+ ions from aqueous solutions using tururi fibers as an adsorbent, Journal of Applied Polymer Science 131(20) (2014) 40883.

[187] D. Mohan, K. Singh, Single- and Multi-Component Adsorption of Cadmium and Zinc Using Activated Carbon Derived From Bagasse—An Agricultural Waste, Water research 36 (2002) 2304-18.

[188] M. Visa, L. Isac, A. Duta, Fly ash adsorbents for multi-cation wastewater treatment, Applied Surface Science 258 (2012) 6345–6352.

[189] J. Hanzlík, J. Jehlicka, O. Sebek, Z. Weishauptová, V. Machovic, Multi-component adsorption of Ag(I), Cd(II) and Cu(II) by natural carbonaceous materials, Water research 38 (2004) 2178-84.

[190] C. Dong, F. Zhang, Z. Pang, G. Yang, Efficient and Selective Adsorption of Multi-metal Ions Using Sulfonated Cellulose as Adsorbent, Carbohydrate Polymers 151 (2016) 230-236.

Annexe A

List of publications (Articles)

[1] Brandes, R.; Brouillette, F.; Chabot, B. Phosphorylated cellulose/electrospun chitosan nanofibers media for removal of heavy metals from aqueous solutions, Journal of Applied Polymer Science, 2020, e50021, https://doi.org/10.1002/app.50021

[2] Brandes, R.; Brouillette, F.; Chabot, B. Cd^{2+} removal by nonwoven Chitosan/Phosphorylated Microcellulose Nanocomposite, Water, Air, & Soil Pollution, *Submitted (29 March 2020).*

[3] Brandes, R.; Belosinschi, D.; Brouillette, F.; Chabot, B. A new electrospun Chitosan/Phosphorylated Nanocellulose biosorbent for the removal of cadmium ions from aqueous solutions, Journal of Environmental Chemical Engineering, 7 (6) 2019, 103477, https://doi.org/10.1016/j.jece.2019.103477.

List of publications (Oral presentations)

[1] R. Brandes, F. Brouillette, B. Chabot, Development of Electrospun Chitosan/Phosphorylated Nanocellulose Sorbent Nanocomposite for Removal of Metal Ions from Aqueous Solutions, CQMF - 2nd Advanced Materials Annual Conference, Montreal, Canada, http://cqmf-qcam.ca/wp-content/uploads/2018/10/booklet-AM18.pdf.

[2] R. Brandes, F. Brouillette, B. Chabot, Membranes nanofibreuses électrofilées à base de chitosane et de microcellulose phosphorylée pour l'élimination de métaux lourds des eaux usées, 87e Congrès de l'ACFAS, Gatineau, Canada, https://www.acfas.ca/evenements/congres/programme/87/200/216/c.

List of publications (Posters)

[1] R. Brandes, F. Brouillette, B. Chabot, Chitosan/Phosphorylated Microcellulose nanofibers membrane produced by electrospinning, 26e édition du Concours d'affiches scientifiques (2019), Trois Rivieres, Canada.

[2] R. Brandes, F. Brouillette, B. Chabot, Electrospun Chitosan/Phosphorylated Cellullose nanofibers for the removal of cadmium ions from aqueous solutions, 25e édition du Concours d'Affiches scientifiques (2018), Trois-Rivières, Canada.

Annexe B

Proof of submission: Article 2

Article 2 in Chapter 5 entitled: "Cd2+ removal by nonwoven Chitosan/Phosphorylated Microcellulose Nanocomposite" was submitted to the scientific journal "Water, Air, & Soil Pollution" in March 2020 for publication. The following email from the journal's editor are evidence that the article was submitted to the scientific journal.

Brandes, Ricardo

From: em.wate.0.6a4332.830e2f88@editorialmanager.com on behalf of WATE <em@editorialmanager.com>
Sent: March 29, 2020 12:28 PM
To: Brandes, Ricardo
Subject: WATE-D-20-00650 - Submission Notification to co-author

Submission ID: WATE-D-20-00650
Re: "Cd2+ removal by nonwoven Chitosan/Phosphorylated Microcellulose Nanocomposite"
Full author list: Ricardo Brandès; François Brouillette, PhD; Bruno Chabot

Dear Mr Ricardo Brandès,

We have received the submission entitled: "Cd2+ removal by nonwoven Chitosan/Phosphorylated Microcellulose Nanocomposite" for possible publication in Water, Air, & Soil Pollution, and you are listed as one of the co-authors.

The manuscript has been submitted to the journal by Dr. Dr. Bruno Chabot who will be able to track the status of the paper through his/her login.

If you have any objections, please contact the editorial office as soon as possible. If we do not hear back from you, we will assume you agree with your co-authorship.

Thank you very much.

With kind regards,

Springer Journals Editorial Office
Water, Air, & Soil Pollution

As a result of the significant disruption that is being caused by the COVID-19 pandemic we are very aware that many researchers will have difficulty in meeting the timelines associated with our peer review process during normal times. Please do let us know if you need additional time. Our systems will continue to remind you of the original timelines but we intend to be highly flexible at this time.

This letter contains confidential information, is for your own use, and should not be forwarded to third parties.

Recipients of this email are registered users within the Editorial Manager database for this journal. We will keep your information on file to use in the process of submitting, evaluating and publishing a manuscript. For more information on how we use your personal details please see our privacy policy at https://www.springernature.com/production-privacy-policy. If you no longer wish to receive messages from this journal or you have questions regarding database management, please contact the Publication Office at the link below.

In compliance with data protection regulations, you may request that we remove your personal registration details at any time. (Use the following URL: https://www.editorialmanager.com/wate/login.asp?a=r). Please contact the publication office if you have any questions.